

**Control Authority Issues
in
Aircraft Conceptual Design:
Critical Conditions, Estimation Methodology,
Spreadsheet Assessment, Trim and Bibliography**

by

J. Kay, W. H. Mason, W. Durham, F. Lutze and A. Benoliel

VPI-Aero-200

November 1993
(minor revisions and typos fixed, November 1996)

Supported in part by the
NASA/USRA Advanced Design Program
and Navy/NASA Aircraft Control Requirements Grant NCC1-158

Department of Aerospace and Ocean Engineering
Virginia Polytechnic Institute and State University
Blacksburg, Virginia 24061

Control Authority Issues
in
Aircraft Conceptual Design:
Critical Conditions, Estimation Methodology,
Spreadsheet Assessment, Trim and Bibliography

by

J. Kay, W. H. Mason, W. Durham, F. Lutze and A. Benoliel

ABSTRACT

All aircraft must meet controllability requirements to be certified for commercial use or adopted by the military. Many military aircraft also have additional maneuverability requirements. An aircraft's ability to meet these requirements is often limited by the amount of control authority available. Thus, it is essential for designers to evaluate the control authority of candidate concepts early in the conceptual design phase. Normally the designer considers numerous possible configurations before the stability and control group starts their analysis. An early evaluation by the designer, before detailed control system design starts, makes the design process much more efficient. In this report a methodology for rapid control power evaluation of conceptual and early preliminary design configurations against requirements at the critical flight conditions is established.

First, the critical flight conditions to be considered using this methodology are discussed. Next, to examine a variety of aircraft configurations and accelerate the process of estimating stability and control derivatives, a FORTRAN program using the vortex-lattice method to estimate subsonic, low angle-of-attack aerodynamics is described. Then, a simple spreadsheet is used to combine the aerodynamic and geometric data to assess whether the design concept possesses adequate control power to satisfy the requirements at the critical flight conditions. This allows the designer to perform "what if" studies to decide how to change the design to satisfy the requirements. To trim configurations with three lifting surfaces or two lifting surfaces and thrust vectoring, a program implementing a recent NASA Langley method is provided. For further study, a bibliography relevant to control power issues is included.

As an educational document, both the report and the software will be continually refined. The authors solicit comments on ways to improve the material. Users should request the latest editions of the report and software.

Acknowledgments

We acknowledge the NASA/USRA Aeronautics Advanced Design Program for the support of the first and fifth authors. The bibliography was developed under partial Navy/NASA support through Navy/NASA Aircraft Control Requirements Grant NCC1-158. Portions of this work are based on work done by Mason's co-workers at Grumman, where Rudy Meyer and Richard Mercadante investigated the same issues.

Software

The software described here is being used and continually updated by the students of the senior aircraft design class at Virginia Tech. Although it is not a commercial grade product, it may prove useful for designers. It is available and could form the basis for further work by other engineers. Requests for the software should be directed to the second author.

Table of Contents

1. Introduction	1
2. Specifications: Critical Flight Conditions and Maneuvers	4
2.1 Equilibrium/Performance Considerations	5
2.1.1 Normal Trimmed Flight	5
2.1.1.2 Classical 1G trim	5
2.1.1.3 Elementary Control Allocation Examples	9
- Three Surface Configurations	
- Thrust Vectoring	
2.1.1.4 Longitudinal Maneuvering Flight	10
2.1.2 Steady Sideslip	12
2.1.3 Engine-Out Trim	13
2.2 Dynamic Considerations	15
2.2.1 Takeoff & Landing Rotation	17
2.2.2 Time-to-Bank	20
2.2.3 Inertia Coupling: Pitch Due to Velocity Axis Roll	27
2.2.4 Inertia Coupling: Yaw Due to Loaded Roll	30
2.2.5 Coordinated Velocity Axis Roll and Roll Acceleration	31
2.2.6 Short Period & CAP Requirements	32
2.2.7 High Angle-of-Attack/Departure	34
2.3 Other Considerations Not Currently Included in Spreadsheet	35
2.3.1 Gust	35
2.3.2 Non-linear Aerodynamics	36
2.3.3 Aeroelasticity	36
2.3.4 Special Requirements	37
3. Discussion of Overall Assessment Methodology	38
3.1 Flight Condition Variables	40
3.2 Stability and Control Derivatives	45
3.3 Control Power Evaluation for Requirements	45

4. Subsonic Linear Aerodynamic Estimation:	
A Vortex-Lattice Method	47
4.1 Code Implementation: Concept and Limitations	47
4.2 Comparison with DATCOM Estimates Wind Tunnel Data	52
4.2.1 Stability Derivatives	53
4.2.2 Control Derivatives	60
5. Assessment Computer Codes: User Instructions	65
5.1 JKayVLM	65
5.2 FLTCOND	72
5.3 CPRCHECK	72
5.4 TRIM3S	72
5.5 TRIMTV	76
6. Control Authority Assessment Example: The F-18	80
6.1 1-G Trim	80
6.2 Maneuver Flight (Pull-up)	80
6.3 Steady Sideslip	81
6.4 Engine-out Trim	81
6.5 Takeoff & Landing Rotations	82
6.6 Time-to-Bank	83
6.7 Pitch Due to Velocity Axis Roll	83
6.8 Rolling Pullout & Coordinated Roll	84
6.9 Short Period & CAP	85
6.10 Overall Assessment	86
7. Conclusions	87
7.1 Future Work	87
References	89
Appendices	93
A. Program and Spreadsheet Documentation	93
A1. Program VLM	93
A2. Spreadsheet to Check Control Authority Requirements	95
A3. Program FLTCOND	104
A4. Programs TRIM3S and TRIMTV	105
B. Annotated Bibliography and Extended Reference List: Control Power Requirements	107

List of Figures

1.	Forces and Moments for Take-off Ground Run	19
2.	MIL-STD-1797 Short Period Flying Qualities Requirements	33
3.	Control Authority Assessment Methodology	38
3.	Sample Input Spreadsheet for program FLTCOND	31
4.	Vortex Rings & Control Points of VLM Implementation	48
5.	Prandtl-Glauert Correction Rule Used in VLM To Account for Compressibility	49
6.	Surface Velocity Distribution due to Pitching Rate	49
7.	Spanwise Vortex Strength Distribution for Asymmetric Loading	51
8.	Use of Mirror Vortex System to Model Ground Effect	51
9.	VLM Grid Representation of F-18 Showing Individual Sections	52
10.	Angle-of-Attack Derivatives & Static Margin	54
11.	Pitch Rate Derivatives	55
12.	Sideslip Derivatives	56
13.	Yaw Rate Derivatives	57
14.	Roll Rate Derivative	58
15.	Elevator (Horizontal Tail) Effectiveness	61
16.	Inboard Trailing Edge Flap Effectiveness	62
17.	Aileron Effectiveness	62
18.	Rudder Effectiveness (One-Rudder Deflection)	63
19.	Order of Points for Each Trapezoidal Panel	68
20.	Convention for Geometry Input Files	68
21.	Convention for Positive Control Surface Deflection	70
22.	Estimated Maximum Stability Axis Roll Rate of F-18 Limited @ SL, Mach 0.6	84

List of Tables

1.	Flying Quality Level Specifications	15
2.	Airplane Classification	16
3.	Flight Phase Categories	16
4.	Roll performance for Class I and II Aircraft	20
5.	Class II Aircraft Speed Definitions for Roll for Performance Requirements	21
6.	Roll Performance Requirements for Class III Aircraft	21
7.	Class IV Aircraft Speed Definitions for Roll Performance Requirements	21
8.	Time-to-Bank Requirements from MIL-STD-1797	
	a. General Roll Performance for Class IV Airplanes	22
	b. Air-to-Air Combat Roll Performance (360° rolls)	22
	c. Air-to-Air Combat Roll Performance Requirements	23
	d. Ground Attack Roll Performance Requirements	23
9.	Minimum Flying Qualities for Normal States in Atmospheric Disturbances	35
10.	Minimum Flying Qualities for Failure States in Atmospheric Disturbances	36
11.	Sample Input Spreadsheet for Program FLTCOND	43
12.	Sample Output File of Program FLTCOND	44
13.	Trimmed 1-g Flight Worksheet	46
14.	Pitch Due to Roll Coupling Worksheet	46
15.	Reliability of Stability Derivative Predictions	59
16.	Sample Longitudinal Geometry Input File	69
17.	Sample Lateral/Directional Geometry Input File	69
18.	Sample Parameter Input File	70
19.	VLM Code Output (Longitudinal and Lateral Data for F-18)	71
20.	Sample Input Data for the Three Surface Code TRIM3S	74
21.	Sample Output from TRIM3S	75
22.	Sample Case for Thrust Vectoring Code, TRIMTV	78
23.	Sample Output for TRIMTV	79

24.	1-G Trim Assessment	80
25.	Maneuver Flight (Pull-up) Assessment	81
26.	Engine-out Trim Assessment at Mach 0.2 at S.L.	82
27.	Time-to-Bank Performance at SL ($I_x = 26,000$ slug ft ²)	83
28.	Rolling Pullout & Coordinated Roll Assessment at SL, Mach 0.6	85
29.	Short Period & Control Anticipation Parameter (CAP) Assessment	85

List of Symbols

Symbol	Definition	Dimension
b	wing/planform span	ft
CAP	control anticipation parameter	rad/(g s ²)
c, \bar{c}	reference chord	ft
g	gravitational acceleration	ft/s ²
$I_{x,y,z}$	Inertia about x-, y-, z- axis (body reference frame)	slug ft ²
i_T	vertical thrust incident angle with respect to fuselage reference line (+ for jet exhaust downward, + for jet creating positive yawing moment)	rad
l	rolling moment,	ft-lb
L_p	$(dl/dp)/I_x$	rad/s
L_r	$(dl/dr)/I_x$	rad/s
$L_{\delta R}$	$(dl/d\delta R)/I_x$	rad/s ²
$L_{\delta A}$	$(dl/d\delta a)/I_x$	rad/s ²
M	Mach number	
m	airplane mass	slugs
n	yawing moment	ft-lb
N_p	$(dn/dp)/I_z$	rad/s
N_r	$(dn/dr)/I_z$	rad/s
$N_{\delta R}$	$(dn/d\delta R)/I_z$	rad/s ²
$N_{\delta A}$	$(dn/d\delta A)/I_z$	rad/s ²
$n_{O(-)}, n_{O(+)}$	minimum & maximum operational load factor	g
n_z	normal load factor	g
p	velocity axis roll rate	rad/s
q	pitch rate	rad/s

List of Symbols (Cont'd)

Symbol	Definition	Dimension
\hat{q}	non-dimensional pitch rate	
\bar{q}	dynamic pressure	lb/ft ²
r	velocity axis yaw rate	rad/s
S	wing reference area	ft ²
T	thrust	lb
T	aileron servo time constant	s
V	speed	ft/s
W	airplane weight	lb
x, z	horizontal & vertical distance between C.G. and Main Gear Axle (+ for axle behind and below CG)	ft
ξ_T, ζ_T	horizontal & vertical distance between engine nozzle and C.G. (+ for nozzle behind and above C.G.)	ft
α	angle of attack	rad
β	sideslip angle	rad
β	Prandtl-Glauert correction factor	
ΔT	thrust difference	lb
$\delta_e, \delta_f, \delta_a, \delta_r$	elevator, flap, aileron, rudder deflection	rad
ϕ	bank angle	rad, deg
γ	climb angle	rad, deg
μ	rolling friction coefficient	
ω_{nsp}	short period natural frequency	/s
ρ	air density	slug/ft ³
$\theta_{tipback}$	tipback angle (arctan(x/z))	rad
ζ	damping ratio	

Non-dimensional Stability & Control Derivative System:

C_{xy}	Variation of x with non-dimensionalized y
C_{lp}	$\frac{\partial C_{lp}}{\partial \left(\frac{pb}{2V} \right)}$
C_{mq}	$\frac{\partial C_{mq}}{\partial \left(\frac{q\bar{c}}{2V} \right)}$
C_{nr}	$\frac{\partial C_{nr}}{\partial \left(\frac{rb}{2V} \right)}$

Subscripts:

α	alpha, angle of attack
$\dot{\alpha}$	alpha-dot, angle of attack rate
β	beta, sideslip angle
δ_a	delta A, aileron deflection
δ_e	delta E, elevator deflection
δ_f	delta F, flap deflection
δ_r	delta R, rudder deflection
D	drag
L	lift
l	rolling moment, body axis
m	pitching moment (about CG)
n	yawing moment, body axis
p	roll rate
q	pitch rate
r	yaw rate
T	thrust
y	sideforce
C_{L0}, C_{m0}	C_L & C_m at 0° angle of attack

Symbols for the VLM Program

CL0	C_L at 0-deg AOA with x -axis as the fuselage reference line.
CM0	C_m at 0-deg AOA with x -axis as the fuselage reference line.
CL-alpha	$C_{L\alpha}$ (/rad)
Cm/CL	dC_m/dC_L
CL-q	C_{Lq} (/rad)
CM-q	C_{mq} (/rad)
DCL(i,j)	$dC_L/d\delta$ control surface (i = section #, j = 1 for LE flap; j = 2 for TE flap) with symmetric deflection for control surfaces modeled in the longitudinal case
DCM(i,j)	$dC_m/d\delta$ control surface (i = section #, j = 1 for LE flap; j = 2 for TE flap) with symmetric deflection
Cl-p	C_{lp} (/rad)
Cn-p	C_{np} (/rad)
DCroll(i,j)	$dC_l/d\delta$ control surface (i = section #, j = 1 for LE flap; j = 2 for TE flap) with antisymmetric deflection for control surfaces modeled in the longitudinal case
DCyaw(i,j)	$dC_n/d\delta$ control surface (i = section #, j = 1 for LE flap; j = 2 for TE flap) with antisymmetric deflection for control surfaces modeled in the longitudinal case
Cy-beta	$C_{y\beta}$ (/rad)
Cn-beta	$C_{n\beta}$ (/rad)
Cl-beta	$C_{l\beta}$ (/rad)
Cy-r	C_{yr} (/rad)
Cn-r	C_{nr} (/rad)
Cl-r	C_{lr} (/rad)
DCy(i,j)	$dC_y/d\delta$ control surface (i = section #, j = 1 for LE flap; j = 2 for TE flap) for control surfaces modeled in the lateral/directional case
DCn(i,j)	$dC_n/d\delta$ control surface (i = section #, j = 1 for LE flap; j = 2 for TE flap) for control surfaces modeled in the lateral/directional case
DCl(i,j)	$dC_l/d\delta$ control surface (i = section #, j = 1 for LE flap; j = 2 for TE flap) for control surfaces modeled in the lateral/directional case

1. Introduction

Aircraft control authority is determined by the size and placement of control surfaces. With increasing demand for agility, and use of advanced flight control systems coupled with relaxed static stability, consideration of control power has become an important issue in aircraft design. Excessive control authority can translate into increased weight and drag, while inadequate control power can result in a failed design. Putting it succinctly, Dave Wyatt¹ has stated, “Having a Process to properly size the control power is essential to, optimize the configuration.” Thus, the designer’s goal when sizing and placing control surfaces is to provide sufficient, yet not excessive, control power to meet the requirements of prescribed maneuvers, military specifications, MIL-STD-1797,² or certification guidelines, FAR Parts 23 or 25.³

Low airspeed and gusts traditionally place the greatest demands on control authority of an aircraft. In addition, agile maneuvers accomplished by frequent excursions into high angle-of-attack regimes and high roll performance can result in critical control power conditions, including adverse coupling effects. To achieve a successful design, it is important to assess the control power of a proposed design concept against the performance requirements early in the conceptual design stage. The development of control power and flying qualities requirements has not been straightforward. An account of the development of the flying qualities requirements as specified in Ref. 2 has been given by Vincenti.⁴

The primary objective of this work is to establish a methodology that can be used easily by designers with a PC or workstation to rapidly assess the control power of conceptual-stage design concepts against their requirements. The intent is not be encyclopedic, or to replace the stability and control engineers. Rather, the intent is to improve the quality of the initial design concepts used to decide which concepts should be pursued further. This should provide a much better starting point for more detailed work.

First, requirements of maneuvers and flight conditions that are known to place critical demands on control power are identified. The related parameters and the governing equations are presented for each maneuver requirement. The critical flight condition variables such as altitude, airspeed, *cg* location, load factor, *etc.* will vary widely for different requirements. A FORTRAN program with spreadsheet input was created to identify the critical combinations of these variables for each requirement evaluation for a particular design concept.

To evaluate the design for control power, stability and control derivatives must be estimated from the geometry of the design configuration. Traditionally, early in design studies, when many concepts are being considered, designers use their experience and historical data in the form tail volume coefficients, *etc.*, to include control considerations in the concept. If further analysis is required, a quick US Air Force Stability and Control DATCOM⁵ type calculation is made. However, this approach is limited to more conventional configurations and can be very time consuming for this stage of the design process. Once the specialists get involved, more detailed CFD methodology is used. However, those methods cannot yet respond to the “dozen a day” type configuration evaluations desired in the initial conceptual design stages.

Therefore, a subsonic vortex-lattice method code was written to expedite the estimation of stability and control derivatives for the subsonic (up to around Mach 0.6-0.9) and low angle-of-attack flight regimes. Once the aerodynamic characteristics are estimated, they can be used in the appropriate equations to determine if the design has sufficient control power using a series of simple spreadsheets.

A similar systematic approach can be found prescribed as a series of design steps in Roskam.⁶ A good early discussion of stability and control issues appropriate for designers was given by Woodcock and Drake.⁷ A more advanced study including control system

design was done by Thomas.⁸ More recently, control power requirements have been surveyed by Simon, Blake and Multhopp⁹ in a study of the feasibility of a vertical tailless fighter concept.

Note that the present control authority evaluation process does not address high angle-of-attack stability and control requirements for two reasons. First, the requirements are only recently emerging, and second, it is difficult to estimate the high- α aerodynamic characteristics accurately. Designers are cautioned that high angle of attack requirements may dictate the control concept for some designs. The current status of research to establish control power requirements is described in Ref. 10 and 11.

As currently developed, the methods do not include aeroelastic effects, gust effects, or, in most cases, power effects on trim. These effects should be included after experience is gained with the current methodology. However, codes have been written to implement the three surface and two surface with thrust vectoring methodology developed at NASA Langley.¹² Further insight can be gained by examining the compilation of references included in Appendix B.

The methods are currently being used by students studying airplane design. However, designers can also use them. To apply the methodology, the following information regarding the candidate concept is needed:

1. Layout of the major components and control surfaces
2. Mass properties: *cg* travel, weight and inertia variations (can be estimated using Ref. 13 and 14).
3. Extreme performance objectives: Maximum Mach vs. altitude; Maximum load factor and maximum and minimum thrust limits

The FORTRAN programs used in this study were written in FORTRAN 77 and run on most PC and workstation level computer systems. Lotus 1-2-3 was used to create the worksheet on which the control authority is tested against the requirements.

2. Specifications: Critical Flight Conditions and Maneuvers:

This chapter discusses requirements of maneuvers and flight conditions that are known to place critical demands on control power to achieve desirable flight characteristics. The related parameters and the governing equations are presented for each maneuver requirement. Specifications set by MIL-STD-1797 (Ref. 2) and MIL-F-8785C (Ref. 15) are the basis of the requirements. MIL-STD 1797 replaced MIL-F-8785 and allows the customer to tailor the requirements, providing guidance primarily based on lessons learned and MIL-F-8785. Thus MIL-F-8785 is still useful in providing specific values for requirements. The scope of this study does not, except for a few exceptions, include unsteady characteristics such as the rate limits of the control servos, the effects of aeroelasticity, and thrust effects. The maneuvers are considered in the following order.

- 2.1 *Equilibrium/Performance Considerations*
 - 2.1.1 Normal Trimmed Flight
 - 2.1.1.2 Classical 1G trim
 - 2.1.1.3 Elementary Control Allocation Examples
 - Three Surface Configurations
 - Thrust Vectoring
 - 2.1.1.4 Longitudinal Maneuvering Flight
 - 2.1.3 Steady Sideslip
 - 2.1.4 Engine-Out Trim
- 2.2 *Dynamic Considerations*
 - 2.2.1 Takeoff and Landing Rotation
 - 2.2.2 Time-to-Bank
 - 2.2.3 Inertia Coupling: Pitch Due to Velocity Axis Roll
 - 2.2.4 Inertia Coupling: Yaw Due to Loaded Roll
 - 2.2.5 Coordinated Velocity Axis Roll and Roll Acceleration
 - 2.2.6 Short Period & CAP Requirements
 - 2.2.7 High Angle-of-Attack/Departure
- 2.3 *Other Considerations Not Currently Included in Spreadsheet*
 - 2.3.1 Gust
 - 2.3.2 Non-linear Aerodynamics
 - 2.3.3 Aeroelasticity
 - 2.3.4 Special Requirements

Control power requirements can also be categorized in a manner proposed by Wyatt.¹ He suggests that the requirements should be divided into *i*) non-performance related flying qualities (primarily dependent on control law design (*i.e.*, short period frequency and damping, stick force per *g*, spiral mode, PIO tendencies, *etc.*), *ii*) performance related flying qualities (primarily dependent on airframe capabilities (*i.e.*, roll performance, nose wheel liftoff, minimum control speed, departure resistance, *etc.*), and *iii*) degraded-state flying qualities (performance related flying qualities for degraded systems can impact control system layout, probability-of-occurrence requirements can drive system redundancy and reliability). In addition, Wyatt suggests that control requirements can be categorized as either deterministic or stochastic. Deterministic demands on control power are the focus of this report, although stochastic requirements are equally important. Examples of deterministic demands are trim requirements, maneuvers in clean air, *etc.* They are relatively easy to quantify and repeatable. Examples of stochastic demands on control power are requirements for turbulence and aerodynamic uncertainties. They are uncertain and non-repeatable. Early in the conceptual design phase the stochastic demands should be included by allowing for a margin of control power beyond that required for the deterministic demands. The estimation of the size of the margin requires further research.

2.1 Equilibrium/Performance Considerations

Here we consider the control required to fly the airplane under a variety of situations which occur in steady flight. This includes the purely longitudinal cases for trimmed flight both at cruise and maneuver conditions. A special situation considered in detail only recently occurs when more than one control is available to provide a desired force or moment to control the airplane. We also consider cases involving lateral directional characteristics. This occurs when trimming for a steady sideslip or in an engine out condition.

2.1.1 Normal Trimmed Flight

Here we consider cases where only the longitudinal aerodynamics are involved. The aerodynamic characteristics are assumed to be linear.

2.1.1.2 Classical 1-g Trim

The pitch controller must be capable of attaining steady 1-g level flight at all service altitudes between stall and maximum speed. Experience shows that this scenario may become important only at the limits of the flight envelope. To maintain level flight the plane's forces and moments must be balanced. In the classical case, only the elevator is available to trim the aircraft. Further, assuming the neutral point is invariant with respect to angle of attack change, a simple analysis leads to the required result. Following Etkin¹⁶ (Eq. 6.4,2 on page 213) we write the lift and moment balance equations,

$$C_{Ltrim} = C_{L0} + C_{L\alpha} \alpha_{trim} + C_{L\delta_e} \delta_{e_{trim}} \quad (1)$$

$$C_m = 0 = C_{m0} + C_{m\alpha} \alpha_{trim} + C_{m\delta_e} \delta_{e_{trim}}. \quad (2)$$

and solve (1) for α_{trim} ,

$$\alpha_{trim} = \frac{C_{Ltrim} - C_{L0} - C_{L\delta_e} \delta_{e_{trim}}}{C_{L\alpha}}, \quad (3)$$

separate out the elevator term in (2),

$$C_{m\delta_e} \delta_{e_{trim}} = -C_{m0} - C_{m\alpha} \alpha_{trim}, \quad (4)$$

and substitute in for α_{trim} from (3):

$$C_{m\delta_e} \delta_{e_{trim}} = -C_{m0} - \frac{C_{m\alpha}}{C_{L\alpha}} \left(C_{Ltrim} - C_{L0} - C_{L\delta_e} \delta_{e_{trim}} \right). \quad (5)$$

Next we recognize that

$$\frac{C_{m\alpha}}{C_{L\alpha}} = \frac{\partial C_m}{\partial C_L}. \quad (6)$$

Substituting this into (5):

$$C_{m\delta_e} \delta_{e_{trim}} = -C_{m_0} - \frac{\partial C_m}{\partial C_L} (C_{L_{trim}} - C_{L_0} - C_{L\delta_e} \delta_{e_{trim}}) \quad (7)$$

and collecting the coefficients of $\delta_{e_{trim}}$ we obtain:

$$\left(C_{m\delta_e} - \frac{\partial C_m}{\partial C_L} C_{L\delta_e} \right) \delta_{e_{trim}} = -C_{m_0} - \frac{\partial C_m}{\partial C_L} (C_{L_{trim}} - C_{L_0}). \quad (8)$$

Finally, solve for $\delta_{e_{trim}}$:

$$\delta_{e_{trim}} = \frac{C_{m_0} + \frac{\partial C_m}{\partial C_L} (C_{L_{trim}} - C_{L_0})}{-C_{m\delta_e} + \frac{\partial C_m}{\partial C_L} C_{L\delta_e}}. \quad (9)$$

Recognize that for 1-g flight,

$$C_{L_{trim}} = \frac{W}{\bar{q}S}, \quad (10)$$

and the desired result is,

$$\delta_{e_{trim}} = \frac{C_{m_0} + \frac{\partial C_m}{\partial C_L} \left(\frac{W}{\bar{q}S} - C_{L_0} \right)}{-C_{m\delta_e} + \frac{\partial C_m}{\partial C_L} C_{L\delta_e}}. \quad (11)$$

The required α is found by returning to (2), and solving for α_{trim} ,

$$\alpha_{trim} = \frac{-\left(C_{m_0} + C_{m\delta_e} \delta_{e_{trim}} \right)}{C_{m\alpha}} \quad (12)$$

or

$$\alpha_{trim} = \frac{-\left(C_{m_0} + C_{m\delta_e} \delta_{e_{trim}} \right)}{C_{L\alpha} \frac{\partial C_m}{\partial C_L}}. \quad (13)$$

Note that a special case arises when the airplane is neutrally stable, and the denominator of (13) is zero. Eqn.(11) can still be used to find the deflection required. The trim deflection is

now independent of the lift, and equal to zero if C_{m0} is zero. Since (12) and (13) are not valid for this case, use (1) with $C_{m\alpha} = 0$. The trim angle of attack is then

$$\alpha_{trim} = \frac{C_{Ltrim} - C_{L0} + C_{L\delta_e} \left(\frac{C_{m0}}{C_{m\delta_{e_{trim}}}} \right)}{C_{L\alpha}}. \quad (14)$$

The resulting elevator deflection angle should not exceed its range of effectiveness. This generally means the deflection should be less than about 25° . These equations can also be used to determine the 1-g trim schedule. When there are two or more controls available to produce the moment, a decision has to be made about how to choose the means of generating the moment. Currently, this is research area generally known as control allocation. It is discussed in more detail in the next section.

In this discussion, trim is considered without direct connection to the design. The specifics of the design enter through the stability derivatives. In particular, the static margin, defined as

$$sm = -\frac{\partial C_m}{\partial C_L}, \quad (15)$$

is important, as seen in (11). Normally designers try to create a design with only a small trim drag penalty. In general, the surface with the largest span should carry most of the load. For airplanes without stability augmentation systems, the location of the center of gravity is usually limited by stability considerations and is placed ahead of the location for minimum trimmed drag. One of the fundamental reasons for designing statically unstable airframes and using active controls to provide stability is to reduce trim drag.¹⁷ Configurations where this is an especially big concern are airplanes that fly both supersonically and subsonically, so that the aerodynamic shift with Mach number must be considered, and variable sweep wings, where the aerodynamic center changes location as

the wings sweep. Generally, the trim drag analysis is carried out independently of the control power analysis. Methods to size tails efficiently have been presented by Kroo¹⁸ and Swanson.¹⁹

Many methods that find the trimmed drag as a function of the center of gravity location, and hence sm , are available. In particular, a code by John Lamar²⁰ works well for two surfaces, and has been modified to include effects of profile drag variation with local lift coefficient by Mason.²¹

2.1.1.3 Elementary Control Allocation Considerations

When multiple surfaces are available to provide moments, the best choice of control combinations is usually not clear. This problem is currently receiving considerable attention, and is known as the control allocation problem. Examples of recent studies in this area include the work of Durham^{22,23} and Lallman.²⁴ For the cases considered here, the selection is typically based on finding the control coordination producing the minimum trimmed drag.

For the case of three lifting surfaces, or two lifting surfaces and thrust vectoring, the analysis for the minimum trimmed drag at 1- g has been examined by several researchers. The issue of trim drag did not arise in the choice of the deflection in the previous analysis. There was no freedom to consider it directly. The trim drag is related to the distance between the center of gravity and the aerodynamic center. In the two-surface case, it's connection to the design has to be studied indirectly. However, with three surfaces, a degree of freedom arises to include other considerations. Trim drag minimization has typically been chosen as the condition to use in selecting which control surfaces to use to obtain trim. The correct analysis has been given by Goodrich, Sliwa and Lallman.¹² The original NASA TP should be consulted for details. In general, the addition of a third surface allows for a much wider cg range without incurring a severe trim drag penalty.

Two computer programs were written based on the analysis in Ref. 12 to determine the optimal longitudinal trim solution for aircraft with 3 lifting-surface or 2 lifting-surfaces and thrust vectoring. The operation of these programs is described in Sections 5.4 and 5.5. Considerably more information has to be provided in the three surface problem to obtain results compared to the two surface code of Ref. 20. The method of Ref. 20 could be extended to include more surfaces, but this has not been done yet.

2.1.1.4 Longitudinal Maneuvering Flight

MIL-STD-1797 requires that within the operational flight envelope the configuration should be able to develop, by use of pitch control alone, load factors between $n_{O}(+)$ and $n_{O}(-)$, the maximum and minimum operational load factors. Using linear theory analysis, the pitch controller deflection required for the maneuvers must not exceed its range of effectiveness. Assuming the airplane is performing a pull-up from a trimmed 1-g level flight an analysis (derived based on the discussion in Section 6.10 of Etkin,¹⁶ below Eq. 6.10,5 on page 240) can be made to determine the change in α and the *additional* elevator deflection angle above the trim value required to achieve the desired load factor. Here, the idea is find the control deflection increment from the 1-g flight condition required to obtain the desired load factor. The analysis differs from the one given in Section 2.1.1.2 by the inclusion of the pitch rate terms in the equations.

To start, we relate the number of g 's specified for the pull-up to the change in lift and required pitching rate. For an n -g pull-up the required lift is

$$L - W = nW - W = (n - 1)W \quad (16)$$

and the additional lift above that required for 1-g level flight is

$$\Delta L = (n - 1)W, \quad (17)$$

which in coefficient form this becomes:

$$\Delta C_L = \frac{\Delta L}{\bar{q}S} = \frac{(n-1)W}{\bar{q}S}. \quad (18)$$

The associated pitch rate can be found to be

$$q = \frac{(n-1)g}{V}, \quad (19)$$

which is normally non-dimensionalized as

$$\hat{q} = \frac{q\bar{c}}{2V} \quad (20)$$

so that the non-dimensional pitch rate is:

$$\hat{q} = \frac{(n-1)\bar{c}g}{2V^2}. \quad (21)$$

Thus, for a specified g level pull-up, we know the required ΔC_L and \hat{q} . We then use these values in the relations for lift and moment:

$$\Delta C_L = C_{L\alpha} \Delta\alpha + C_{Lq} \hat{q} + C_{L\delta_e} \Delta\delta_e \quad (22)$$

$$\Delta C_m = C_{m\alpha} \Delta\alpha + C_{mq} \hat{q} + C_{m\delta_e} \Delta\delta_e \quad (23)$$

where,

$$C_{Lq} = \frac{\partial C_L}{\partial \hat{q}}, \quad C_{mq} = \frac{\partial C_m}{\partial \hat{q}}. \quad (24)$$

And for trimmed flight,

$$\Delta C_m = 0 \quad (25)$$

We then use Eqs. (18), and (21) in Eqs. (22) and (23), observing (25) to obtain two equations for the two unknowns, $\Delta\alpha$ and $\Delta\delta_e$, required to obtain the required load factor.

The result is:

$$C_{L\alpha} \Delta\alpha + C_{L\delta_e} \Delta\delta_e = (n_z - 1) \left[\frac{W}{\bar{q}S} - C_{Lq} \frac{g\bar{c}}{2V^2} \right] \quad (26)$$

$$C_{m\alpha} \Delta\alpha + C_{m\delta_e} \Delta\delta_e = -(n_z - 1) C_{mq} \frac{g\bar{c}}{2V^2} \quad (27)$$

If the load factor is one, the right hand side is zero, and hence the increments are zero. If we ignore the q terms (frequently done by designers in making performance estimates), the result reduces to the 1- g trim solution applied at higher lift coefficient. It is informative to examine the impact of including the pitch rate terms in the analysis. Using the spreadsheet later to experiment, it will become clear that for typical configurations the effect of including the pitch rate terms on the required elevator deflection is very small.

The system of equations, (26) and (27), can be solved to obtain a result in a similar fashion to the analysis by Etkin:

$$\begin{aligned} \left\{ \frac{\Delta\alpha}{n-1} \right\} &= \frac{1}{\Delta} \left[\left(\frac{W}{qS} - C_{Lq} \frac{g\bar{c}}{2V^2} \right) C_{m\delta} + C_{mq} \frac{g\bar{c}}{2V^2} C_{L\delta} \right] \\ \left\{ \frac{\Delta\delta_e}{n-1} \right\} &= \frac{1}{\Delta} \left[\left(-C_{mq} \frac{g\bar{c}}{2V^2} \right) C_{L\alpha} - \left(\frac{W}{qS} - C_{Lq} \frac{g\bar{c}}{2V^2} \right) C_{m\alpha} \right] \end{aligned} \quad (28)$$

where

$$\Delta = C_{L\alpha} C_{m\delta} - C_{L\delta} C_{m\alpha} \quad (29)$$

and $\frac{W}{qS} = C_L @ n = 1$, where $\Delta\alpha = \Delta\delta_e = 0$.

2.1.2 Steady Sideslip

This requirement is for the design to have adequate roll and yaw power to perform steady sideslip maneuvers. This can become significant during cross-wind landing, when the sideslip angle is the greatest because of low airspeed. To maintain a steady sideslip, the net sideforce, rolling and yawing moment must vanish. In the usual analysis it is assumed that the aileron and rudder are used to maintain a specified sideslip angle. Furthermore, it is usual to assume that the aileron does not generate sideforce, leaving the rudder as the only sideforce generator. Once the rudder deflection is found, the bank angle required to obtain zero sideforce is found. The designer must check to see if the required control deflections and bank angle are acceptable. If not, the design needs revision. The steady state sideforce,

roll and yaw equilibrium equations are (rewritten from Eq. 10.4,2 and 10.4,1 of Etkin, Ref. 16, page 422):

$$C_{y\beta}\beta + \frac{W}{\bar{q}S} \cos\gamma \cdot \phi + C_{y\delta_r} \delta_r = 0 \quad (30)$$

$$C_{l\beta} \beta + C_{l\delta_r} \delta_r + C_{l\delta_a} \delta_a = 0 \quad (31)$$

$$C_{n\beta} \beta + C_{n\delta_r} \delta_r + C_{n\delta_a} \delta_a = 0 \quad (32)$$

To solve for the rudder and deflection angles requires the simultaneous solution of the second and third equations, (31) and (32), given the sideslip angle, β . Once that solution is obtained, the first equation, (30), is used to find the bank angle. The solution of (31) and (32) is found to be:

$$\delta_r = \beta \frac{-C_{n\delta_a} C_{l\beta} + C_{l\delta_a} C_{n\beta}}{C_{l\delta_r} C_{n\delta_a} - C_{n\delta_r} C_{l\delta_a}}, \quad (33)$$

$$\delta_a = \beta \frac{C_{n\delta_r} C_{l\beta} - C_{l\delta_r} C_{n\beta}}{C_{l\delta_r} C_{n\delta_a} - C_{n\delta_r} C_{l\delta_a}}. \quad (34)$$

The resulting bank angle, given by Eq. (30), is:

$$\phi = -\frac{C_{y\beta}\beta + C_{y\delta_r}\delta_r}{\frac{W}{\bar{q}S} \cos\gamma}. \quad (35)$$

Generally, it is sufficient to demonstrate that no more than 75% of the roll and yaw control authority be devoted to maintaining steady sideslip. Typically, the bank angle must be less than 5.° Note that this requirement does not include sensitivity to a lateral gust.

2.1.3 Engine-Out Trim

The analysis given above can easily be extended to include asymmetric thrust situations. For multi-engine airplanes, the roll and yaw controllers must also be sufficiently

powerful to cope with asymmetric propulsion failure. Similar to steady sideslip, this requirement becomes most demanding when operating at very low speed. To maintain steady straight flight, the roll and yaw controllers must counter the effect of asymmetric thrust to produce zero sideforce and no rolling and no yawing moments. The following system of equations (derived based on the addition of asymmetric thrust contribution to Eq. 10.4,2 of Etkin, Ref. 6, page 422, which are the sideforce, rolling and yawing moment equations) must be simultaneously satisfied:

$$C_y = 0 = C_{y\beta} \beta + C_{y\delta_r} \delta_r + C_{y\delta_a} \delta_a + C_{y\Delta T} + \frac{W}{\bar{q}S} \cos\gamma \phi \quad (36)$$

$$C_l = 0 = C_{l\beta} \beta + C_{l\delta_r} \delta_r + C_{l\delta_a} \delta_a + C_{l\Delta T} \quad (37)$$

$$C_n = 0 = C_{n\beta} \beta + C_{n\delta_r} \delta_r + C_{n\delta_a} \delta_a + C_{n\Delta T} \quad (38)$$

where:

$$C_{y\Delta T} = \frac{-\Delta T \cos(\delta_{eng_{vert}}) \sin(\delta_{eng_{horiz}})}{\bar{q}S} \quad (39)$$

$$C_{l\Delta T} = \frac{\Delta T \cos(\delta_{eng_{vert}})}{\bar{q}Sb} \left[\sin(\delta_{eng_{horiz}}) \Delta x - \cos(\delta_{eng_{horiz}}) \Delta y \right] \quad (40)$$

$$C_{n\Delta T} = \frac{-\Delta T \cos(\delta_{eng_{horiz}}) \sin(\delta_{eng_{vert}}) \Delta y}{\bar{q}Sb} \quad (41)$$

The bank angle is specified (5° is generally the maximum value) and the sideslip angle and aileron and rudder deflections are found. Because of control power limitations, the achievable bank angle may be limited to a certain range, *i.e.*, wings-level attitude may not be possible. It is recommended that no more than 75% of the yaw and roll control be allocated to compensate for asymmetric loss of thrust.

2.2 Dynamic Considerations

Several key control power issues arise from dynamic maneuvers. The analysis of these maneuvers is given here. Before considering the maneuvers, several important classifications used to gage dynamic maneuvers must first be defined. First, we define a measure of the flying qualities according to the definitions in Table. 1. These are used to define the capability of the aircraft. Control power adequate to achieve Level 2 flying qualities may not be adequate to achieve Level 1 flying qualities.

Table 1. - Flying quality level specification

Level 1	Adequate for mission flight phase		
Level 2		Some increase in pilot workload and/or degradation in mission effectiveness	
Level 3			Pilot workload is excessive or mission effectiveness is inadequate

Another important consideration is the type of aircraft. The control power required for a fighter is not necessarily the same as that required for a transport. To differentiate, aircraft requirements are often defined differently for different types of airplanes. Table 2 provides the definitions used in the specifications for different types of aircraft.

Table 2. Airplane classification

Classification	Aircraft Type	Examples
Class I	Small, light airplanes	Light utility, primary trainer, light observation
Class II	Medium-weight, low-to-medium maneuverability	Heavy utility/search and rescue, light or medium transport/cargo/tanker, recon, tactical bomber
Class III	Large, heavy, low-to-medium maneuverability	heavy transport/cargo/tanker, heavy bomber
Class IV	High maneuverability	fighter/interceptor, attack, tactical recon

Finally, a distinction is made for different tasks. Table 3 defines the different flight categories that occur in the specification of requirements.

Table 3. - Flight phase categories

Flight Phase	Flight requirements	Included mission flight phase
Nonterminal flight phase		
Category A	Rapid maneuvering, precision tracking, or precise flight-path control	Air-to-air combat, ground attack, weapon delivery/launch, aerial recovery, recon, terrain following, in-flight refueling (receiver), etc.
Category B	Gradual maneuvers, without precision tracking, but with accurate flight-path control	Climb, cruise, loiter, descent, aerial delivery, in-flight refueling (tanker), emergency deceleration and descent
Terminal flight phases		
Category C	Gradual maneuvers with accurate flight-path control	Take-off, catapult take-off, wave-off, go-around, approach, and landing

2.2.1 Takeoff & Landing Rotations

According to the section 4.2.7.3 of MIL-STD-1797, at $0.9 V_{min}$ the aircraft must be able to obtain the pitch attitude that will result in takeoff at V_{min} for dry, prepared runways. For conventional nose-wheeled aircraft, this scenario is most critical for maximum takeoff gross weight, or with a stores arrangement or cargo loading resulting in the cg being located at its most forward location. To verify compliance with this requirement, one must first determine the minimum rotation speed. This speed occurs when the aircraft first obtains enough dynamic pressure for its pitch controller to generate a net nose-up moment with the nose wheel clear of the ground (*i.e.*, providing no force contribution). The lift-off velocity is calculated by setting the moment about the center of gravity and the normal force on the nose-gear equal to zero. The following equation for the moment about the center of gravity can be derived from statics using Fig. 1 (based on the discussion in section 2.5.3.1 of Roskam, Ref. 6).

$$\begin{aligned}
 M_{CG} = & -[W - S\bar{q}C_L - T\sin(i_T + \alpha)] \cdot \\
 & \left[\sin(\theta_{tipback} - \alpha) + \mu \cos(\theta_{tipback} - \alpha) \sqrt{x_{cg}^2 + z_{cg}^2} \right] \\
 & - T[z_T \cos i_T + x_T \sin i_T] + \bar{c} S\bar{q} C_m
 \end{aligned} \tag{42}$$

The aerodynamic moment coefficient, C_m , includes the contribution of lift and drag to the aerodynamic moment about the center of gravity. Thus the lift, L , is the total lift from the wing-body and horizontal tail. The thrust incidence angle, i_T , (not shown in Fig. 2.2.1) is measured positive clockwise from the horizontal. The total moment about the center of gravity and the nose-gear normal force are zero at the start of rotation (the nose-gear normal force is already assumed to be zero in Eq. 42). By setting M_{CG} equal to zero the equation can now be solved for the velocity, V_{LO} :

$$V_{LO} = \sqrt{\frac{\left(\frac{W}{S} - \frac{T}{S} \sin i_T\right)(x_{cg} + \mu z_{cg}) + \frac{T}{S}(z_T \cos i_T + x_T \sin i_T)}{\frac{1}{2}\rho[\bar{c} C_m + C_L(x_{cg} + \mu z_{cg})]}}. \quad (43)$$

C_L and C_m are the total aerodynamic lift and pitching moment coefficients in ground effect with flaps set in takeoff position and pitch controllers fully deflected for nose-up moment. The nose-wheel lift-off speed must be smaller than $0.9 V_{min}$. In addition, one must also check to determine if adequate control power exists to continue rotating to takeoff pitch attitude prior to reaching $0.9 V_{min}$. This can be accomplished by performing a simulation of the rotation process using Eq. 42.

The dynamic pressure, angle-of-attack, and aerodynamic lift and pitching moment are all time-dependent variables. The total lift and pitching moment can be approximated by:

$$C_L = C_{I_{\alpha=0}} \alpha + C_{I_{\delta F}} \Delta \delta F_{Takeoff} + C_{I_{\delta E}} \Delta \delta E_{max} \quad (44)$$

$$C_m = C_{m_{\alpha=0}} \alpha + C_{m_{\delta F}} \Delta \delta F_{Takeoff} + C_{m_{\delta E}} \Delta \delta E_{max}, \quad (45)$$

and the rotation motion can be simulated using:

$$M_{cg} = I_{yy_{cg}} \ddot{\theta}. \quad (46)$$

For landing requirements, after the main gear touches down, the pitch controller must be sufficiently powerful to gently lower the nose wheel at velocity as low as $0.9 V_{min}$ in the landing configuration. The design configuration must demonstrate that it can provide a net nose-up moment in the landing configuration down to the specified speed using Eq. 42. Note this requirement does not address the potentially large nose-down moment as a result of extremely high sink rate at touch down.

2.2.2 Time-to-Bank

The roll response to full roll control input must meet the performance requirements prescribed by Section 4.5.8.1 of MIL-STD-1797. The input is to be abrupt, with time measured from the application of force. The requirements vary depending on the class of airplane. For class I and II aircraft, the requirement is for the aircraft to be able to make a bank angle change in the time prescribed in Table 4.

Table 4. Roll performance requirements for Class I and II aircraft

Time to achieve stated bank angle change, in seconds							
Class	Level	Category A		Category B		Category C	
		60 deg	45 deg	60 deg	45 deg	30 deg	25 deg
I	1	1.3		1.7		1.3	
	2	1.7		2.5		1.8	
	3	2.6		3.4		2.6	
II-L	1		1.4		1.9	1.8	
	2		1.9		2.8	2.5	
	3		2.8		3.8	3.6	
II-C	1		1.4		1.9		1.0
	2		1.9		2.8		1.5
	3		2.8		3.8		2.0

source: MIL STD 1797

For Class III aircraft the requirements are given in terms of the time to achieve a 30° bank angle. The requirement varies with airspeed, in terms of low (L), medium (M), and high (H) speed. Table 5 provides the definitions. The corresponding requirements are given in Table 6.

Table 5. Class III aircraft speed definitions for roll performance requirements.

Speed Range Symbol	Equivalent Airspeed Range
L	$V_{min} \leq V \leq 1.8 V_{min}$
M	$1.8 V_{min} \leq V \leq 0.7V_{max}$
H	$0.7 V_{max} \leq V \leq V_{max}$

Table 6. Roll performance requirements for Class III Aircraft

Time to achieve 30° bank angle, in seconds				
	Speed Range	Category A	Category B	Category C
Level 1	L	1.8	2.3	2.5
	M	1.5	2.0	2.5
	H	2.0	2.3	2.5
Level 2	L	2.4	3.9	4.0
	M	2.0	3.3	4.0
	H	2.5	3.9	4.0
Level 3	All	3.0	5.0	6.0
source: MIL STD 1797				

For class IV aircraft, the pitch control is to be held fixed while the yaw control pedals shall remain free throughout the maneuver. The speed ranges used to define Class IV level-1 flying quality requirements are given in Table 7. The roll performance requirements for Class IV aircraft are listed in Tables 8a to 8d.

Table 7. Class IV aircraft speed definitions for roll performance requirements.

Speed Range Symbol	Equivalent Airspeed Range
VL	$V_{min} \leq V < V_{min} + 20 kt$
L	$V_{min} + 20 kt \leq V < 1.4V_{min}$
M	$1.4 V_{min} \leq V < 0.7 V_{max}$
H	$0.7 V_{max} \leq V \leq V_{max}$

Table 8a. General Roll Performance for Class IV Airplanes.

Time to Achieve Bank Angle Change (sec)						
		Category A			Category B	Category C
		30 deg	50 deg	90	90	90
Level 1	VL	1.1			2.0	1.1
	L	1.1			1.7	1.1
	M			1.3	1.7	1.1
	H		1.1		1.7	1.1
Level 2	VL	1.6			2.8	1.3
	L	1.5			2.5	1.3
	M			1.7	2.5	1.3
	H		1.3		2.5	1.3
Level 3	VL	2.6			3.7	2.0
	L	2.0			3.4	2.0
	M			2.6	3.4	2.0
	H		2.6		3.4	2.0

source: MIL STD 1797

Table 8b. Air-to-Air Combat Roll Performance Requirements (360° rolls)
(Initial Load Factor = 1 G)

Time to Achieve Bank Angle Change (sec)					
		30 deg	90 deg	180 deg	360 deg
		Level 1	VL	1.0	
L			1.4	2.3	4.1
M			1.0	1.6	2.8
H			1.4	2.3	4.1
Level 2	VL	1.6			
	L	1.3			
	M		1.3	2.0	3.4
	H		1.7	2.6	4.4
Level 3	VL	2.5			
	L	2.0			
	M		1.7	3.0	
	H		2.1		

source: MIL STD 1797

Table 8c. Air-to-Air Combat Roll Performance Requirements

		Time to Achieve Bank Angle Change (sec)			
		30 deg	50 deg	90 deg	180 deg
Level 1	VL	1.0			
	L		1.1		
	M			1.1	2.2
	H		1.0		
Level 2	VL	1.6			
	L	1.3			
	M			1.4	2.8
	H		1.4		
Level 3	VL	2.5			
	L	2.0			
	M			1.7	3.4
	H		1.7		

source: MIL STD 1797

Table 8d. Ground Attack Roll Performance Requirements

		Time to Achieve Bank Angle Change (sec)			
		30 deg	50 deg	90 deg	180 deg
Level 1	VL	1.5			
	L		1.7		
	M			1.7	3.0
	H		1.5		
Level 2	VL	2.8			
	L	2.2			
	M			2.4	4.2
	H		2.4		
Level 3	VL	4.4			
	L	3.8			
	M			3.4	6.0
	H		3.4		

source: MIL STD 1797

Because requirements of Table 8b, 8c and 8d apply to air-to-air and air-to-ground combat flight phases with more stringent guidelines, they take precedence over the requirements of Table 8a. Roll maneuvers specified in Tables 8b are to be initiated at 1-g while those specified in Tables 8a, 8c & 8d are to be initiated at load factors between $0.8n_0(-)$ and $0.8n_0(+)$. The roll performance requirements for Class IV airplane in the ground attack flight phase with large complements of external stores may be relaxed from Table 8b (but not beyond those stated in Table 8d) with the approval of the procuring activity.

The ability of the airplane to meet the time to bank requirement is usually assessed by considering one-degree of freedom motion. The following ordinary differential equations represent the rolling motion:

$$\dot{\phi} = p \quad (47)$$

$$\dot{p} = \frac{\bar{q}Sb}{I_x} \left[\left(C_{l_{\delta_a}} \delta_a \right) + \left(C_{l_p} p \right) \left(\frac{b}{2V} \right) \right] \quad (48)$$

where ϕ is the bank angle, p is the roll rate, $C_{l_{\delta_a}} = \frac{\partial C_l}{\partial \delta_a}$ and $C_{l_p} = \frac{\partial C_l}{\partial \left(\frac{pb}{2V} \right)}$.

Here we see that the roll performance is dominated by the ability to generate rolling moment (here taken to mean the aileron), the roll damping, and the moment of inertia. Roll performance is often degraded by aeroelastic effects. The deflection of the aileron may induce a wing twist which negates the desired effects. Recently research has been conducted to exploit this property through the use of active control to reduce wing weight.

If the aileron deflection is a constant, an analytic expression for the roll rate can be obtained. The result is given by

$$p = -\frac{2V}{b} \frac{C_{l_{\delta_a}} \delta_a}{C_{l_p}} \left(1 - e^{-L_p t} \right) \quad (49)$$

where

$$L_p = \frac{\bar{q} S b^2}{2 V I_x} C_{l_p} \quad (50)$$

and $-L_p^{-1}$ is the roll time constant. A roll mode time constant of about 1 second is considered desirable. The minus sign should not be confusing. C_{l_p} is negative, and hence the final result is actually a positive roll rate. Note from Eq. 49 that the steady state roll rate is:

$$p_{ss} = -\frac{1}{b} \frac{C_{l_{\delta_a}} \delta_a}{C_{l_p}} \quad (51)$$

or

$$\frac{p_{ss} b}{2V} = -\frac{C_{l_{\delta_a}} \delta_a}{C_{l_p}}. \quad (52)$$

Values of this parameter used to be specified to define roll performance. Finally, the value of the bank angle can be found by integrating the expression for the roll rate. Assuming that the initial bank angle is zero, we obtain

$$\phi(t) = -\frac{2V}{b} \frac{C_{l_{\delta_a}} \delta_a}{C_{l_p}} \left[t + \frac{1}{L_p} (1 - e^{L_p t}) \right]. \quad (53)$$

If the aileron deflection is specified as a function of time, simulating finite rate deflections, Eq. 47 and 48 define a system of ordinary differential equations which can be numerically integrated to show compliance with requirements. Note that this approximation does not consider the rudder deflection needed to maintain coordinated rolling motion (to be discussed in Section 2.2.4). In this analysis, the time scale might be small enough to warrant including the roll controller rate limit in the estimation. Assuming the maximum aileron servo rate is a constant, the actual aileron surface deflection prior to reaching the maximum position is:

$$\delta_a = \left(\frac{d\delta_a}{dt} \right)_{\max} (t - t_0) \quad \text{for } t_0 < t < t' \quad (54)$$

followed by a constant,

$$\delta_a = \delta_{a_{\max}} \quad \text{for } t > t' \quad (55)$$

where t' is given by

$$t' = \frac{\delta_a}{\left(\frac{d\delta_a}{dt} \right)_{\max}}. \quad (56)$$

The value of t' is the time between roll input to the time the ailerons reach their maximum deflection. Typically, this is only a significant factor during the initial instant of the roll input. Since Eq. (48) is a single linear first order equation, an analytic solution is available for the linear increase in aileron deflection given by Eq. (54) which occurs between t_0 and t' . This is:

$$p(t) = \frac{-L_{\delta_a} \left(\frac{d\delta_a}{dt} \right)_{\max}}{L_p^2} \left[(1 + L_p t) - e^{L_p t} \right] \quad (57)$$

with the corresponding bank angle solution:

$$\phi = \frac{-L_{\delta_a} \left(\frac{d\delta_a}{dt} \right)_{\max}}{L_p^2} \left[\frac{1}{L_p} (1 - e^{L_p t}) + t + \frac{L_p}{2} t^2 \right] \quad (58)$$

where

$$L_{\delta_a} = \frac{\bar{q} S b}{I_x} C_{l_{\delta_a}} \quad (59)$$

is an alternate stability parameter form, which has been introduced to simplify the notation. The solution for $t > t'$ can then be found using the constant aileron solution, Eqs. (49) and (53), altered to use the values of p and ϕ at t' from Eq.(57) and (58) as initial conditions. Thus, for $t > t'$, use:

$$p(t) = p(t')e^{L_p(t-t')} - \frac{L\delta_a\delta_a}{L_p}\left(1 - e^{L_p(t-t')}\right) \quad (60)$$

and

$$\phi(t) = \phi(t') + \left(p(t') + \frac{L\delta_a\delta_a}{L_p} \right) \left(\frac{e^{L_p t} - e^{L_p t'}}{L_p} \right) - \frac{L\delta_a\delta_a}{L_p}(t - t'). \quad (61)$$

Eqns. (60) and (61) reduce to (49) and (53) if there is a step change in the aileron.

Another representation of the aileron deflection could also be used,

$$\delta_a = \left(1 - e^{-\frac{t}{T}} \right) \delta_{a_{command}}, \quad (62)$$

where T is the 1st order time constant associated with the lag between the actual aileron deflection and the step aileron deflection command. The spreadsheet contains a numerical integration, of Eq. (48) using the aileron schedule given by Eq. (54) and (55).

2.2.3 Inertial Coupling: Pitch due to Velocity Axis Roll

The aircraft concept must also possess sufficient nose-down pitch authority to compensate for the nose-up moment as a result of inertial cross-coupling during high angle-of-attack stability axis roll maneuvers (Chody, Hodgkinson, and Skow²⁵). Assuming the flight path is confined to a straight line without sideslip, at constant α and also without variations in speed, the pitching moment due to velocity axis roll can be estimated from the pitching moment equation of motion in the body axis. Our analysis follows that of Nguyen, *et al.*, in Ref. 26. Start with the basic body axis equation given in Etkin, (Eq. 5.6,10, page 145):

$$M = I_y \dot{q} - I_{zx}(r^2 - p^2) - (I_z - I_x)rp. \quad (63)$$

Then use the relation between angular rates in the body and wind axis for the case of a pure roll about the velocity axis with zero sideslip, β , and $q_w = r_w = 0$, so that Eq. 4.5,5 of Etkin (page 117) becomes:

$$\begin{bmatrix} p_b \\ q_b \\ r_b \end{bmatrix} = \begin{bmatrix} \cos\alpha & 0 & -\sin\alpha \\ 0 & 1 & 0 \\ \sin\alpha & 0 & \cos\alpha \end{bmatrix} \begin{bmatrix} p_{stab} \\ 0 \\ 0 \end{bmatrix}. \quad (64)$$

Here we introduced the subscript b to make the body axis component clear. We will now drop the subscript. The resulting angular rates used in Eq. (63) are thus:

$$p = p_{stab} \cos\alpha \quad (65)$$

$$r = p_{stab} \sin\alpha \quad (66)$$

and $q = 0.$ (67)

Substituting into Eq. (63) we obtain

$$M_{IC} = -I_{zx}(\sin^2\alpha - \cos^2\alpha)p_{stab}^2 - (I_z - I_x)\sin\alpha\cos\alpha p_{stab}^2 \quad (68)$$

where the moment is due to inertial coupling, and is denoted by the subscript IC . Using trigonometric identities, we can rewrite the equation as:

$$M_{IC} = -\left[I_{zx} \cos(2\alpha) - \frac{1}{2}(I_z - I_x)\sin(2\alpha) \right] p_{stab}^2 \quad (69)$$

which illustrates dramatically the effect of roll rate on the required pitching moment. Recall that here p_{stab} is the velocity-axis roll rate, and α , I_x and I_z are measured with respect to the body axis system. Currently, the problem of developing aerodynamic forces to handle this moment is considered critical at high angle of attack. If we assume that the body and principal axis are nearly coincident, such that I_{zx} is small,* we obtain the usual approximation for the moment due to inertial coupling:

$$M_{IC} = \frac{1}{2}(I_z - I_x)\sin(2\alpha)p_{stab}^2 \quad (70)$$

* For the F-16 studied by Nguyen, *et. al.*²⁶, , $I_x = 9,496$, $I_z = 63,100$ and $I_{zx} = 982$, all in slug-ft².

This nose-up moment due to coupling reaches its maximum at $\alpha = 45^\circ$. The pitch control deflection required to compensate for the roll coupling can thus be estimated from:

$$\delta_{eIC} = \frac{-M_{IC}}{C_{m\delta_e} \bar{q} S \bar{c}}. \quad (71)$$

All of the pitch controller deflection must not be used to counter the moment due to inertial coupling. Additional control power must be available for normal flight path control. This requirement for M_{IC} does not address the pitch authority needed to maintain attitude with zero roll rate. For unstable aircraft, the situation may be most critical around the pinch point,¹⁰ which is the angle of attack where the margin for nose-down moment is at its minimum (often near $\alpha = 35^\circ - 45^\circ$).

The classical solution for the pitching moment requirement has been extended by Durham.²⁷ He developed an analysis which integrates the equations of motion assuming a perfectly coordinated velocity vector roll. In this case the velocity vector is not straight, but varies rapidly due to the effect of gravity. Approximate but highly accurate analytic expressions for the maximum moment required were also obtained and compared with numerical integrations. The approximate maximum pitching moment solution was found to be:

$$M_{\max} = \frac{1}{2} (I_{x_p} - I_{z_p}) \sin(2\alpha) p_{stab}^2 - \left(\frac{g}{V_{\min}} \right) \left[(I_{x_p} - I_{z_p}) \cos(2\alpha) + I_y \right] p_{stab}. \quad (72)$$

Here, the maximum depends on the aircraft attitude. For a right roll, Eq. (72) applies at $\gamma = 0$, $\mu = -\pi/2$, and at an α of:

$$\tan(2\alpha) = -\frac{V_{\min} p_{\max}}{2g} \quad (73)$$

This equation was found to provide enough accuracy to use in conceptual design studies. Results indicate that the pitching moment given in Eq. (70), which is the first term of Eq. (72) is too small for the perfectly coordinated velocity axis roll by as much as a factor of two! The paper should be consulted for complete details.

2.2.4 Inertia Coupling: Yaw Due to Loaded Roll

The yaw controller must possess adequate authority to overcome the yawing moment as a result of inertia coupling during a rolling pullout maneuver. According to Mercadante,²⁸ (derived from the total yawing moment equation), the adverse yawing moment coefficient in a rolling pullout can be approximated by:

$$C_{n_{couple}} = \frac{(I_x - I_y) \cos \alpha p q}{\bar{q} S b} \quad (74)$$

The pitch rate q is determined by the bank angle of the aircraft and the normal load factor applied to the airframe. The adverse yawing moment is most severe (result of highest pitch rate, q) when the loading occurs while the airplane is inverted (due to the additional contribution from gravity). The pitch rate of the aircraft in this orientation is:

$$q = \frac{(n_z + 1)g}{V}. \quad (75)$$

Combining Eqs. (74) and (75), the rudder deflection needed to counter the adverse yawing moment during a pullout maneuver can be obtained from:

$$C_{n_{\delta_r}} \delta_r = -\frac{(I_x - I_y) \cos \alpha p (n_z + 1)g}{\bar{q} S b V}. \quad (76)$$

2.2.5 Coordinated Stability Axis Roll and Roll Acceleration

To perform coordinated stability-axis rolls, both roll and yaw controllers are used to maintain zero sideslip. At low angles-of-attack there is usually adequate rudder power to obtain the desired motion. However, as the angle-of-attack increases, the demand on rudder authority increases rapidly. Consider the stability-axis roll rate (p) and roll acceleration (\dot{p}), α , and normal load factor as specified requirements. Resolving the forces and moments in the principal body axes system and expanding the aerodynamically generated rolling and yawing moments (Eqs. 5.8,3 a & c of Etkin,¹⁶ page 149) which involve the rolling and yawing moments, can be rewritten as:

$$L_{\delta_r} \delta_r + L_{\delta_a} \delta_a = -(L_p \cos \alpha + L_r \sin \alpha) p + \cos \alpha \dot{p} - \frac{(I_y - I_z)}{I_x} \sin \alpha p q \quad (77)$$

and

$$N_{\delta_r} \delta_r + N_{\delta_a} \delta_a = -(N_p \cos \alpha + N_r \sin \alpha) p + \sin \alpha \dot{p} - \frac{(I_x - I_y)}{I_z} \cos \alpha p q. \quad (78)$$

The rudder and aileron deflections are found by solving Eq. (77) & (78) simultaneously. This problem can be reformulated into the rolling pullout maneuver. Again, the most critical control power demand due to pitch rate arises when the maneuver occurs while the airplane is inverted. Similar to the rolling pullout, the conservative approach is to define pitch rate (q) as:

$$q = (n_z + 1) \frac{g}{V} \quad (79)$$

2.2.6 Short Period and CAP Requirements

Although this requirement is not specifically related to any control surface, horizontal tail volume strongly influences the value of the pitch rate damping coefficient. The requirement is to achieve level-1 flying qualities for the equivalent (with augmentation) short period damping requirements and satisfy the control anticipation parameter (CAP) requirement in Fig. 2 taken from the requirements in Section 4.2.1.2 of MIL STD 1797.² The following short-period approximation equations (based on Eq. 4.80 & 4.81 of Nelson,²⁹ page 131) can be used to estimate non-augmented flight characteristics:

$$\omega_{n_{sp}} = \sqrt{-C_{m_q} C_{L_\alpha} \frac{(\bar{c} S \bar{q})^2}{2V^2 m I_y} - \frac{C_{m_\alpha} \bar{c} S \bar{q}}{I_y}} \quad (80)$$

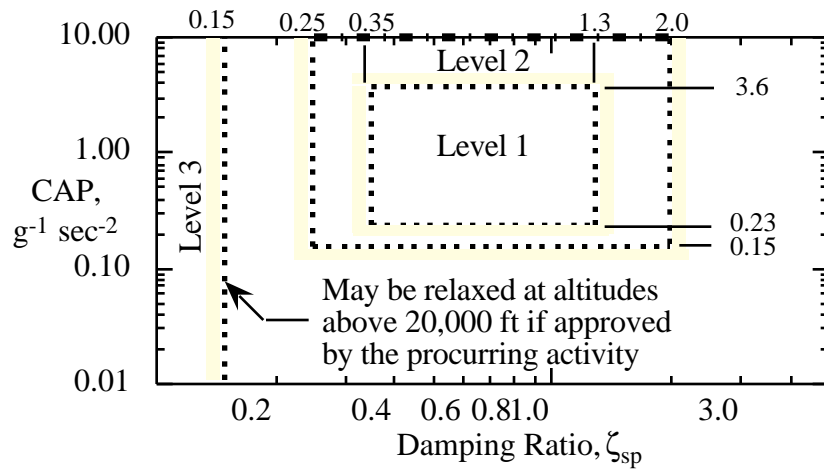
$$\zeta = -\frac{1}{2\omega_{n_{sp}}} \left[\left(C_{m_{\dot{\alpha}}} + C_{m_q} \right) \frac{\bar{c}^2 S \bar{q}}{2V I_y} - C_{L_{\dot{\alpha}}} \frac{\bar{q} S}{mV} \right] \quad (81)$$

Note that Eq. (47) and (48) are intended for non-augmented airplanes. Aircraft with longitudinal stability augmentation (such as unstable airplanes) must account for the dynamics of the control system. To use Fig. 2, the definitions in Section 4.2.1.2 of Ref. 2 are:

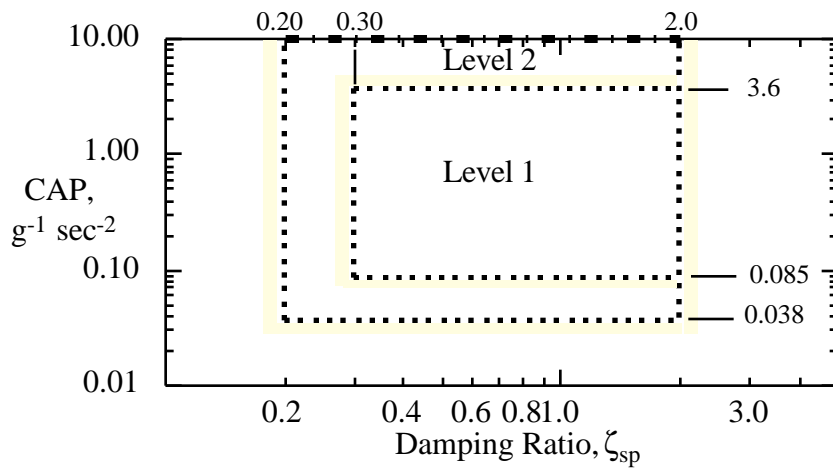
$$n/\alpha \cong \frac{C_{L_\alpha} \bar{q} S}{W} \quad (82)$$

$$CAP = \frac{\omega_{n_{sp}}^2}{n/\alpha} \quad (83)$$

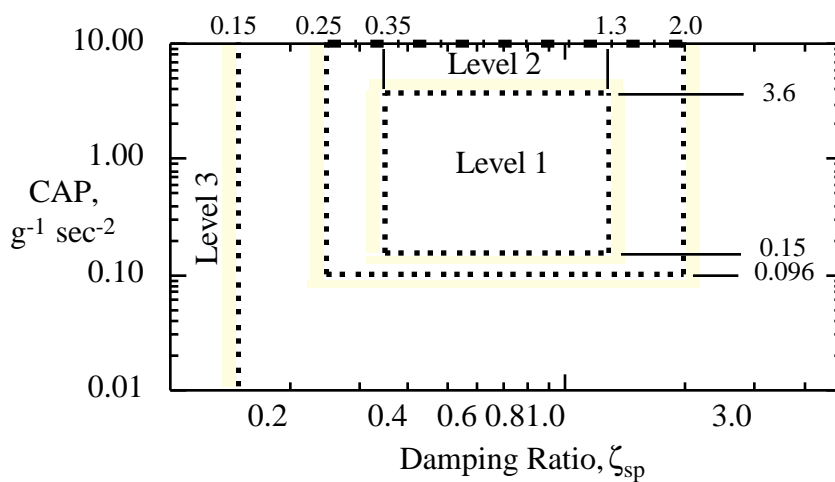
It should be noted that some configurations simply do not fit the standard requirements, and there continue to be debates between experts about the adequacy and the merits of these requirements.



a) Category A flight phases



b) Category B flight phases



c) Category C flight phases

Figure 2. Short period flying qualities requirements

2.2.7 High Angle-of-Attack/Departure

This section identifies some parameters that are found to be useful in determining the susceptibility of the airplane to departure during high angle of attack operation. However, the inability to estimate high angle of attack aerodynamic characteristics makes it difficult to assess the stability and control authority requirements at high angle of attack in the conceptual design stage. Therefore, high-angle of attack stability is not included as part of the control power assessment methodology for conceptual designs.

Many parameters have been proposed as the measure of departure tendency. An overview of the connection between various proposed criteria and the related theoretical foundation has been given recently by Lutze *et al.*³⁰ Although not ideal, two parameters, $C_{n\beta_{DYN}}$ and LCDP are the most commonly used.

While not directly related to control power, the open-loop directional stability can be roughly evaluated from $C_{n\beta_{DYN}}$:

$$C_{n\beta_{DYN}} = C_{n\beta} \cos\alpha - \frac{I_z}{I_x} C_{l\beta} \sin\alpha \quad (84)$$

Note that $C_{n\beta}$ and $C_{l\beta}$ are in principal axis. Aircraft with positive values for this parameter over the angle of attack range (> 0.0040 per deg.) tend to exhibit little yaw departure tendency. In fact, $C_{n\beta_{DYN}}$ is linearly related to the static directional stability in the wind axis.

The second (closed-loop) parameter, which includes controls, is frequently used to measure departure tendency. it is known as the Lateral Control Departure Parameter (LCDP):

$$LCDP = C_{n\beta} - \frac{C_{n\delta A}}{C_{l\delta A}} C_{l\beta} \quad (85)$$

A value of *LCDP* greater than zero generally indicates that the configuration tends to be spin resistant (Ref. 25) and less susceptible to aileron induced departure (Ref. 31). Despite suggestions by Chody et al. (Ref. 25) and Bihrlé & Barnhart (Ref. 32) of the imperfection of using these two parameters as design figures of merits, they continue to be used to assess lateral departure tendency at high angle-of-attack (Ref. 25).

2.3 Other Considerations Not Currently Included in Spreadsheet

2.3.1 Atmospheric Disturbances (Gusts)

Gusts must also be accounted for in determining control power requirements at critical conditions. A degradation of flying qualities in atmospheric disturbances, such as turbulence, wind shear, and gusts, are permitted. The minimum required flying qualities are specified for conditions in normal states and failure states. Both the quantitative level and qualitative minimum requirements are shown in Tables 9 and 10. Requirements for failure state I are to be such that in the operational flight envelope the probability of encountering degraded levels of flying qualities due to failure is less than one per 100 flights. Requirements for failure state II are to be such that the probability of encountering degraded levels of flying qualities due to failure is less than one per 10000 flights and one per 100 flights in the service flight envelope.

Table 9. - Minimum flying qualities for normal states in atmospheric disturbances.

Atmospheric Disturbances	Requirements in Operational Flight Envelope	Requirements in Service Flight Envelope
Light to Calm	Level I; Qualitatively: Satisfactory	Level II; Qualitatively: Acceptable or better
Moderate to Light	Level I; Qualitatively: Acceptable or better	Level II; Qualitatively: Controllable or better
Severe to Moderate	Qualitatively: Controllable or better	Qualitatively: Recoverable or better

Table 10. - Minimum flying qualities for failure states in atmospheric disturbances.

Atmospheric Disturbances	Failure State I	Failure State II
Light to Calm	Level II; Qualitatively: Acceptable or better	Level III; Qualitatively: Acceptable or better
Moderate to Light	Level II; Qualitatively: Acceptable or better	Level III; Qualitatively: Controllable or better
Severe to Moderate	Qualitatively: Controllable or better	Qualitatively: Recoverable or better

Verification of the flying qualities in the presence of atmospheric disturbances may be in the form of analysis, simulation, or flight test. If analysis or simulation is used, a suitable atmospheric disturbance model is used to verify that the flying qualities meet the minimum requirements. Separate models are used for low and high altitude and carrier landings. Quantitative values of turbulence intensity, gust length, gust magnitude and wind shear values based on severity and altitude, for use in the models, are given in a series of tables and graphs found in MIL-STD-1797.

2.3.2 *Non-linear Aerodynamics*

Many of the key problems occur at high angle of attack where the flow is separated, and the use of linear aerodynamics is invalid. In this situation more sophisticated methods are required.

2.3.3 *Aeroelasticity*

At high dynamic pressure conditions, the flexibility of the airplane can have an important effect on the stability and control characteristics. This should also be considered. This is difficult without more details of the structure than are usually available in conceptual design. One method for making the calculation was given by Roskam and Dusto.³³

2.3.4 Special Requirements

Naval aircraft have special considerations associated with carrier landings which may also be important in determining critical control power requirements. One example is the recent study of roll requirements for carrier approach by Citurs, Buckley and Doll.³⁴

3. Discussion of Overall Assessment Methodology

The goal of our control authority assessment methodology is to evaluate a given design concept during the conceptual and early preliminary design stage against the requirements of the potentially critical maneuvers and flight conditions listed in Section 2. Figure 3 outlines the procedure involved to complete the task.

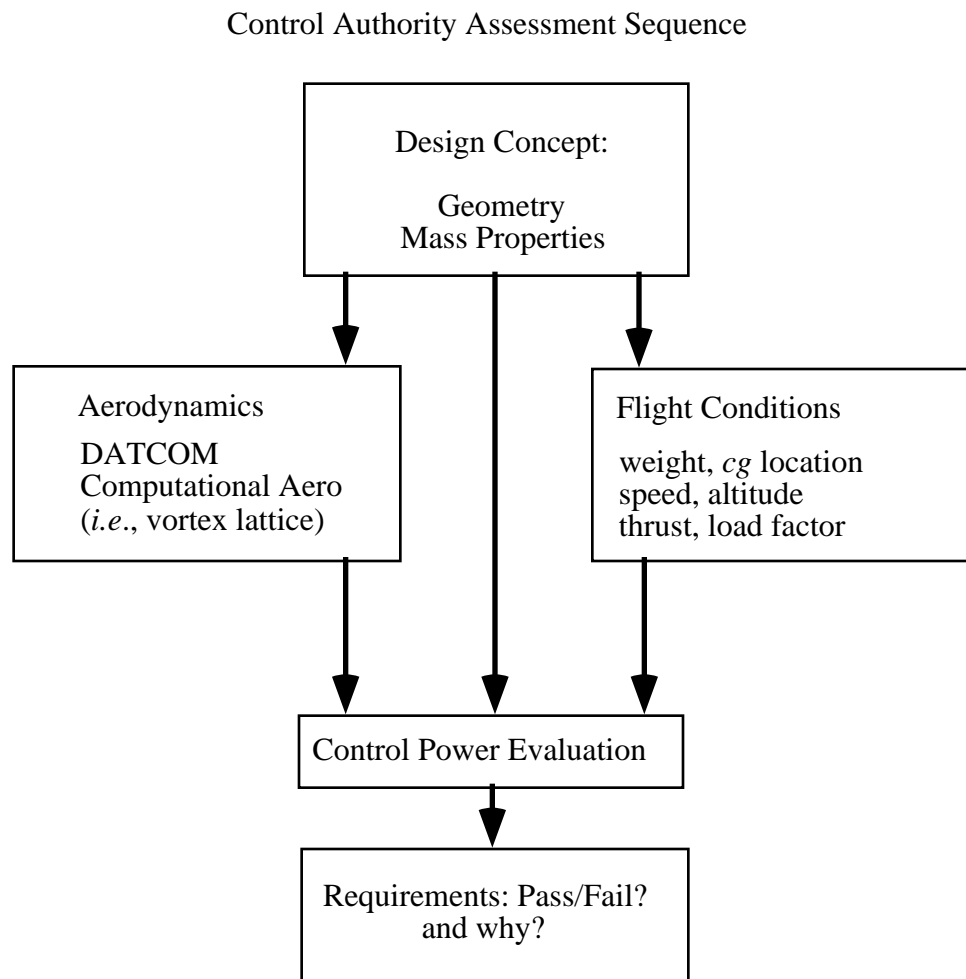


Figure 3. Control authority assessment methodology.

For each requirement discussed in Section 2, there is a set of combinations of flight condition variables such as weight, *cg* location, load factor, altitude and speed, that affect the performance of the airplane. Therefore the methodology must evaluate the configuration concept's control power for the conditions producing the greatest demand. For example, when checking the nose-wheel lift-off capability of a configuration, maximum gross takeoff weight with most forward *cg* location will define the most critical nose-up pitch authority condition. It is important to perform the control authority analysis with these critical flight condition variables so that the most severe cases are tested.

With the airplane geometry and the flight condition variables corresponding to each requirement, one needs to obtain the necessary aerodynamic characteristics in the form of stability and control derivatives. Early in the preliminary design phase, wind tunnel data or results from sophisticated CFD analysis are usually not available. In this study, a subsonic vortex-lattice method is adapted to supplement DATCOM in estimating subsonic, low angle of attack aerodynamic characteristics. The estimated stability and control derivatives along with the corresponding flight conditions are then applied to the airplane dynamics equations examined in Section 2. The results typically are in the form of control surface deflections which are indications of how much of the available control authority is used. The designer must judge whether the required deflections are realistic. In the cases of nose-wheel lift-off and time-to-bank performance requirements, one must check whether the maneuvers can be accomplished according to the specifications. For short period & CAP requirements, the configuration must demonstrate flight characteristics within the defined tolerance. Note that Equations 47 and 48 given in Section 2.2.6 cannot be used for unstable configurations. If the vehicle is unstable, it is assumed that stability augmentation will be used, and the control system designed to satisfy the flight characteristic requirements.

If the design concept fails to meet some of the requirements, the designer must adjust the configuration in terms of sizing, geometry, weight properties, and/or relax the performance requirements. Increasing control authority by geometry changes alone to satisfy certain performance requirements may not always be practical due to the resulting weight and drag penalties. If any changes are made, the new design's control power must be re-evaluated.

3.1 Flight Condition Variables

For a design concept there are variables independent of aerodynamic properties that can change the demands on control authority. These parameters vary considerably as functions of flight phase category and store configuration. The objective of this section is to qualitatively identify the variables of each requirement critical to assessing the control power. The variables to be considered are:

- Weight
- Inertia
- *cg* location
- Engine thrust
- Thrust deflection angle(s)
- Load Factor
- Altitude
- Speed

Note that not all of these variables need to be specified for each requirement evaluation.

For the nose-wheel lift-off requirement, airplane weight should be the maximum gross takeoff weight with the *cg* located at its most forward position. Use of the maximum value of I_y with maximum thrust at sea level should lead to a conservative estimation. Future advanced aircraft may employ thrust vectoring to shorten the ground roll distance during takeoff. Pointing the thrust (jet exhaust) upward (for aft-engine configurations) decreases the nose-wheel lift-off speed by providing additional nose-up moment but leads to increased downward force. However, diverting the exhaust downward adds to the total lift

but requires additional nose-up control authority from another pitch controller. Thrust deflections at both extremes should be examined. Similar combinations of variables should be used for landing, with the airplane weight set to its maximum landing weight.

For 1-g trim requirements, the analysis should be performed at all corners of the operational 1-g V-h diagram, with particular emphasis near the stall boundary. Center of gravity locations at both extremes should be considered.

Variation of load factors, speed, altitude, and weight are most significant in the maneuvering flight requirement analysis. It is conservative to use maximum weight in conjunction with maximum load factor, however, structural limits may not allow such conditions to occur. It is important to explore all boundaries of the V-h diagram for all load factors, with special emphasis in the low speed regime.

For short period & CAP specifications, Mach number and cg location can significantly influence the flying qualities. However, it is impractical and unnecessary to examine all possible combinations. Emphasis should be placed at the nominal design points. One should keep in mind that the actual flying qualities may be significantly different from the prediction here for highly augmented airplanes.

Three of the flight condition variables are important in evaluating pitch control effectiveness against roll-induced pitch-up. Maximum I_z and minimum I_x should be used. While low speed tends to result in saturating the pitch controller, high roll rate usually does not occur near this regime. Therefore speeds between the range of L and H (as defined in Section 2.2.2) should be used for the test.

Achieving a large sideslip angle is usually most critical during landing approach. Evaluation of this requirement should be carried out at minimum landing speed. Lateral thrust vectoring angle (if available) should be varied to reduce the burden on the yaw controller or produce the worst-case scenario.

Antisymmetric thrust becomes most critical during low-speed operations. Minimum speed and maximum asymmetric thrust should be considered in the analysis. If lateral thrust vectoring is available, it should be directed so that the thrust line passes through cg to alleviate the burden on the yaw controller.

For time-to-bank performance evaluation, the speed range defined in Section 2.2.2 should be considered. The lowest value of each of the four speed ranges defined in Section 2.8 should be used in the analysis. In addition, I_x should assume the largest value corresponding to the flight phase under consideration to produce conservative estimates.

In the case of the rolling pullout maneuver and a coordinated roll, the largest adverse yawing moment is produced when the difference between the values of I_x and I_y are the largest. Therefore the minimum I_x and maximum I_y and I_z should be used in the analyses. Because high stability axis roll rate and high load factors are not possible at very low speeds, speed ranges between L and H should be used while applying maximum load factor allowed by the speeds to produce the most critical conditions.

A FORTRAN program, FLTCOND, was written with a spreadsheet, shown in Table 11, as input to help accelerate the process of isolating the most critical combinations of flight condition variables for each requirement. A typical output of FLTCOND is shown in Table 12. The flight condition variables listed, such as cg location, inertia, etc., are to be used in the final control authority assessment check. It serves to provide candidate combinations of flight condition variables that may result in the most critical demand on control power for each requirement. However, it may, for some cases, be too stringent and repetitive. The user must make the necessary adjustment based on the overall design objectives. Input details are contained in Section 5.2

Table 11. Sample Input spreadsheet for program FLTCOND

CONTROL POWER ASSESSMENT PROGRAM

Part 1. Flight Condition Variables

Prepared by Jacob Kay Feb. 1992

Variables	Units	Value
Minimum Gross Weight	(lbs)	25000
Maximum Gross Weight	(lbs)	45000
Minimum I-x	(slug-ft ²)	23168
Maximum I-x	(slug-ft ²)	80000
Minimum I-y	(slug-ft ²)	100000
Maximum I-y	(slug-ft ²)	123936
Minimum I-z	(slug-ft ²)	120000
Maximum I-z	(slug-ft ²)	200000
Most Forward C.G. Location	(ft)	31.5
Most Aft C.G. Location	(ft)	32.5
Max. Thrust with Thrust Vectoring	(lbs)	35000
Max. Thrust w/o Thrust Vectoring	(lbs)	25000
Max. Thrust Deflection Angle--Up	(deg)	20
Max. Thrust Deflection Angle--Down	(deg)	15
Max. Thrust Deflection Angle--Yaw	(deg)	10
Maximum Normal Load Factor	(g's)	9.5
Altitude/Speed Range:		
Number of Entries:		3
Altitude	(ft)	0
Minimum Speed	(knots)	130
Maximum Speed	(knots)	890
Altitude	(ft)	10000
Minimum Speed	(knots)	180
Maximum Speed	(knots)	992
Altitude	(ft)	20000
Minimum Speed	(knots)	220
Maximum Speed	(knots)	998

Table 12. Sample Output file of program FLTCOND

NOSE-WHEEL LIFT-OFF:												
W (lbs)	I-x	I-y	I-z	Xcg (ft)	T (lbs)	Load Factor	ALT (ft)	Spd (kts)	V	T	DEF	H T
Def(deg)												
.519E+05	.900E+16	.140E+06	.900E+16	.311E+02	.337E+05	.900E+16	.000E+00	.900E+16	.000E+00	.000E+00	.000E+00	
.519E+05	.900E+16	.140E+06	.900E+16	.311E+02	.337E+05	.900E+16	.000E+00	.900E+16	.000E+00	.000E+00	.000E+00	
.519E+05	.900E+16	.140E+06	.900E+16	.311E+02	.337E+05	.900E+16	.000E+00	.900E+16	.000E+00	.000E+00	.000E+00	
LANDING:												
W (lbs)	I-x	I-y	I-z	Xcg (ft)	T (lbs)	Load Factor	ALT (ft)	Spd (kts)	V	T	DEF	H T
Def(deg)												
.519E+05	.900E+16	.140E+06	.900E+16	.311E+02	.900E+16	.100E+01	.000E+00	.900E+16	.000E+00	.000E+00	.000E+00	
.519E+05	.900E+16	.140E+06	.900E+16	.311E+02	.900E+16	.100E+01	.000E+00	.900E+16	.000E+00	.000E+00	.000E+00	
.384E+05	.900E+16	.900E+16	.900E+16	.320E+02	.900E+16	.100E+01	.500E+05	.326E+03	.000E+00	.000E+00	.000E+00	
.384E+05	.900E+16	.900E+16	.900E+16	.320E+02	.900E+16	.100E+01	.500E+05	.103E+04	.000E+00	.000E+00	.000E+00	
1-G TRIM:												
W (lbs)	I-x	I-y	I-z	Xcg (ft)	T (lbs)	Load Factor	ALT (ft)	Spd (kts)	V	T	DEF	H T
Def(deg)												
.519E+05	.900E+16	.900E+16	.900E+16	.311E+02	.900E+16	.100E+01	.000E+00	.120E+03	.000E+00	.000E+00	.000E+00	
.519E+05	.900E+16	.900E+16	.900E+16	.311E+02	.900E+16	.100E+01	.000E+00	.100E+04	.000E+00	.000E+00	.000E+00	
.384E+05	.900E+16	.900E+16	.900E+16	.320E+02	.900E+16	.100E+01	.500E+05	.326E+03	.000E+00	.000E+00	.000E+00	
.384E+05	.900E+16	.900E+16	.900E+16	.320E+02	.900E+16	.100E+01	.500E+05	.103E+04	.000E+00	.000E+00	.000E+00	
MANEUVERING FLIGHT:												
W (lbs)	I-x	I-y	I-z	Xcg (ft)	T (lbs)	Load Factor	ALT (ft)	Spd (kts)	V	T	DEF	H T
Def(deg)												
.519E+05	.900E+16	.900E+16	.900E+16	.311E+02	.900E+16	.150E+01	.000E+00	.120E+03	.000E+00	.000E+00	.000E+00	
.519E+05	.900E+16	.900E+16	.900E+16	.311E+02	.900E+16	.900E+01	.000E+00	.100E+04	.000E+00	.000E+00	.000E+00	
.384E+05	.900E+16	.900E+16	.900E+16	.320E+02	.900E+16	.150E+01	.500E+05	.326E+03	.000E+00	.000E+00	.000E+00	
.384E+05	.900E+16	.900E+16	.900E+16	.320E+02	.900E+16	.855E+01	.500E+05	.103E+04	.000E+00	.000E+00	.000E+00	
SHORT PERIOD & CAP REQUIREMENTS:												
Perform evaluation at design points.												
PITCH DUE TO STABILITY AXIS ROLL												
W (lbs)	I-x	I-y	I-z	Xcg (ft)	T (lbs)	Load Factor	ALT (ft)	Spd (kts)	V	T	DEF	H T
Def(deg)												
.900E+16	.200E+05	.900E+16	.220E+06	.320E+02	.900E+16	.900E+16	.000E+00	.120E+03	.000E+00	.000E+00	.000E+00	
.900E+16	.200E+05	.900E+16	.220E+06	.320E+02	.900E+16	.900E+16	.000E+00	.560E+03	.000E+00	.000E+00	.000E+00	
.900E+16	.200E+05	.900E+16	.220E+06	.320E+02	.900E+16	.900E+16	.000E+00	.100E+04	.000E+00	.000E+00	.000E+00	
.900E+16	.200E+05	.900E+16	.220E+06	.320E+02	.900E+16	.900E+16	.100E+05	.160E+03	.000E+00	.000E+00	.000E+00	
.900E+16	.200E+05	.900E+16	.220E+06	.320E+02	.900E+16	.900E+16	.100E+05	.655E+03	.000E+00	.000E+00	.000E+00	
.900E+16	.200E+05	.900E+16	.220E+06	.320E+02	.900E+16	.900E+16	.100E+05	.115E+04	.000E+00	.000E+00	.000E+00	
.900E+16	.200E+05	.900E+16	.220E+06	.320E+02	.900E+16	.900E+16	.500E+05	.326E+03	.000E+00	.000E+00	.000E+00	
.900E+16	.200E+05	.900E+16	.220E+06	.320E+02	.900E+16	.900E+16	.500E+05	.679E+03	.000E+00	.000E+00	.000E+00	
.900E+16	.200E+05	.900E+16	.220E+06	.320E+02	.900E+16	.900E+16	.500E+05	.103E+04	.000E+00	.000E+00	.000E+00	
TIME-to-BANK PERFORMANCE:												
W (lbs)	I-x	I-y	I-z	Xcg (ft)	T (lbs)	Load Factor	ALT (ft)	Spd (kts)	V	T	DEF	H T
Def(deg)												
.900E+16	.390E+05	.900E+16	.220E+06	.320E+02	.900E+16	.100E+01	.000E+00	.120E+03	.000E+00	.000E+00	.000E+00	
.900E+16	.390E+05	.900E+16	.220E+06	.320E+02	.900E+16	.100E+01	.000E+00	.413E+03	.000E+00	.000E+00	.000E+00	
.900E+16	.390E+05	.900E+16	.220E+06	.320E+02	.900E+16	.100E+01	.000E+00	.707E+03	.000E+00	.000E+00	.000E+00	
.900E+16	.390E+05	.900E+16	.220E+06	.320E+02	.900E+16	.100E+01	.000E+00	.100E+04	.000E+00	.000E+00	.000E+00	
.900E+16	.390E+05	.900E+16	.220E+06	.320E+02	.900E+16	.100E+01	.100E+05	.160E+03	.000E+00	.000E+00	.000E+00	
.900E+16	.390E+05	.900E+16	.220E+06	.320E+02	.900E+16	.100E+01	.100E+05	.490E+03	.000E+00	.000E+00	.000E+00	
.900E+16	.390E+05	.900E+16	.220E+06	.320E+02	.900E+16	.100E+01	.100E+05	.820E+03	.000E+00	.000E+00	.000E+00	
.900E+16	.390E+05	.900E+16	.220E+06	.320E+02	.900E+16	.100E+01	.100E+05	.115E+04	.000E+00	.000E+00	.000E+00	
.900E+16	.390E+05	.900E+16	.220E+06	.320E+02	.900E+16	.100E+01	.500E+05	.326E+03	.000E+00	.000E+00	.000E+00	
.900E+16	.390E+05	.900E+16	.220E+06	.320E+02	.900E+16	.100E+01	.500E+05	.561E+03	.000E+00	.000E+00	.000E+00	
.900E+16	.390E+05	.900E+16	.220E+06	.320E+02	.900E+16	.100E+01	.500E+05	.797E+03	.000E+00	.000E+00	.000E+00	
.900E+16	.390E+05	.900E+16	.220E+06	.320E+02	.900E+16	.100E+01	.500E+05	.103E+04	.000E+00	.000E+00	.000E+00	
STEADY SIDESLIP												
W (lbs)	I-x	I-y	I-z	Xcg (ft)	T (lbs)	Load Factor	ALT (ft)	Spd (kts)	V	T	DEF	H T
Def(deg)												
.384E+05	.900E+16	.900E+16	.900E+16	.329E+02	.900E+16	.100E+01	.000E+00	.120E+03	.000E+00	.000E+00	.000E+00	
.384E+05	.900E+16	.900E+16	.900E+16	.329E+02	.900E+16	.100E+01	.000E+00	.120E+03	.000E+00	.000E+00	.000E+00	
ENGINE-OUT TRIM:												
W (lbs)	I-x	I-y	I-z	Xcg (ft)	T (lbs)	Load Factor	ALT (ft)	Spd (kts)	V	T	DEF	H T
Def(deg)												
.248E+05	.900E+16	.900E+16	.900E+16	.329E+02	.169E+05	.100E+01	.000E+00	.120E+03	.000E+00	.000E+00	.000E+00	
.248E+05	.900E+16	.900E+16	.900E+16	.329E+02	.169E+05	.100E+01	.000E+00	.120E+03	.000E+00	.000E+00	.000E+00	
COORDINATED ROLL & ROLLING PULLOUT:												
W (lbs)	I-x	I-y	I-z	Xcg (ft)	T (lbs)	Load Factor	ALT (ft)	Spd (kts)	V	T	DEF	H T
Def(deg)												
.900E+16	.200E+05	.140E+06	.900E+16	.329E+02	.900E+16	.150E+01	.000E+00	.120E+03	.000E+00	.100E+01	.100E+01	
.900E+16	.200E+05	.140E+06	.900E+16	.329E+02	.900E+16	.550E+01	.000E+00	.560E+03	.000E+00	.100E+01	.100E+01	
.900E+16	.200E+05	.140E+06	.900E+16	.329E+02	.900E+16	.900E+01	.000E+00	.100E+04	.000E+00	.100E+01	.100E+01	
.900E+16	.200E+05	.140E+06	.900E+16	.329E+02	.900E+16	.100E+01	.500E+05	.326E+03	.000E+00	.100E+01	.100E+01	
.900E+16	.200E+05	.140E+06	.900E+16	.329E+02	.900E+16	.100E+01	.500E+05	.679E+03	.000E+00	.100E+01	.100E+01	
.900E+16	.200E+05	.140E+06	.900E+16	.329E+02	.900E+16	.100E+01	.500E+05	.103E+04	.000E+00	.100E+01	.100E+01	

3.2 Stability & Control Derivatives

The values of stability and control derivatives of a design configuration vary considerably depending on flight condition variables, such as Mach number and *cg* location. Once these flight condition variables are selected, the stability and control derivatives can be estimated using a computational aerodynamics method or taken from experimental data. The use of a subsonic linear aerodynamic prediction method is described in Chapter 5.

3.3 Control Power Evaluation for Requirements

Because each of the requirements may be evaluated several times under different flight conditions, a spreadsheet was constructed using *LOTUS 1-2-3* to speed up the process. An EXCEL version is now available also. In general, each requirement has an input section where all pertinent variables are entered. For some requirements, intermediate calculations are performed to arrive at the output. Some control power requirements require solving systems of linear equations. Macros are included so that simple commands from the user can initiate the necessary re-calculation. For nosewheel lift-off and time-to-bank requirements, simulation of the motions are necessary. The worksheet includes numerical integration (using Euler's method) to determine the time-dependent results.

Examples of the worksheets are presented in Tables 13 and 14. They show how the designer can easily check the design, investigate changes, and become familiar with the relative importance of various effects. Although these are some of the simpler worksheets, they illustrate the desirability of using this type of simple system. Examples of all the spreadsheets are shown in Appendix A.

Table 13. - Trimmed 1-g flight worksheet

```
*****
Trimmed 1-G Flight
*****
```

Input: Weight (lbs)	51900
Reference Area (ft ²)	400
Speed (ft/s)	400
Air Density (slug/ft ³)	0.002376
C-m-0	0.0181
C-m-delta E (/rad)	-1.117
C-L-0	-0.0685
C-L-delta E (/rad)	0.8688
C-m/C-L (-Static Margin)	-0.13
C-L-alpha (/rad)	4

Output:

C-L Required for 1-g trim	0.6826073
Elevator Deflection for Trim (deg)	-4.53912205
AOA Required for 1-g Trim (deg)	11.744717

Table 14. - Pitch due to roll coupling worksheet

```
*****
Pitch Due to Roll Inertial Coupling
*****
```

Input: Weight (lbs)	500
I-x (slug ft ²)	23168
I-y (slug ft ²)	123936
I-z (slug ft ²)	143239
Reference Area (ft ²)	400
Reference Chord (ft)	11.52
Density (slug/ft ³)	0.002376
Speed (ft/s)	400
Velocity Axis Roll Rate (deg/sec)	147
Angle of Attack (deg)	60
C-m-delta-E (/rad)	-1.23

Output:

Dynamic Pressure, q (lbf/ft ²)	533.2932
Pitch Moment Coeff. due to Roll Coupling (+ or -)	0.2786349
Additional Elev. Deflection to Counter Coupling (rad)	0.2264511
Counter Coupling (deg)	12.974695

4. Subsonic Linear Aerodynamic Estimation: A Vortex-Lattice Method

Vortex lattice methods (VLM) are widely used for estimating the neutral point and other aircraft aerodynamic characteristics. They have been incorporated in conceptual airplane design to predict the configuration neutral point, lift-curve slope and lifting surface interaction. In this study, a simplified VLM is used to predict the stability and control derivatives. Limited to subsonic flight speeds, this computational approach is better than using DATCOM in that unconventional geometric arrangements can be accommodated and the user's calculations are less time consuming. The Prandtl-Glauert correction is used to account for Mach number effects. Since the VLM is based on potential flow theory, its validity is restricted to the linear aerodynamics region, and hence is valid in the low-angle of attack flight regime. It does not account for viscous effects or leading-edge vortex lift effects. The best theoretical introduction to typical VLM schemes is given in Chapter 7 of Bertin and Smith (Ref. 35).

4.1 Code Implementation: Concept and Limitations

Many variations of the vortex lattice method have been developed. The VLM scheme used in this study is a direct implementation of the method presented in Section 12.3 of the recent text by Katz and Plotkin (Ref. 36). A series of closed trapezoidal vortex rings, rather than horseshoe vortices, are used to represent the airplane surfaces, as illustrated in Figure 4. The actual vortex ring is displaced downstream by a quarter chord of each panel. The control point is located at the center of each ring, where the non-penetration surface boundary condition is satisfied. The result is equivalent to the commonly used $1/4 - 3/4$ rule for horseshoe vortices and control points.

To obtain the aerodynamic characteristics, the strengths of each of the vortex rings must be found so that the vector sum of their induced velocity and the free-stream contribution at each control point satisfies the boundary conditions. The induced velocity at a point due to a straight line segment of a vortex filament is given by the Biot-Savart Law. Since the Helmholtz vortex theorem says that a vortex cannot end in fluid, the vortex filament must form a closed ring (such as those representing the lifting surface) or extend to infinity as a horseshoe vortex at the trailing edge of a surface (Fig. 4). After solving a system of equations for the vortex strengths they can then be integrated over the surface to obtain the forces and moments.

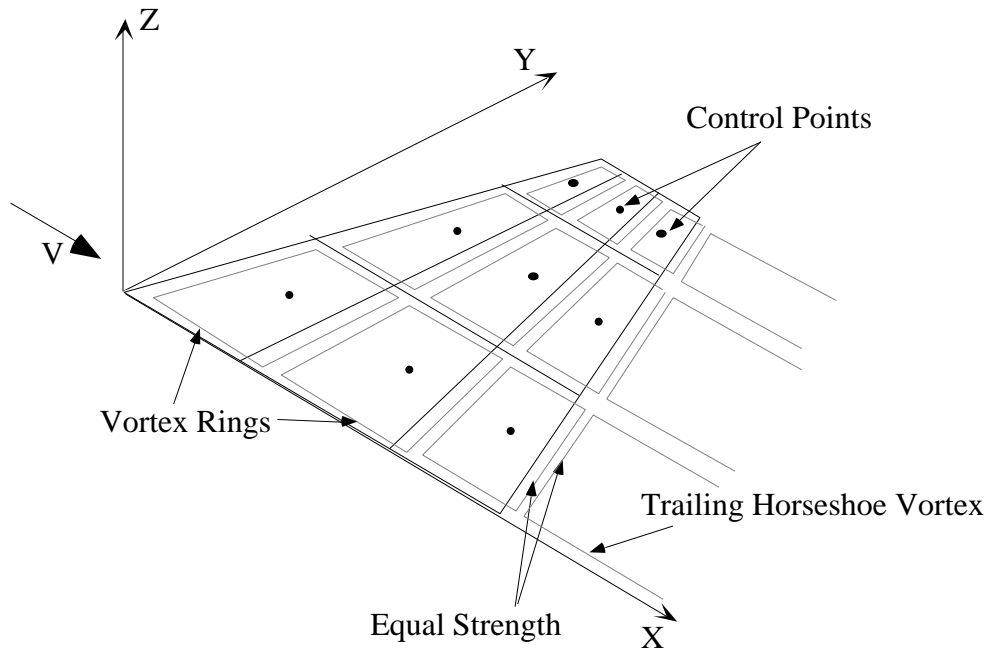


Figure 4. - Vortex rings and control points of VLM implementation.

The effect of compressibility is included using the Prandtl-Glauert rule as illustrated in Figure 5. This approximation stretches the x -coordinate of the distributed singularities (vortex rings) as the Mach number increases. The resulting pitching and yawing moments (now over estimated because of the elongation in the x -coordinate) are re-adjusted with the Prandtl-Glauert correction factor β . Generally, this approximation is good up to $M = 0.8$.

Derivatives are approximated by finite differences of linear small perturbations. The program first solves for the forces and moments of the configuration at a reference condition. It then alters the problem by introducing a perturbation in the flow such as surface deflection or angle of attack change. The desired non-dimensional derivatives are then calculated by dividing the difference of the forces or moments by the perturbation.

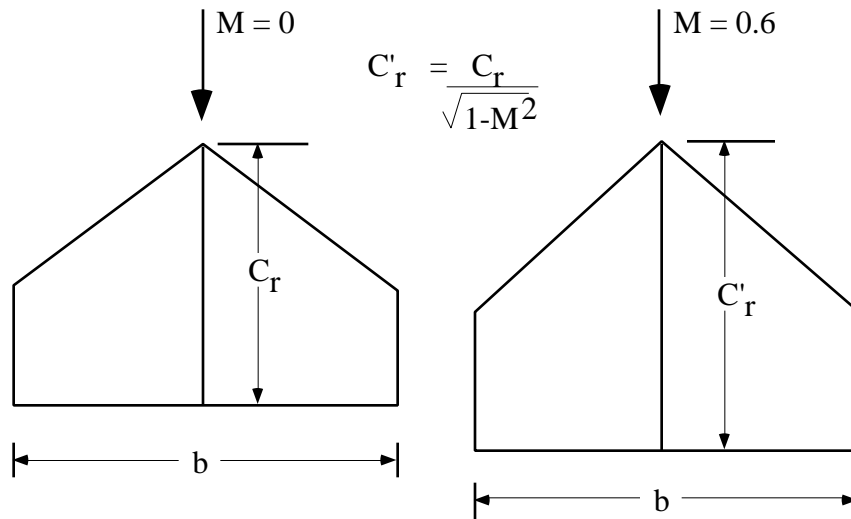


Figure 5. - Prandtl-Glauert correction rule used in VLM to account for compressibility effects.

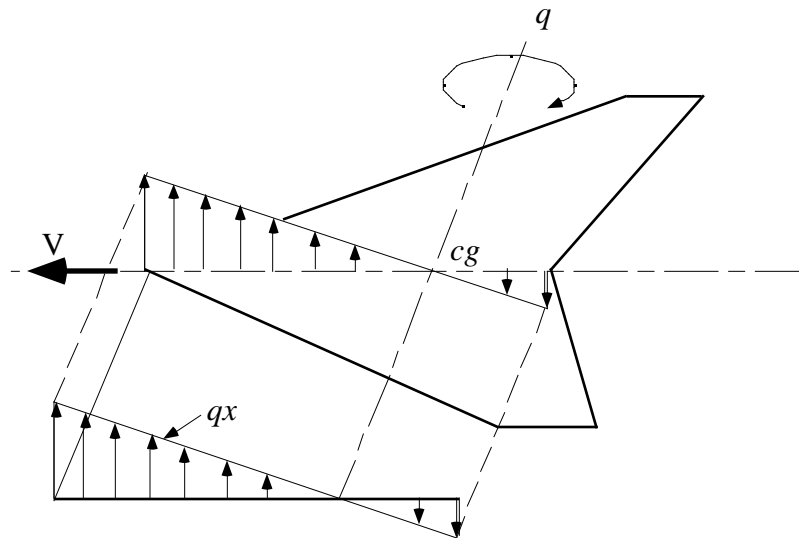


Figure 6. Surface velocity distribution due to pitch rate (ref. 16)

To approximate pitch-, roll- and yaw-rate derivatives, an additional velocity component distribution (Fig. 6) is added to the free-stream velocity at the control points. Since the program takes full advantage of symmetric flow about the x -axis, the following assumptions are made to obtain the approximate solution for asymmetric flow problems, such as antisymmetric aileron deflections and roll-rate derivatives, without doubling the number of equations and unknowns: *i*) the net lift is unchanged from that of the reference condition, and *ii*) the change in vortex distribution caused by the asymmetry is antisymmetric about the x -axis. With these assumptions, the vortex distribution in the asymmetric flow can be decomposed into a symmetric and an antisymmetric pattern as shown in Figure 7. The symmetric distribution is already known from the reference condition, and its influence at each control point can be calculated. Under this formulation, the idea is to solve for the antisymmetric distribution alone. For each control surface listed in the longitudinal geometry file, the program first deflects it individually symmetrically to estimate its effect on the lift and pitching moment. Its effect on roll and perhaps yaw moment (such as in the case of V-tail) is then calculated using the approach discussed above.

The VLM program is also capable of performing the longitudinal stability and control derivative estimation in ground effect. Ground effect is modeled with the imaginary presence of a vortex system with opposite vortex strength distribution placed $2h$ (h is the height of the center of gravity above the ground) below the real vortex system (see Figure 8). The number of unknowns (the strength of each vortex ring) remain the same due to the symmetry.

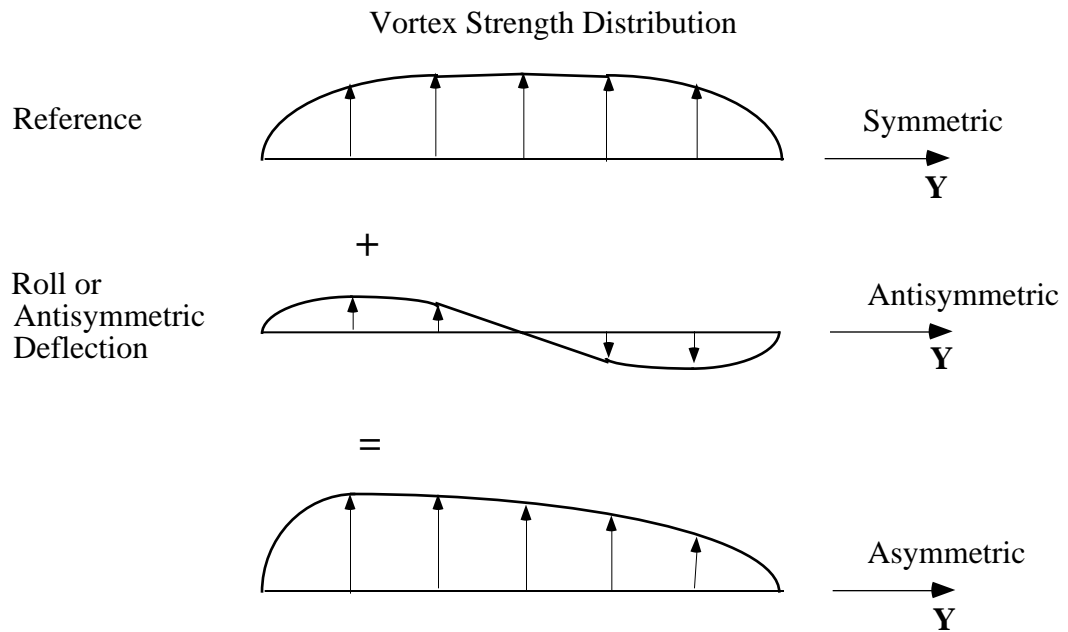


Figure 7. - Spanwise vortex strength distribution for asymmetric loading.

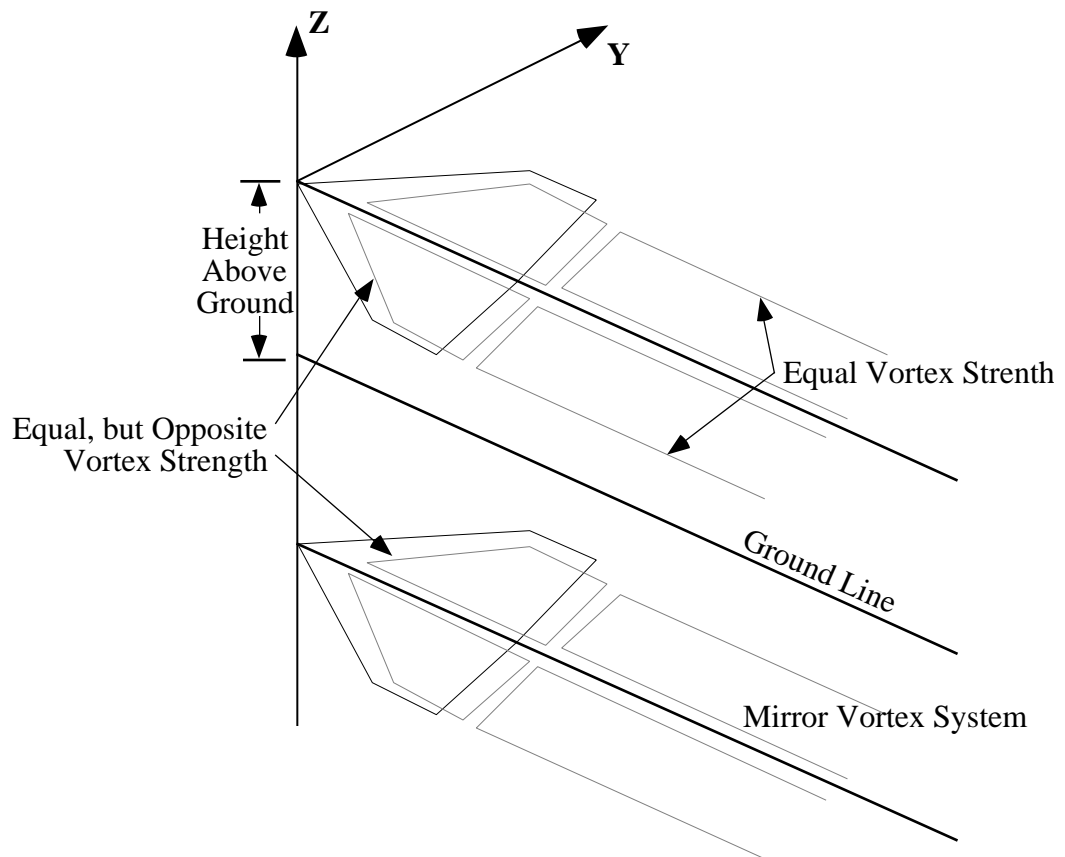


Figure 8. - Use of mirror vortex system to model ground plane.

4.2 Code Validation: Comparison with DATCOM Estimates and Wind Tunnel Data

An F-18 model was constructed to be used for VLM validation. The resulting longitudinal and lateral/directional grid points are shown in Figure 9. Four sections are used to represent the longitudinal geometry as illustrated in Figure 9a. With 40 panels per section, this results in a total of 160 panels. In the lateral/directional geometry, five sections are used to represent the lateral profile of the F-18 as shown in Figure 9b. Note the two vertical tails are placed on the two sides of the fuselage section. There are 200 panels representing the lateral geometry.

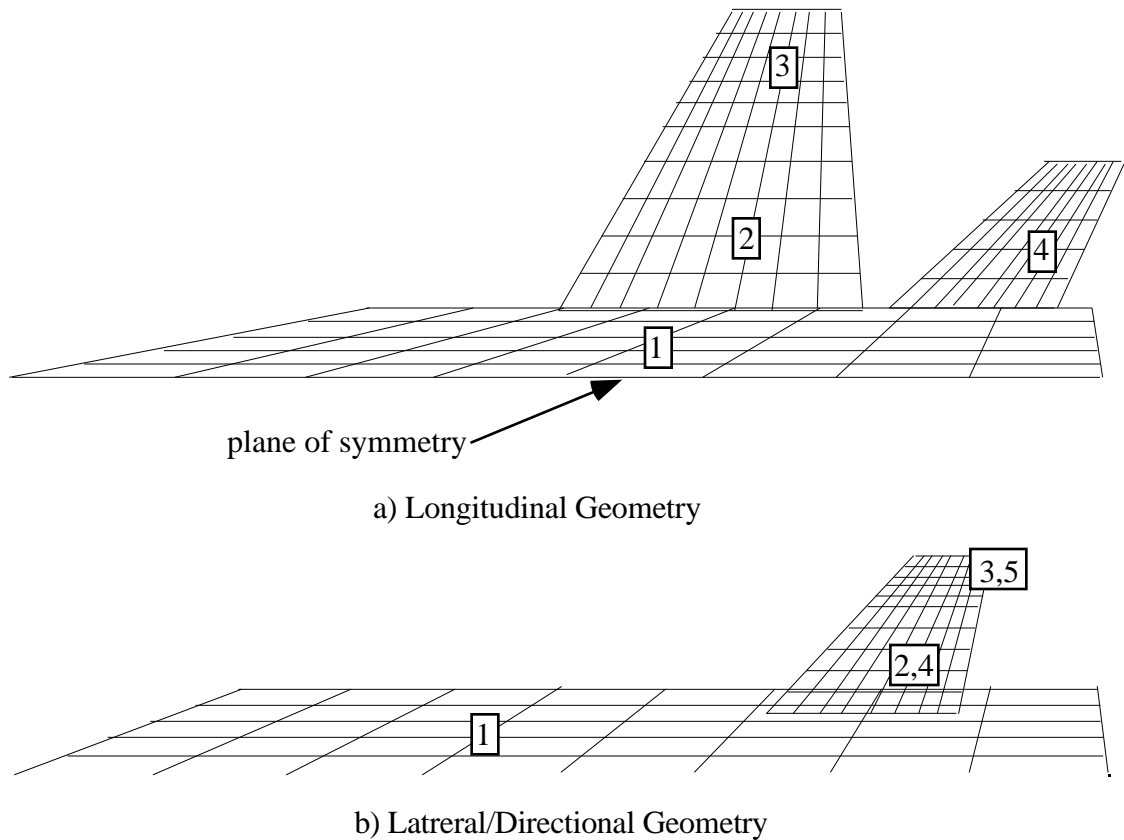


Figure 9 - VLM grid representation of F-18 showing individual sections.

A complete analysis (at one Mach number and one cg location) requires about 55 minutes on an IBM 386 compatible computer, or 1 to 2 minutes on a workstation. A long time is required because there are five control surfaces in the longitudinal model and two in the lateral geometry. Each stability and control derivative requires several solutions. Most of the computing time is spent computing the influence coefficients (the contribution of a vortex ring to the induced velocity at a control point), and solving the resulting large system of equations.

The results are compared to values obtained using the procedures outlined in Ref. 37, which is based on the US Air Force DATCOM, and the aerodynamic coefficients used in a flight simulation of the aircraft. The comparisons are conducted at Mach 0.2 and Mach 0.6 out of ground effect, with the cg located at the quarter chord of the wing's mean chord. Note that the data and the two estimation methods all exclude aeroelastic effects.

4.2.1 Stability Derivatives

Figure 10 contains the comparison of the angle of attack-derivatives and the static margin estimates. For the lift-curve slope, the VLM and DATCOM predictions are 7% and 13% respectively lower than the wind tunnel value for Mach 0.2. The difference can partially be explained by the fact that the contribution of the twin vertical tails are ignored in both the VLM and the DATCOM estimates. Although VLM appears to have under-estimated the static margin at higher Mach number, the difference is only slightly over an inch (less than 1% of the mean chord) when converted to the scale of the actual aircraft.

Figure 11 contains pitch rate estimates and indicates that the lift-due-to-pitch rate prediction of the VLM is poor. Investigation has shown that the difference is caused primarily by over-estimating the contribution from the wing. The VLM results obtained here agree with the Lamar code (Ref. 38) predictions, so that it appears that the problem is

not due to an error in this particular VLM implementation. The exact cause of this problem is still unclear. Due to the wing's shorter moment arm to the c_g , the influence of the over-estimation of the wing's contribution is less profound on the prediction of C_{m_q}

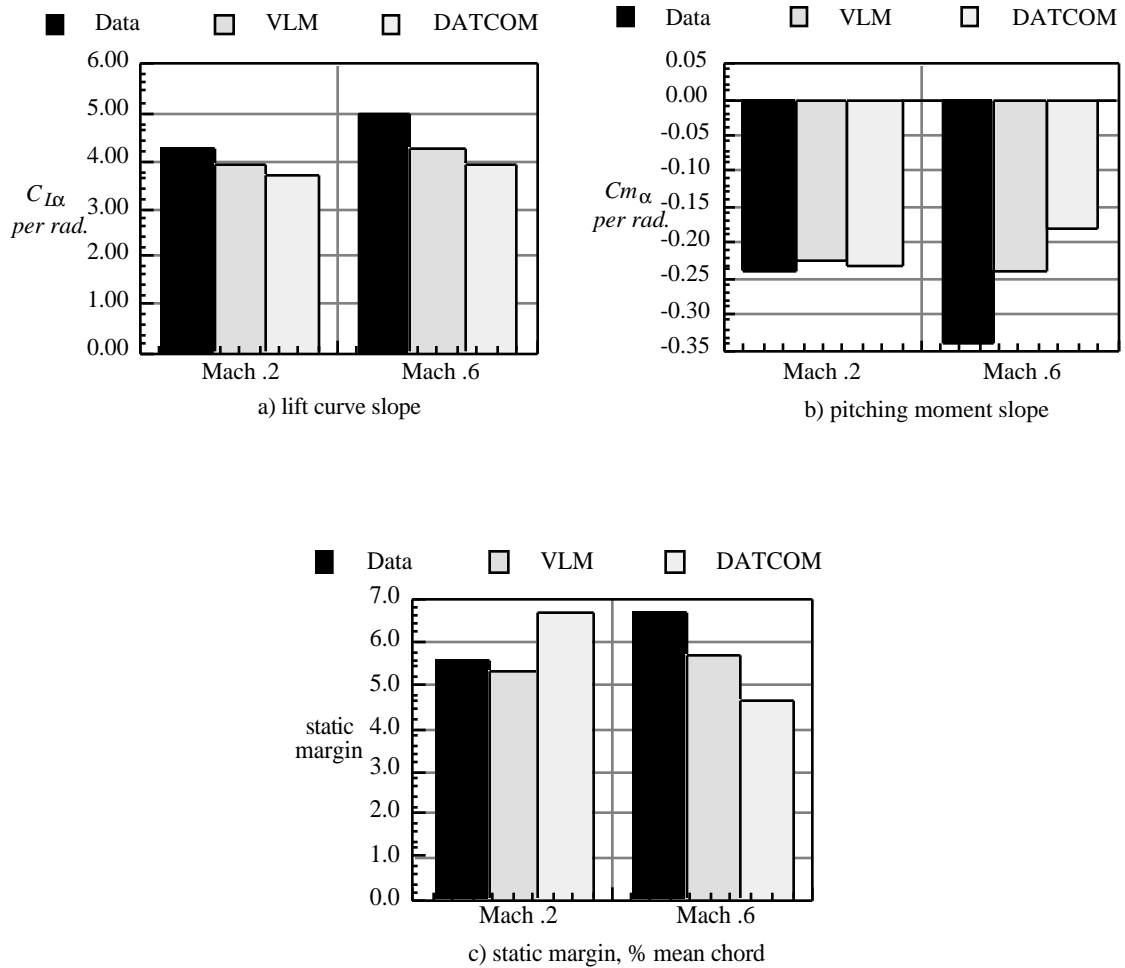


Figure 10. - Angle of attack derivatives

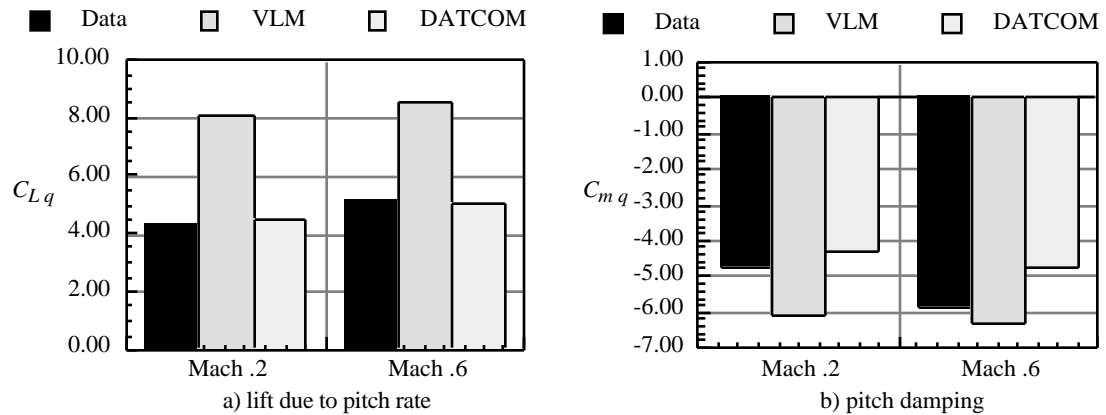


Figure 11. - Pitch rate derivatives

Sideslip derivatives are shown in Figure 12. Both VLM and DATCOM underestimate the change in side-force due to sideslip ($C_{y-\beta}$) by 45 to 55%. In this case, the simplified fuselage representation (see Figure 9) is probably inadequate. The variation of roll moment due to sideslip angle ($C_{l-\beta}$) is poorly predicted because the wing and horizontal tail are not modeled in the VLM geometry. Thus the dihedral effect is not included. The VLM's prediction of the yawing moment due to sideslip ($C_{n-\beta}$) is within 10% of the wind tunnel value at both Mach numbers since this derivative is mostly dictated by the vertical tail(s).

The yaw-rate derivatives are shown in Figure 13. The VLM program over-predicted the side-force variation due to yaw rate (C_{y-r}) in a manner similar to the problem with the pitch rate derivative described above. Fortunately, this parameter is not often of importance. The rolling moment variation with yaw rate (C_{l-r}) is also inaccurate for the same reason. Ignoring the wing's contribution in the lateral/directional model worsens the problem. Since the variation of yawing moment with changes in yaw rate (C_{n-r}) is generally dictated by the vertical tail volume coefficient, the VLM is able to provide a prediction to within 18% of the wind tunnel value.

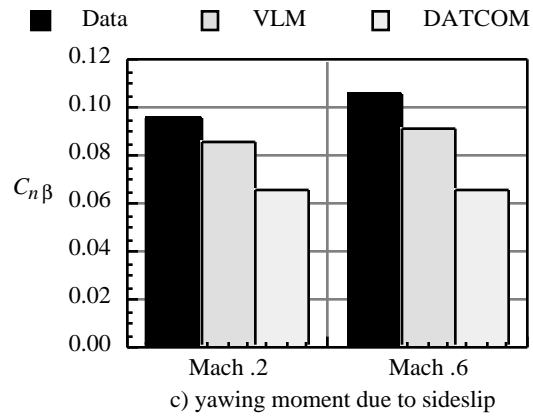
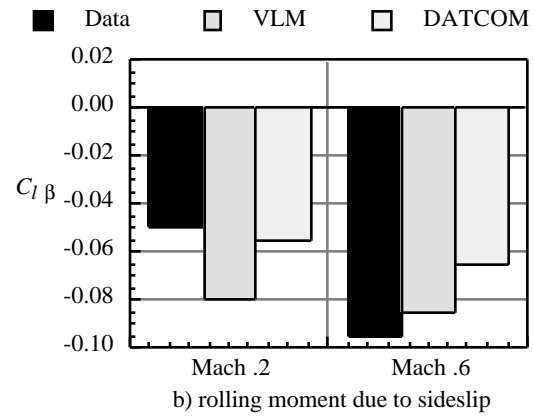
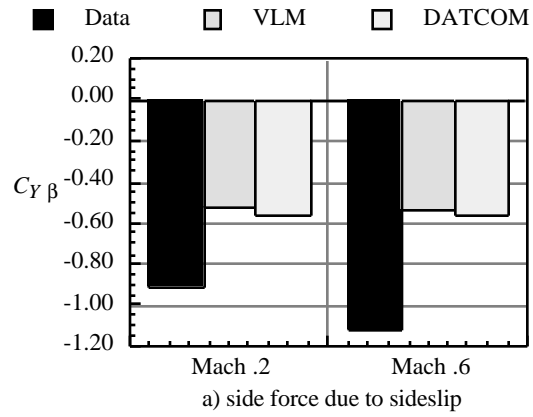


Figure 12. - Sideslip derivatives

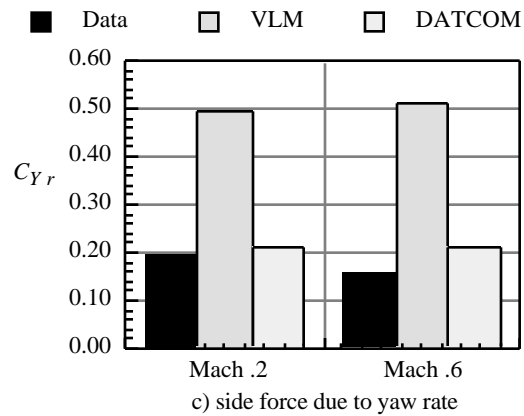
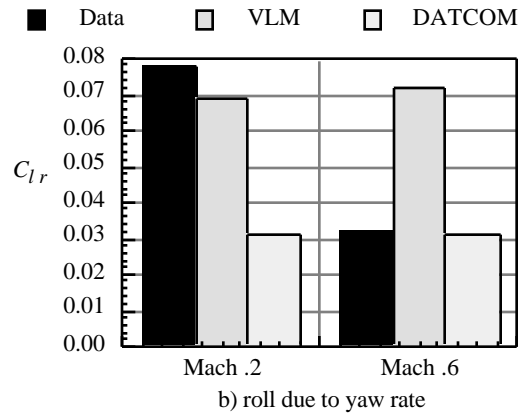
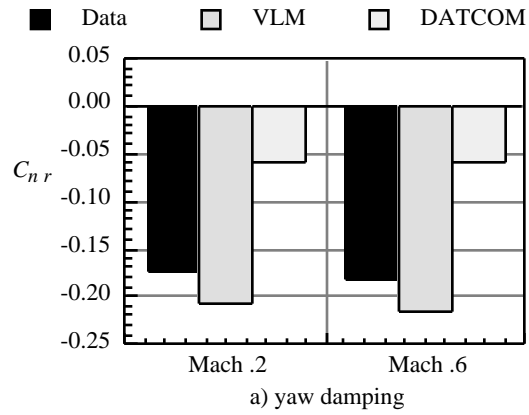


Figure 13. - Yaw rate derivatives

The VLM approach is able to accurately predict roll rate damping coefficient (C_{l-p}) as shown in Figure 14. The slight over prediction is caused by the poor fuselage model in both the longitudinal and lateral/directional model. The value of the yawing moment due to roll rate (C_{n-p}) is affected by: *i*) the dihedral of the horizontal tail, *ii*) the difference of the induced drag on the two sides of the wing during roll if the wing is generating net lift, and *iii*) the vertical tail. The VLM is unable to accurately predict this stability derivative.

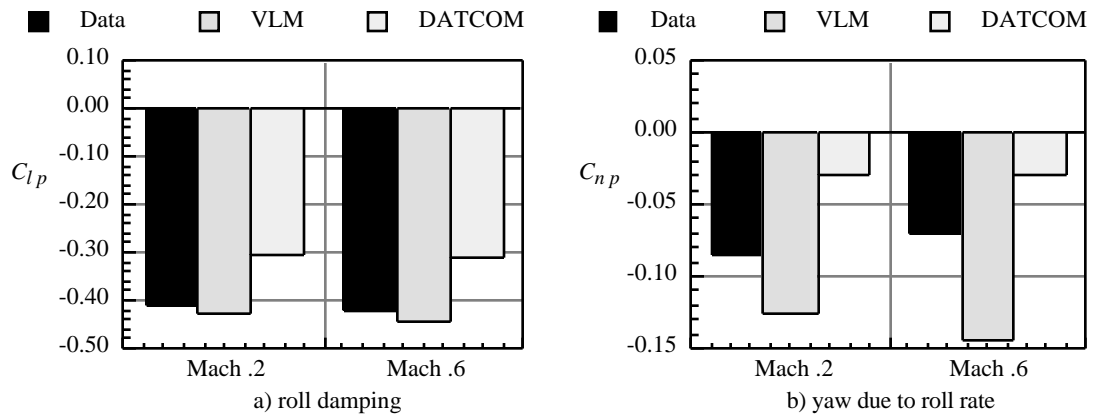


Figure 14. - Roll rate derivatives

Table 15 is the qualitative comparison the overall stability derivative estimation capability of the VLM program against DATCOM. While the VLM approach exhibits poor accuracy in certain cases (pitch and yaw rate derivatives), it appears to provide more accurate overall results than DATCOM.

Table 15. Reliability of Stability Derivative Predictions

	VLM	DATCOM
AOA-Derivatives	good	acceptable
q -Derivatives	poor	good
C-y- β & C-l- β	poor	poor
C-n- β	good	poor
C-y-r & C-l-r	poor	good
C-n-r	good	poor
p -Derivatives	good	acceptable

4.2.2 Control Derivatives

The aerodynamic simulation program generates data for control effectiveness of symmetrical control surfaces, such as flaps and elevators, on one side of the x -axis at a time. The values presented in the comparison figures are twice the magnitude of the one-side deflection values. This approximation can introduce significant error when the lateral separation between the surfaces is small as in the case of flap and elevator deflections.

Figure 15 illustrates the predictions of the elevator (horizontal tail) control effectiveness. Both VLM and DATCOM produce accurate results (VLM predictions are less than 10% from the wind tunnel values) for lift and pitching moment variations with elevator deflections ($C_L\text{-}\delta E$ & $C_m\text{-}\delta E$). This is to be expected because the aircraft has an all flying tail. In addition, VLM is able to predict the rolling moment due to antisymmetric elevator deflections. Note the loss of control effectiveness with increasing Mach number is shown in the data. This phenomenon is observed for most control surfaces. Viscous effect may be the primary cause.

The control effectiveness of the inboard flap is shown in Figure 16. For the change of total lift and pitching moment with flap deflection ($C_L\text{-}\delta F$ and $C_m\text{-}\delta F$), the VLM results show good agreement with wind tunnel measurements. The VLM prediction of the rolling moment due to antisymmetric flap deflection ($C_l\text{-}\delta F$) is larger than the wind tunnel data due to the reason stated at the beginning of this section.

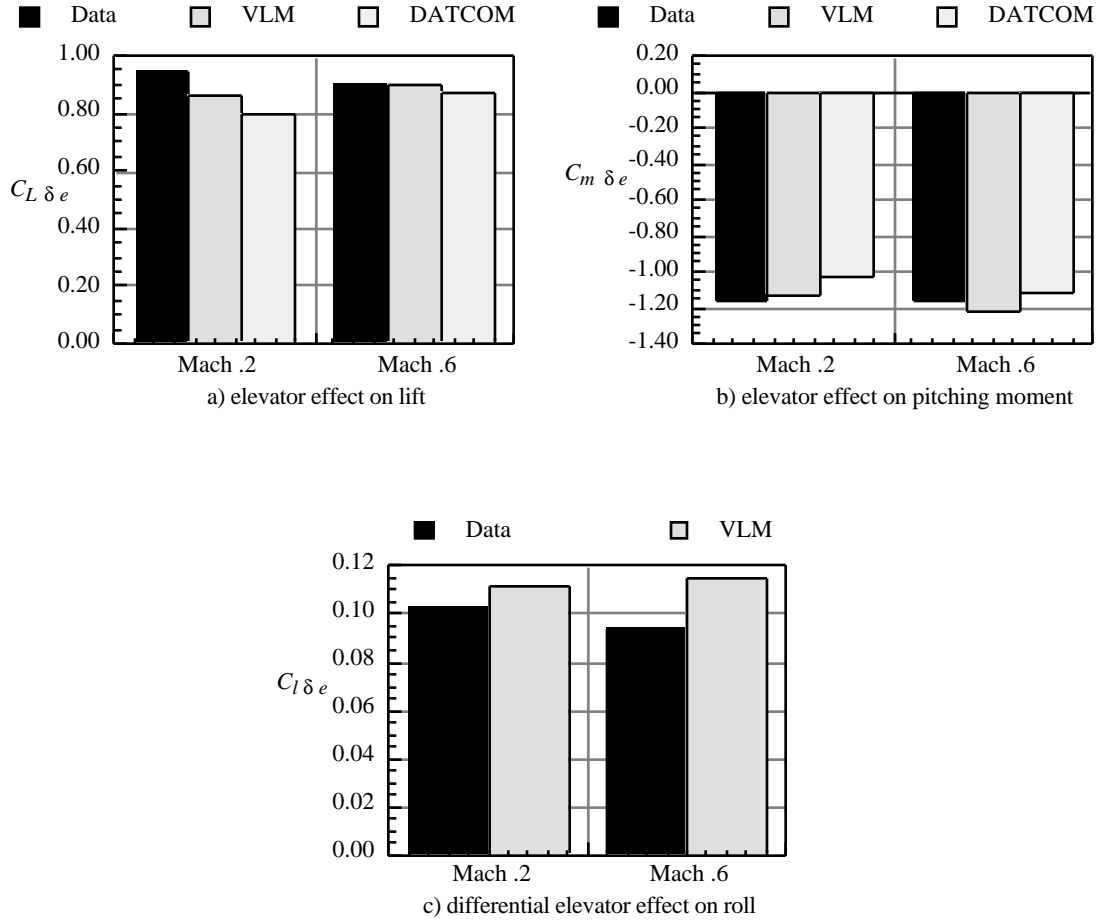


Figure 15. - Elevator effectiveness

The aileron roll power ($C_l \delta_A$) is shown in Figure 17. DATCOM produces slightly more accurate results than the VLM approach.

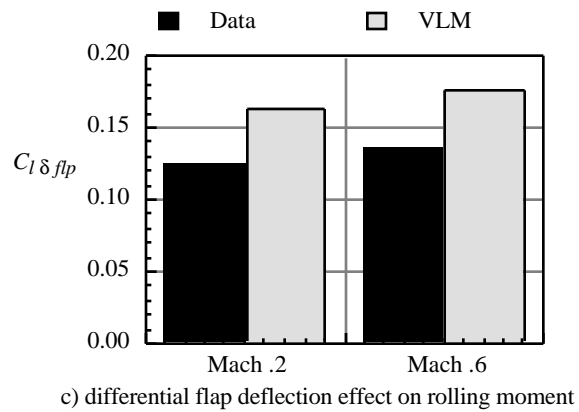
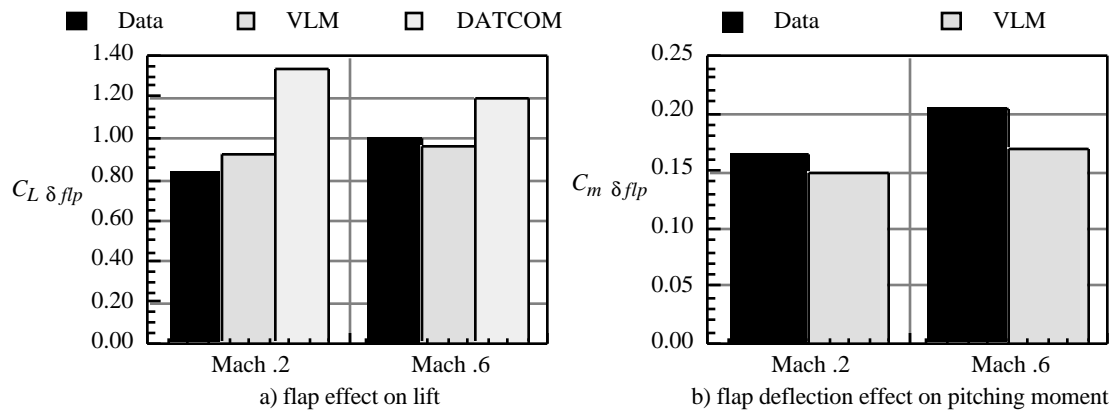


Figure 16. - Inboard flap effectiveness

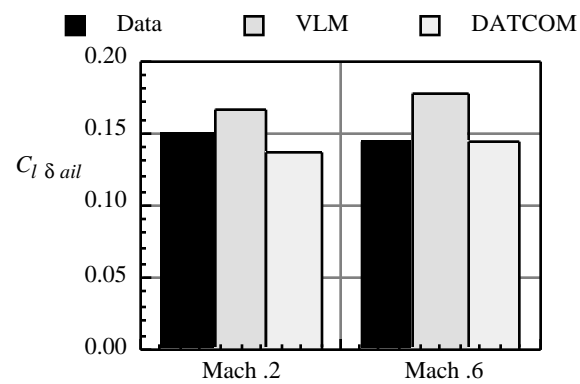


Figure 17. - Aileron effectiveness

The comparison of the rudder control effectiveness is shown in Figure 24. The VLM program is able to produce estimates for the side-force and yawing moment (C_y -delta R and C_n -delta R) with rudder deflection to within 15% of the wind tunnel results. However, DATCOM produces more accurate rolling moment due to rudder (C_l -delta R).

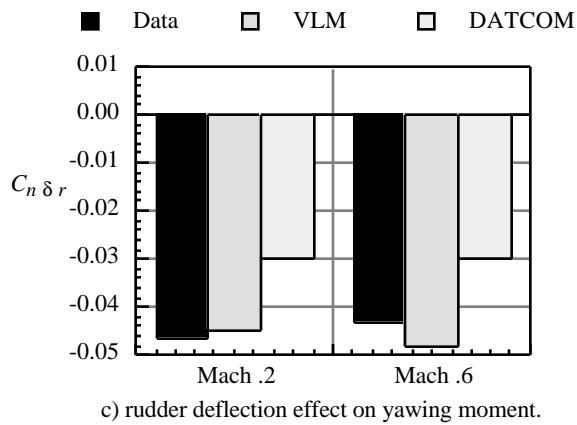
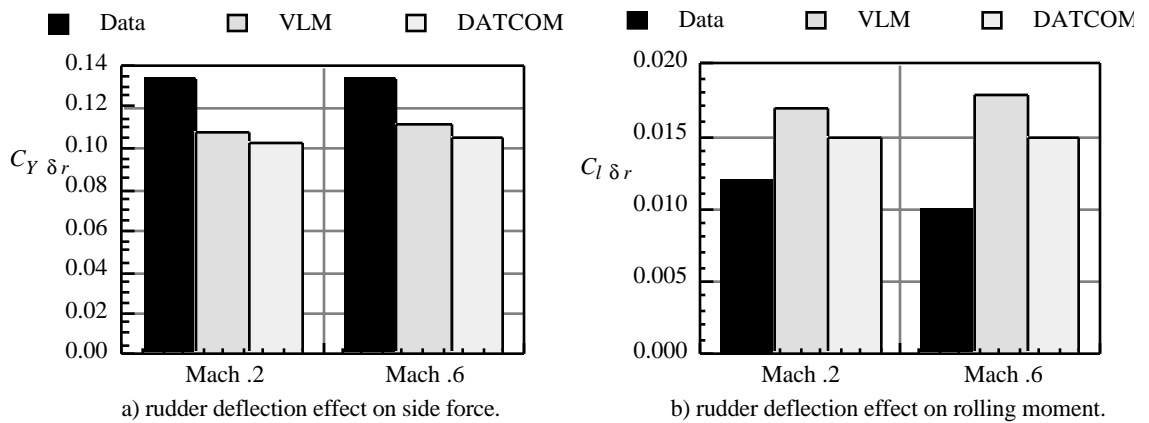


Figure 18. - Rudder effectiveness

The following three conclusions can be made about using VLM to perform control derivative estimation.

- 1). The primary control derivatives are well predicted. i.e.: C_L - δF , C_m - δE , and C_l - δA
- 2). Cross-coupling control derivatives that are caused mainly by change in induced drag during deflection are not well-predicted. i.e.: C_n - δA . Fortunately, these values usually are of less importance compared to the primary control derivatives at low angle of attack.
- 3). As the Mach number increases, the experimentally obtained control derivatives tend to decrease in magnitude, apparently due to viscous effects. The users should be aware of this phenomenon when the VLM control derivatives are calculated at higher Mach numbers.

5. Assessment Computer Codes: User Instructions

5.1 JKayVLM

This section describes the use of the vortex-lattice method program (JKayVLM) to calculate the subsonic stability and control derivatives. The detailed discussion of the VLM code has been given in Chapter 4.

The geometry of the aircraft is defined into a series of zero thickness trapezoidal sections with the option to include twist and dihedral. Effects of camber are not calculated. Each trapezoidal section is divided into 40 panels (8 streamwise and 5 spanwise). The program can handle a maximum of 5 trapezoidal sections.* Wing twist and dihedral can be modeled by entering the appropriate z -coordinate for the corner points. The program assumes that the twist distribution obeys the “straight-line wrap” rule where the hinge line is straight throughout the span of a section. Sections need not be in the same plane. For example, consider a horizontal tail in a T-tail configuration. Winglets may be modeled but must not have dihedral angles exactly equal to +90 or -90 degrees. The notation for each trapezoidal section is given in Fig. 19. Note that corner points 1 & 4 and 2 & 3 should line up streamwise. The y -coordinates of point 1 and 2 of the section must be of different value. The typical combination of trapezoidal sections to model a configuration are shown in Fig. 2, which illustrates the coordinate system definition used in developing an input data file.

Two geometries are incorporated: a longitudinal model (defined in the x - y plane) and a lateral/directional model (defined in the x - z plane). A right-hand coordinate system is used to define the geometries with all z values positive up. The longitudinal model is symmetric about the x - z plane. The lateral model is not. The overall convention for these input files is

* The code has been modified to allow for more sections. The parameter NSECT in the code can be changed to increase the number of sections. Currently the value is 10. The code has also been changed to double precision because of the larger matrices requiring solution. With these modifications the code is best run on a workstation. Execution time is too high for practical use on a PC.

shown in Fig. 20. The following instructions provide the definition of the required input. Sample input files are presented in Tables 16 and 17.

Geometry Input File:

<u>Line</u>	<u>Length</u>	<u>Format</u>	<u>Description</u>
1	80 Col.		Title Field
2	1 value	Real	Number of Sections (5 maximum)
3-6		3 values	Real (f12.5) x,y,z coordinates of each point in section 1 See Fig. 19. Note that points 1 & 4 and 2 & 3 must line in the same $x-z$ plane.
7	2 values	Real (f12.5)	Slat and Flap % chord. For all moving control surface, specify slat = 1, flap = 0
8-11		3 values	Real (f12.5) x,y,z for section 2
.			
.			

For lateral/directional stability analysis the aircraft can be modeled with the side profile alone without the wing or the horizontal tail. Omitting wing and other surfaces with large dihedral angles from the model will result in excluding their contributions to the side-slip and yaw-rate derivatives. In particular, for swept wings an estimate of the wing contribution to $C_{l\beta}$ should be added.

The code parameters (Mach number, span, chord, *etc.*) can be entered interactively or with the use of an input file. When the program is initiated, the user will be prompted to chose either a parameter input file or interactive input. An example of the parameter input file is shown in Table 18 and is self explanatory. Note that the comment lines following each variable must begin AFTER column 12 and that the title field and all files must be present. These comment fields may be changed by the user. All lines must be present in the parameter input file. That is, even if the lateral/directional geometry file does not exist, a comment must be present on this line to avoid input problems. An explanation of some of the parameters is shown below:

- X_{cg} - coordinate of moment reference center (positive aft).
- Z_{cg} - positive up.

- A constant hinge line (which spans the entire section) defined by the percent of the local chord will be assumed.
- Geometry file names are allowed up to 12 characters
- The available cases are:
 - 1 - Longitudinal Parameters Only
 - 2 - Lateral/Directional Parameters Only
 - 3 - Full Aircraft Configuration (Longitudinal & Lateral Directional)
 - 4 - Basic Stability Derivatives Only
- For the longitudinal Geometry file only:
 - o Input related to this file must include the specification of which section numbers correspond to the tail and wing for the calculations of the downwash on the tail.
 - o Specify as many tail sections as you want provided that the total number of sections is less than or equal to NSECT. If there is only one section specify the same section number twice. If there is no tail, specify section “NSECT + 1” for both tail sections.
 - o Wing sections must be in sequential order. If there are more than two wing sections, the input for the “2nd Wing Section” would be the last wing section used.
 Example: When confronted with the situation of three wing sections designated by sections 1, 2, and 3, the response for each query would be:
 Query: “Enter 1st Wing Surface Section:” Response: “1”
 Query: “Enter 2nd Wing Surface Section:” Response: “3”

Output: Stability and control derivatives are in the conventional form (see Etkin, Ref. 16). Standard convention is used in defining positive control surface deflections, as shown in Fig. 21. The user will be prompted for the name of the output file name when the program is run. Program output is written to that file in the form shown in Table 19. $C_{x\delta}$ values for each section are specified by the value $C_{x-\delta} [a,b]$ where x is the force or moment, a is the section number, and b is the control surface (1 for the slat, 2 for the flap). In addition, there is an option to create a file called “lotusout” which contains basic input and output values including aerodynamic coefficients that can be easily imported into the *LOTUS 1-2-3* spreadsheet program.

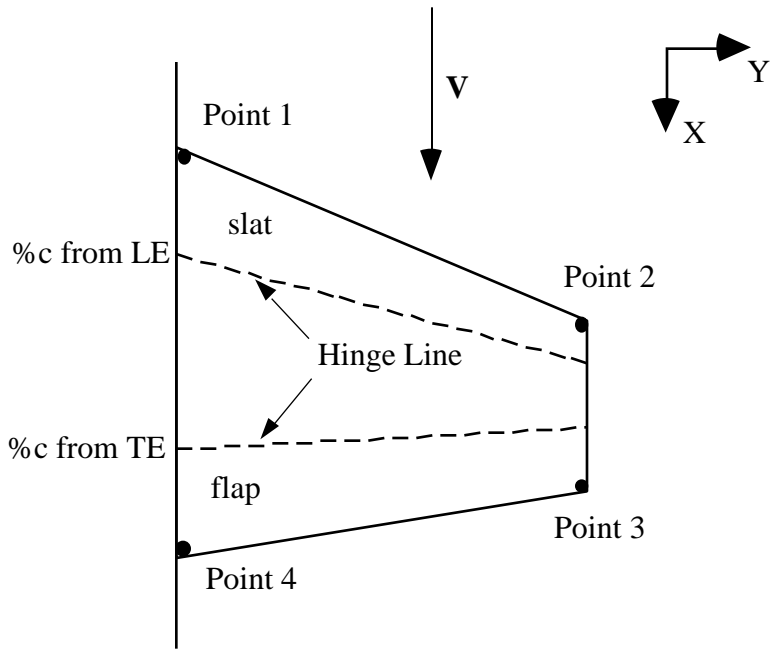


Figure 19 - Order of Points for Each Trapezoidal Panel

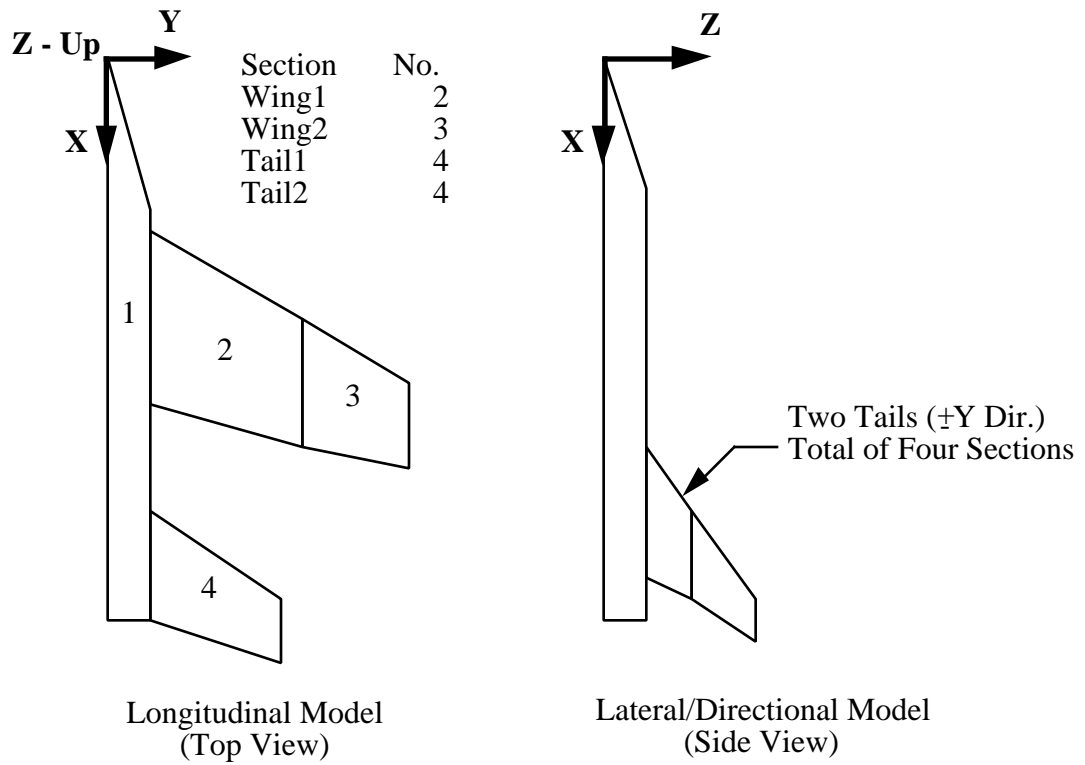


Figure 20 - Convention for Geometry Input Files

Table 16 - Sample Longitudinal Geometry Input File

```

F-18 Longitudinal Geometry Data File
4.
0.0,          0.0,          0.0
17.8,         3.49,         0.0
54.0,         3.49,         0.0
54.0,         0.0,          0.0
.00,          .00
26.85,        3.49,         0.0
32.24,        12.83,        -.4895
41.49,        12.83,        -.1877
42.02,        3.49,         0.0
.20,          .30
32.24,        12.83,        -.4895
35.64,        18.71,        -.7976
41.16,        18.71,        -.4114
41.49,        12.83,        -.1877
.20,          .30
44.946,       3.49,         0.0
52.81,        10.823,       -.256
56.60,        10.823,       -.256
53.17,        3.49,         0.0
1.0,          .00

```

Table 17 - Sample Lateral/Directional Geometry Input File

```

F-18 Lateral Geometry Data File
5.
0.0,          0.0,          0.0
11.5,         0.0,          4.3
54.0,         0.0,          4.3
54.0,         0.0,          0.0
.00,          .00
38.618,       3.2,          3.10
43.67,        5.172,       8.517
49.2,         5.172,       8.517
48.035,       3.2,          3.10
.00,          .20
43.67,        5.172,       8.517
46.00,        6.08,       11.02
49.75,        6.08,       11.02
49.2,         5.172,       8.517
.00,          .00
38.618,       -3.2,         3.10
43.67,        -5.172,      8.517
49.2,         -5.172,      8.517
48.035,       -3.2,         3.10
.00,          .20
43.67,        -5.172,      8.517
46.00,        -6.08,      11.02
49.75,        -6.08,      11.02
49.2,         -5.172,      8.517
.00,          .00

```

Table 18 - Sample Parameter Input File

F-18 Input Parameter File		
0.2	Mach Number(real)	(f4.1)
400.0	Wing Area(real)	(f10.2)
11.7	Wing Mean Chord(real)	(f10.2)
36.0	Wing Span(real)	(f10.2)
8.	Height Above Ground(real)	(f10.2)
4	Case (1-4)(integer)	(i1)
32.4	X-cg (real) (f10.3)	
1.0	Z-cg (real) (f10.3)	
f18longa	Long. Geometry File (8 char.)	(a12)
f18lata	Lateral Geom. file (8 char.)	(a12)
4	1st Horiz. Tail Section	(i1)
4	2nd Horiz. Tail Section	(i1)
2	1st Wing Surface Section	(i1)
3	2nd Wing Surface Section	(i1)

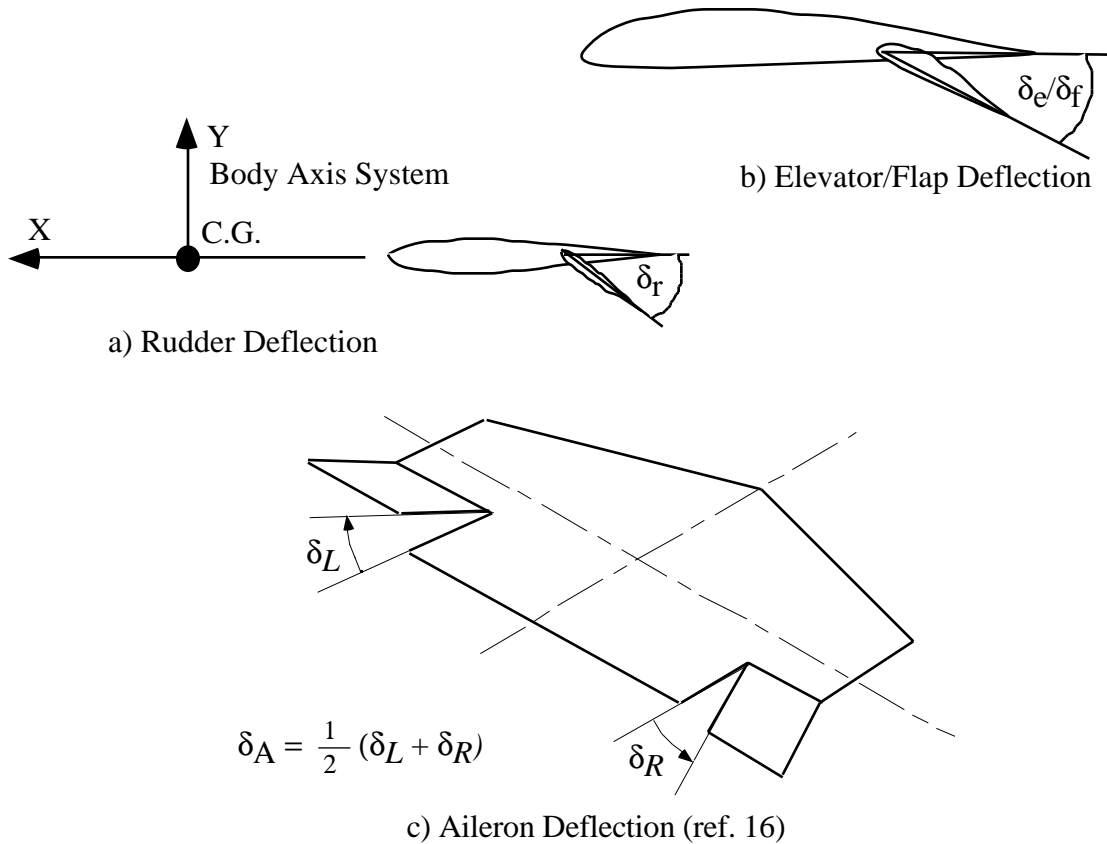


Figure 21. - Convention for positive control surface deflection.

Table 19 - VLM Code Output (Longitudinal and Lateral Data for F-18)

VLM Based Stability & Control Evaluation Code

icase	=	3
MACH NUMBER	=	0.20000
Sref	=	400.00000
c ref	=	11.70000
b ref	=	36.00000
HEIGHT ABOVE GROUND	=	8.00000
X-cg	=	32.40000
Z-cg	=	1.00000
CL0	=	-0.07784
Cm0	=	0.01807
Cdi(at alpha = 0)	=	0.00047
CL-alpha	=	4.93907
Cm-alpha	=	-0.40949
Cm/CL	=	-0.08291
Cdi/CL^2	=	0.06005
CL (at alpha = 5)	=	0.35318
Cdi(at alpha = 5)	=	0.00749
Lift-curve slope of tail due to downwash of wing	=	0.48045
CL-q	=	8.88227
CM-q	=	-5.86070
CL-delta [2 1]	=	0.07212
Cm-delta [2 1]	=	0.14026
CL-delta [2 2]	=	1.15303
Cm-delta [2 2]	=	0.12812
CL-delta [3 1]	=	0.03360
Cm-delta [3 1]	=	0.01560
CL-delta [3 2]	=	0.67143
Cm-delta [3 2]	=	-0.33240
CL-delta [4 1]	=	0.94745
Cm-delta [4 1]	=	-1.13186
Cl-delta [2 1]	=	-0.00830
Cn-delta [2 1]	=	-0.00146
Cl-delta [2 2]	=	-0.17614
Cn-delta [2 2]	=	-0.00436
Cl-delta [3 1]	=	-0.00661
Cn-delta [3 1]	=	-0.00030
Cl-delta [3 2]	=	-0.17322
Cn-delta [3 2]	=	-0.00054
Cl-delta [4 1]	=	-0.10780
Cn-delta [4 1]	=	0.02525
Cy-beta	=	-0.52457
Cn-beta	=	0.07900
Cl-beta	=	-0.10010
Cy-r	=	0.46587
Cn-r	=	-0.18577
Cl-r	=	0.08320
Cl-p	=	-0.43447
Cn-p	=	-0.11396
Cy-delta [2 2]	=	-0.10821
Cl-delta [2 2]	=	-0.02097
Cn-delta [2 2]	=	0.04219
Cy-delta [4 2]	=	-0.10781
Cl-delta [4 2]	=	-0.02099
Cn-delta [4 2]	=	0.04148

5.2 *FLTCOND*

Program *FLTCOND* was written in Microsoft FORTRAN for IBM compatible PCs. Sample input (with *LOTUS 1-2-3* spreadsheet) and output is shown in Figures 3 & 4 respectively. Note the value column in the input worksheet is to be written to a file *FCINPUT.PRN* to be read by *FLTCOND*. In the output of *FLTCOND*, variables with values of *'900E+16'* signifies that the variable need not be specified in the control power requirement check worksheet discussed in A2.

5.3 *CPRCHECK*

A *LOTUS 1-2-3* worksheet, *CPRCHECK*, was created to check if the design configuration is able to meet the control authority requirements. It contains items discussed in sections 2.1 through 2.10. The portion for each condition is listed in App. A. An EXCEL version of the spread sheet is also available, with the name *VPI-NASA.CPC*.

5.4 *TRIM3S*

Two FORTRAN programs were written to find the optimal (minimum trim drag) trim schedule in 1-g, level-flight based on a method by Goodrich, *et al.*¹² *i*) airplanes with three lifting surfaces (*TRIM3S*) and, *ii*) two lifting surfaces plus thrust vectoring (*TRIMTV*). This section discusses the application and limitations of the program *TRIM3S*.

Many recent aircraft configurations use three lifting surfaces. This results in redundant ways of generating moments and forces, leading to a variety of approaches to trim such airplanes. *TRIM3S* is based on the method described in ref. 12, which utilizes the linear optimum trim solution (*LOTS*), derived using a Lagrange formulation. It determines the longitudinal lift distribution (between the three surfaces) resulting in minimum trim drag in level, steady state flight. The program also provides the deflection angles of the controls required to generate the desired lift distribution.

Input:

Airplane geometry and pertinent parameters to the LOTS are listed in the ASCII file '3SURFACE.DAT', which is included here as the sample input file shown in Table 20. Users must be careful to follow the units prescribe for each parameter and not to change the format of the values in the right column. Some input variables require additional discussion, and they are listed below.

- a. l^{cg} (No. 3) is the distance between the cg and the wing AC normalized with the mean chord of the wing. NOTE: for measurements taken with respect to the wing's AC, it is "+" if measured from below and/or behind the wing's AC, and it is "-" if measured from above and/or in front of the wing's AC.
- b. σ/e_{ij} (No.12-17) is the ratio of the Prandtl coefficient and efficiency factor between surface-i and surface-j. They can be obtained by using the approximation in Appendix C of NASA TP-2907 or by a vortex-lattice method (VLM).
- c. δ_f (No. 28) is the optimal wing flap deflection angle (in terms of drag). Typical value is zero.
- d. c_e/c_t (No. 35) is the ratio of the elevator chord to the H. tail chord. If all-moving (variable incident) tail is used, enter zero for this value. The program will determine the proper incident angle.
- e. c_{cf}/c_c (No. 38) is the ratio of the canard's flap chord to the canard chord. Enter zero if an all-moving (variable incident) canard is used.

Output

Six key parameters are generated as the final outputs of the program. CL(1), CL(2) and CL(3) represent the lift coefficients of wing, horizontal tail and canard respectively. The last three angles are the fuselage inclination angle (angle of attack), the horizontal tail deflection angle and the canard deflection angle, respectively. After executing 'TRIM3S,' these values can be found on the screen and in the ASCII file 'RESULTS.' The output corresponding to the sample input of Table 20 is presented here in the Table 21.

Table. 20 Sample input data for the three surface code TRIM3S

1.	Total lift coeff.	(W-bar)	+1.600E-00
2.	Zero-lift Moment Coeff.	(C-m,0)	-1.000E-01
3.	C.G. distance from wing AC	(l^-cg)	-1.500E-01
4.	Area of Wing, ft ²	(S-1)	+1.670E+02
5.	Area of H. tail, ft ²	(S-2)	+4.140E+01
6.	Area of Canard, ft ²	(S-3)	+2.230E+01
7.	Span of Wing, ft	(b-1)	+4.650E+01
8.	Span of H. tail, ft	(b-2)	+1.370E+01
9.	Span of Canard, ft	(b-3)	+1.060E+01
10.	Wing AC to H. tail AC, ft	(l-2)	+1.551E+01
11.	Wing AC to Canard AC, ft	(l-3)	-2.155E+01
12.	Influence coeff-wing	(sigma/e-11)	+1.000E+00
13.	Influence coeff-H tail	(sigma/e-22)	+1.000E+00
14.	Influence coeff-canard	(sigma/e-33)	+1.000E+00
15.	Influence coeff-wing-tail	(sigma/e-12)	+2.030E-01
16.	Influence coeff-wing-canard	(sigma/e-13)	+1.900E-01
17.	Influence coeff-tail-canard	(sigma/e-23)	+1.440E-01
18.	Wing Mean chord length, ft	(c-bar)	+3.591E+00
19.	Free stream Mach number	(M-infinity)	+5.000E-01
20.	Wing max thickness swp, rad	(lambda-t/c-1)	+0.000E+00
21.	Tail max thickness swp, rad	(lambda-t/c-2)	+4.363E-01
22.	Canard max thick. swp, rad	(lambda-t/c-3)	+0.000E+00
23.	Wing chord/4 sweep, rad	(lambda-c/4-1)	+0.000E+00
24.	H tail chord/4 swp, rad	(lambda-c/4-2)	+4.363E-01
25.	Canard chord/4 swp, rad	(lambda-c/4-3)	+0.000E+00
26.	Flap chord/total wing chord	(c-f/c-w)	+2.000E-01
27.	Wing thickness ratio	(t/c-1)	+1.000E-01
28.	Optimal flap deflection,rad	(delta-f)	+1.745E-02
29.	Incident angle of wing,rad	(i-wing)	+3.491E-02
30.	Taper ratio of wing	(TR-1)	+7.500E-01
31.	Taper ratio of H tail	(TR-2)	+8.200E-01
32.	Taper ratio of canard	(TR-3)	+9.000E-01
33.	H. Tail Height, ft	(h-2)	+6.464E+00
34.	Canard height, ft	(h-3)	-2.227E+00
35.	Elevator-tail chord ratio	(c-e/c-t)	+0.000E-00
36.	H tail thickness ratio	(t/c-2)	+1.200E-01
37.	H tail incident angle, rad	(i-tail)	+0.000E-00
38.	Canard flap-chord ratio	(c-cf/c-c)	+0.000E-00
39.	Canard thickness ratio	(t/c-3)	+8.000E-02
40.	Canard incident angle, rad	(i-canard)	+0.000E-00

Table 21. Sample output from TRIM3S:

Trim Drag Code for Three Surface Configurations

NASA TP 2907 by Goodrich, Sliwa and Lallman
 coded by Jacob Kay, Sept. 1991

Input for this case:

wbar	=	1.60000	cmo	=	-0.10000
lccg	=	-0.15000	s(1)	=	167.00000
s(2)	=	41.40000	s(3)	=	22.30000
b(1)	=	46.50000	b(2)	=	13.70000
b(3)	=	10.60000	l(2)	=	15.51000
l(3)	=	-21.55000	sigmaoe(1,1)	=	1.00000
sigmaoe(2,2)	=	1.00000	sigmaoe(3,3)	=	1.00000
sigmaoe(1,2)	=	0.20300	sigmaoe(1,3)	=	0.19000
sigmaoe(2,3)	=	0.14400	cbar	=	3.59100
mfs	=	0.50000	lammt(1)	=	0.00000
lammt(2)	=	0.43630	lammt(3)	=	0.00000
lamqc(1)	=	0.00000	lamqc(2)	=	0.43630
lamqc(3)	=	0.00000	fcowc	=	0.20000
trw	=	0.10000	deltaf	=	0.01745
iwing	=	0.03491	tr(1)	=	0.75000
tr(2)	=	0.82000	tr(3)	=	0.90000
h(2)	=	6.46400	h(3)	=	-2.22700

Output results:

C-L-1 = 1.5553
 C-L-2 = -0.0280
 C-L-3 = 0.3869

CDi = 0.06363
 Effective Span e = 0.98905

CLALPHA(1) = 6.0756
 CLALPHA(2) = 4.1361
 CLALPHA(3) = 4.6556

AOA OF BODY REFERENCE LINE (DEG) = 12.1841

more tail geometry

fcocf = 0.0000
 tocf = 0.1200
 itail = 0.0000

H TAIL INCIDENT ANGLE SHOULD BE: -12.5936

more canard geometry

fcocf = 0.0000
 tocf = 0.0800
 icanard = 0.0000

Canard INCIDENT ANGLE SHOULD BE: -4.6823

5.5 TRIMTV

This section discusses the application and limitations of the program TRIMTV. Several recently proposed aircraft configurations use two lifting surfaces plus thrust vectoring, which results in redundant ways of generating moments and forces. Consequently there are many approaches to trim such airplanes. 'TRIMTV' is based on a method described in Ref. 12, which utilizes the linear optimum trim solution (LOTS), derived using a Lagrange formulation. It determines the longitudinal lift distribution (between the two surfaces and the jet nozzle deflection angle) which produces the minimum trim drag in level, steady state flight. The program also provides the deflection angles for the two lifting surfaces required to generate the desired lift distribution. Table 22 contains an example of the input.

Input

The required airplane geometry and other input parameters are defined in the ASCII file '2SURFACE.DAT.' Because of the constraints set by TRIMTV, users must be careful to use the units prescribe for each parameter and not to change the format of the values on the right column. Some input variables require additional discussion, and they are listed below. This program can also be applied to canard configurations by entering the canard geometry in place of the horizontal tail geometry.

a. l^{cg} (No. 3) is the distance between the *cg* and the wing AC, normalized with the mean chord of wing. NOTE: for measurements taken with respect to wing's AC, it is "+" if measured from below and/or behind the wing's AC, and it is "-" if measured from above and/or in front of the wing's AC.

b. σ_{e-ij} (No. 10-12) is the ratio of the Prandtl coefficient and efficiency factor between surface-*i* and surface-*j*. They can be obtained by using the approximation in Appendix C of NASA TP-2907 or by a vortex-lattice method (VLM).

c. k_1 & k_2 (No. 13 & 14) are the induced lift parameter of wing and horizontal tail due to thrust vectoring. The induced lift coefficient (due to thrust vectoring) is equal to the product of k , deflection angle and thrust coefficient. k is a constant depending on surface and nozzle factors. No analytical approach to determine the value of k was known to the authors of NASA TP-2907 at the time of publication. However, in general, the value of k approaches zero if there exists significant separation between the jet nozzle and the surface.

d. μ_{TL} (No. 15) is the fraction of thrust loss due to thrust vectoring. It is equal to 1 minus the fraction of thrust recovery. Thrust recovery takes the form of reduced induced drag as the consequence of the upwash field created in front of the surfaces of the airplane by the directed jet. μ_{TL} generally has a value between 0.0 and 0.5.

e. C_T (No. 16) is the thrust coefficient which is obtained by dividing thrust by the product of dynamic pressure and reference area. C_T is about equal to the total drag coefficient provided the jet nozzle deflection angle is relatively small.

f. δ_f (No. 26) is the optimal wing flap deflection angle (in terms of drag). The typical value is zero.

g. c_e/c_t (No. 35) is the ratio of the elevator chord to the H. tail chord. If all-moving (variable incident) tail is used, enter zero for this value. The program will determine the proper incident angle.

Table 22. Sample case for thrust vectoring code, TRIMTV

1.	Total lift coeff.	(W-bar)	+2.000E-01
2.	Zero-lift Moment Coeff.	(C-m,0)	-1.000E-01
3.	C.G. distance from wing AC	(l^-cg)	-5.600E-02
4.	Area of Wing, ft ²	(S-1)	+4.000E+02
5.	Area of H. tail, ft ²	(S-2)	+8.810E+01
6.	Span of Wing, ft	(b-1)	+3.750E+01
7.	Span of H. tail, ft	(b-2)	+1.470E+01
8.	Wing AC to H. tail AC, ft	(l-2)	+1.493E+01
9.	Wing AC to jet nozzle, ft	(l-3)	+1.920E+01
10.	Influence coeff-wing	(sigma/e-11)	+1.000E+00
11.	Influence coeff-H tail	(sigma/e-22)	+1.000E+00
12.	Influence coeff-wing-tail	(sigma/e-12)	+1.160E-01
13.	Induced lift parameter W-THR(k1)		+0.000E+00
14.	Induced lift parameter T-THR(k2)		+0.000E+00
15.	Fraction of thrust-loss	(MU-TL)	+5.000E-01
16.	Thrust coefficient	(C-T)	+2.000E-01
17.	Free stream Mach number	(M-infinity)	+5.000E-01
18.	Wing max thickness swp, rad	(lambda-t/c-1)	+3.491E-01
19.	Tail max thickness swp, rad	(lambda-t/c-2)	+6.981E-01
20.	Wing incident angle, rad	(i-1)	+0.000E-00
21.	Exhaust Nozzle height, ft	(z-3)	+0.000E+00
22.	Wing chord/4 sweep, rad	(lambda-c/4-1)	+3.491E-01
23.	H tail chord/4 swp, rad	(lambda-c/4-2)	+6.981E-01
24.	Flap chord/total wing chord	(c-f/c-w)	+2.000E-01
25.	Wing thickness ratio	(t/c-1)	+8.000E-02
26.	Optimal flap deflection,rad	(delta-f)	+0.000E-00
28.	Taper ratio of wing	(TR-1)	+3.500E-01
29.	Taper ratio of H tail	(TR-2)	+4.600E-01
30.	H. Tail Height, ft	(h-2)	+5.335E-01
35.	Elevator-tail chord ratio	(c-e/c-t)	+0.000E-00
36.	H tail thickness ratio	(t/c-2)	+6.200E-02
37.	H tail incident angle, rad	(i-tail)	+9.999E-00

Output

The output includes five key parameters. CL(1) and CL(2) are the lift coefficients of the wing and horizontal tail (or canard). The fuselage inclination angle (angle of attack), the horizontal tail (or canard) deflection angle and the jet nozzle deflection angle are also output. The jet nozzle deflection is measured with respect to the fuselage reference line. It is "+" if pointing down and "-" if pointing up. Because of the uncertainty involved in the estimation of thrust coefficient and the supercirculation parameters such as k1, k2 and Mu-TL, the results generated may require experimental validation. The values can be found in the ASCII file RESULTS, and are shown in Table 23.

Table 23. Sample output from TRIMTV

Trim drag code for two surface configurations
with thrust vectoring for control

NASA TP 2907 by Goodrich, Sliwa and Lallman
coded by Jacob Kay, Sept. 1991

Input for this case:

wbar	=	0.20000	cmo	=	-0.10000
lccg	=	-0.05600	s(1)	=	400.00000
s(2)	=	88.10000	b(1)	=	37.50000
b(2)	=	14.70000	l(2)	=	14.93000
l(3)	=	19.20000	sigmaoe(1,1)	=	1.00000
sigmaoe(2,2)	=	1.00000	sigmaoe(1,2)	=	0.11600
k1	=	0.00000	k2	=	0.00000
mutl	=	0.50000	ct	=	0.20000
mfs	=	0.50000	lammt(1)	=	0.34910
lammt(2)	=	0.69810	iwing	=	0.00000
z(3)	=	0.00000	LAMQC(2)	=	0.69810
LAMQC(1)	=	0.34910	TRW	=	0.08000
FCOWC	=	0.20000	TR(1)	=	0.35000
DELTAf	=	0.00000	H(2)	=	0.53350
TR(2)	=	0.46000	TOCT	=	0.06200
FCOCT	=	0.00000			
ITAIL	=	9.99900			

Output results:

Wing CL	=	0.25837
H. Tail C-L	=	-0.21027
Jet deflection angle (deg)	=	-7.38117

CDi	=	0.00667
Effective Span e	=	0.69181

AOA OF BODY REFERENCE LINE (DEG) = 4.50993

H TAIL INCIDENT ANGLE SHOULD BE = -9.55842

6. Control Authority Assessment Example: The F-18

An example of the control authority assessment process is discussed in this section using the F-18's geometry and mass properties. For this study, a controller is considered saturated when it is deflected by 25 degrees.

6.1 1-G Trim

The level-flight trim capability of the pitch controller was evaluated under various flight conditions. Table 24 summarizes the results. The most critical condition occurs at $V = 250$ ft/sec with maximum weight and the cg at its most forward location. In this case, less than 13 degrees of elevator deflection was needed, and the required angle of attack is nearly 30 deg. This exceeds the realm of linear aerodynamics; the predicted elevator deflection for trim may not be valid. Despite this problem, the configuration appears to exhibit adequate pitch control power to achieve 1-G trim.

Table 24. - 1-g Trim Assessment

Weight (lb)	Static Margin	Altitude (ft)	Speed (ft/sec)	α (deg)	Elevator (deg)
51 900	13.3 %	0	250	28.7	-12.4
51 900	13.3 %	0	1695	0.58	-0.93
38 400	5.4 %	50 000	600	20.5	-2.98
38 400	5.4 %	50 000	1030	3.23	-3.87

6.2 Maneuver Flight (Pull-up)

Table 25 summarizes the tests performed to check the pitch controller's effectiveness to satisfy the pull-up requirements. There may not be enough elevator power to generate the maximum load factor of 9-G's at the maximum speed at an altitude of 50,000 ft.

Table 25. - Maneuver Flight (Pull-up) Assessment

Weight (lb)	Static Margin	Altitude (ft)	Speed (ft/sec)	g's	α (deg)	Elevator (deg)
51 900	13.3 %	0	250	1.5	42.2	-19.1
51 900	13.3 %	0	1695	9.0	4.35	-2.0
38 400	5.4 %	50 000	600	1.5	34.4	-6.35
38 400	5.4 %	50 000	1030	9.0	24.6	-33.9

6.3 Steady Sideslip

The aircraft's ability to maintain sideslip at very low speed was evaluated. To achieve 30 degrees of sideslip, the rudder must be deflected 24.9 degrees. Allowing a 25% yaw control margin as prescribed by MIL-STD-1797, a steady sideslip angle of 18.5 degrees can be achieved in the test case. Therefore the configuration is expected to have enough control authority to land in a 30-knot cross-wind with a landing speed as low as 95 knots.

6.4 Engine-out Trim

The yaw and roll controllers' effectiveness was tested against adverse yaw conditions as a result of asymmetric loss of thrust. In this case, 15,000 lbs thrust is assumed to be generated by the right engine. Note that this asymmetric thrust is chosen near the maximum thrust of one engine to account for the additional drag because of possible sideslip and the asymmetric drag created by the failed engine. The results are shown in Table 26. Depending on the weight of the aircraft, there is sufficient rudder power to create -3.5 to +4.5 degrees of bank angle while complying with the requirement that no more than 75% of the yaw and roll effectiveness be used to cope with asymmetric thrust.

Table 26. - Engine-out Trim Assessment at Mach 0.2 (Sea Level)

Weight (lb)	Bank Angle (deg)	Sideslip (deg)	Aileron (deg)	Rudder (deg)
30 000	+4.5	+10.8	+6.9	+10.1
30 000	0.0	-3.3	+2.9	-3.3
30 000	-2.0	-9.5	+1.1	-9.2
30 000	-4.5	-18.0	-1.3	-17.2
40 000	+4.5	+15.5	+8.2	+14.5
40 000	0.0	-3.3	+2.9	-3.3
40 000	-3.5	-17.1	-1.3	-17.1

6.5 Takeoff and Landing Rotations

Assuming the takeoff flap setting is 10° , elevator trailing setting of 25° up, and maximum rotation angle of 15° , the stall speed (assuming the maximum total lift coefficient occurs when angle of attack reaches the maximum rotation angle) with a maximum weight of 51,900 lbs is estimated to be 303 ft/sec. Note the aerodynamic properties were based on VLM's prediction in ground effect with the *cg* at 6.5 ft above the ground. This model does not reflect the actual F-18 operation, which includes rudder toe-in to generate additional nose-up pitching moment. The results indicate that nose-up rotation can be initiated when the speed reaches 274 ft/s. A numerical integration is performed to check the speed when the maximum rotation angle is reached (which should occur before $0.9 V_{\min}$ according to MIL-STD-1797). The configuration failed to obtain the take-off attitude of 15-deg angle of attack prior to $0.9 V_{\min}$. Another 0.5 seconds of ground run past $0.9 V_{\min}$ is required before the desired angle of attack is reached. This simple simulation represents the worst condition, when the aircraft is configured with its maximum weight with the *cg* at its most forward location.

An analysis was also performed to check whether the pitch controller has enough authority to gently lower the nose down to 0.9 V_{min} in landing configuration. In this case, the flap is assumed to be set at 25 degrees. The touch down speed for maximum weight is estimated at 305 ft/sec. The total moment from touch down to 0.9 V_{min} is positive (nose-up) for all angles of attack. Therefore, the configuration has enough pitch authority to meet the landing requirement.

6.6 Time-to-Bank

The roll performance of the F-18 is assessed against the general time-to-bank requirement of table 8b. Table 27 summarizes the time required to roll through the specified angles along with the speed at which the configuration is tested. When compared to the Level 1 requirements in Table 8b, the F-18 demonstrates superior roll capability.

Table 27. - Time-to-bank Performance at Seal Level ($I_x = 26\ 000$ slug \cdot ft²)

	Speed (ft/sec)	30°		90°		180°		360°	
		Require d	Calc.	Require d	Calc.	Require d	Calc.	Require d	Calc.
VL	334	1.0	0.58						
L	368			1.4	0.91	2.3	1.40	4.1	2.25
M	468			1.0	0.73	1.6	1.10	2.8	1.77
H	1186			1.4	0.40	2.3	0.65	4.1	1.15

6.7 Pitch Due to Velocity Axis Roll

The test of pitch authority to counter velocity-axis roll was performed at Mach 0.6 at sea level. Assuming 60% of the total pitch effectiveness can be allocated to coping with the pitch-up tendency, a plot of maximum stability-axis roll rate vs. angle of attack can be obtained (Figure 22). The results were very similar to the actual aircraft. Depending on the performance requirement, the designer can decide whether the pitch controller will become a limiting factor in the configuration's stability-axis roll capability.

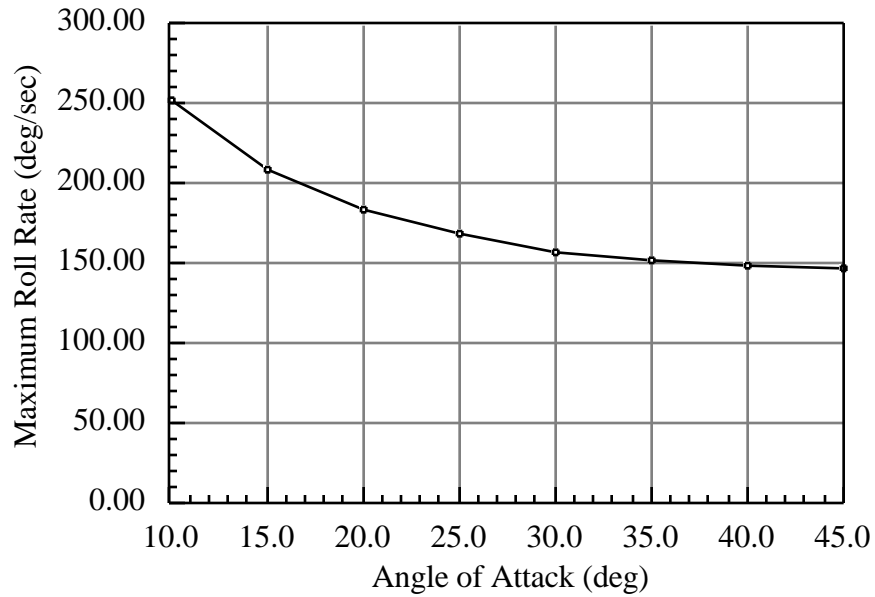


Figure 22. Estimated maximum stability axis roll rate of the F-18 limited by elevator power at sea level, Mach = 0.6

6.8 Rolling Pullout & Coordinated Roll

To assess the configuration's yaw and roll control effectiveness, an analysis was performed at Mach .6 at sea level. Different combinations of roll rate, roll acceleration and normal load factors were applied. Table 28 indicates that coordinated roll performance of the F-18 appears to be limited mainly by the lack of yaw control authority.

Table 28. - Rolling Pullout & Coordinated Roll Assessment at Sea Level (M = 0.6)

P _{stab} (deg/s)	p-dot _{stab} (deg/s ²)	Load Factor (g)	α (deg)	Rudder (deg)	Aileron (deg)
180	0	0.0	0.0	-4.9	+12.5
180	0	2.0	3.1	-8.0	+13.0
180	0	4.0	6.3	-12.2	+13.5
360	0	0.0	0.0	-9.8	+25.0
360	0	2.0	3.1	-17.0	+26.1
0	180	5.0	45.0	-27.1	+7.5
0	360	5.0	18.0	-24.0	+10.7
180	180	5.0	28.0	-23.5	+16.1

6.9 Short Period & CAP Requirements

Short period & Control Anticipation Parameter (CAP) tests were performed at different potentially critical flight conditions (Table 29). All but the Mach 1.2 case satisfy the level-1 flying quality requirements. Inadequate damping resulting in a level-2 condition is observed at Mach 1.2. at an altitude of 10,000 ft. However, the deficiency appears to be small enough to allow the augmented flight control systems to correct the problem.

Table 29. - Short Period & Control Anticipation Parameter (CAP) Assessment

Weight (lb)	Static Margin (%c)	Altitude (ft)	Mach	Natural Frequency	Damping Ratio	CAP (1/g/s ²)
50 000	13.2	0	0.2	0.78	0.42	0.256
24 800	13.2	0	0.2	0.98	0.57	0.202
36 000	5.4	10 000	0.8	3.48	0.40	0.286
36 000	5.4	10 000	1.2	10.06	0.22	1.061

6.10 Overall Assessment

The F-18 appears to lack elevator power to obtain the take-off attitude during the takeoff roll with maximum weight and the *cg* at its most forward location. This problem alone does not warrant increasing the horizontal tail volume. A possible alternative is to decrease the tip-back angle by moving the main gear forward. The rudder power appears to be marginally adequate while there is sufficient roll authority.

7. Conclusions

In this study, a methodology that allows aircraft designers to quickly assess candidate concepts against the control authority requirements early in the design phase was established. Flight conditions and maneuvers that result in great demands on control power were identified. A vortex lattice method program was written to estimate the design's stability and control derivatives for subsonic, low angle-of-attack flight regimes. Finally, a spreadsheet was created to assess whether the configuration possesses sufficient control power by application of the estimated stability and control derivatives to the dynamics equations. Applying this methodology should ensure that the conceptual design team can identify deficient control power early in the preliminary design stage, when design modifications can be made without major complications.

7.1 Future Work

Although this study has identified many critical maneuvers and flight conditions that are known to deplete available control authority, future super agile aircraft with frequent excursions into the high angle-of-attack regime are likely to demand even more control authority. To assure stability and controllability at high angle of attack, the designers will need to be able to evaluate the configurations' aerodynamic characteristics at high angle of attack.

To improve the accuracy of the stability and control derivative estimates for subsonic, low-angle of attack flight, a more sophisticated vortex lattice method with more efficient use of panels should be explored. A better fuselage representation could further enhance accuracy of the stability and control derivative estimates. The calculation of the vortex lift effects would improve the estimation of the high-angle of attack aerodynamic characteristics. In addition, effects of aeroelasticity and viscosity should be approximated

using empirical correlation approach. If sufficient reliability can be achieved, the control authority assessment process can even be incorporated as part of the design optimization cycle. Finally, the incorporation of estimating the supersonic aerodynamic characteristics would allow for the evaluation of the aircraft control power over a larger speed range.

The possibility of using thrust vectoring to augment the longitudinal and lateral/directional controllers introduces a new dimension to the problem. Issues such as control power allocation should be considered in the conceptual design stage due to redundant controllers.

References

1. Dave Wyatt, personal communication, Lockheed-Ft. Worth, Aug. 1993.
2. MIL-STD-1797. *Flying Qualities of Piloted Vehicle*. 1987.
3. FAR Part 23 and Part 25, FAA, Washington, DC.
4. Vincenti, W.G., "Establishment of Design Requirements: Flying Qualities Specifications for American Aircraft, 1918-1943," in *What Engineers Know and How They Know It*, Johns Hopkins Univ. Press, Baltimore, 1990. pp. 51-111.
5. Hoak, D. E.; Ellison, D. E. et al.; USAF Stability and Control DATCOM; Flight Control Division; Air Force Flight Dynamics Laboratory, Wright Patterson Air Force Base, Ohio.
6. Roskam, J. *Airplane Design. Part VII: Determination of Stability, Control and Performance Characteristics: FAR and Military Requirements*. Roskam Aviation and Engineering Corporation, Kansas, 1988.
7. Woodcock, R.J., and Drake, D.E., "Estimation of Flying Qualities of Piloted Airplanes," AFFDL-TR-65-218, 1965.
8. Thomas, R.W., "Analysis of Aircraft Stability and Control Methods," AFWAL-TR-84-3038, May 1984.
9. Simon, J., Blake, W., and Multhopp, D., "Control Concepts for a Vertical Tailless Fighter," AIAA Paper 93-4000, Aug. 1993.
10. Ogburn, M.E., Foster, J.V., Pahle, J.W., Wilson, R.J., and Lackey, J.B., "Status of the Validation of High-Angle-of-Attack Nose-Down Pitch Control Margin Design Guidelines," AIAA Paper 93-3623, Aug. 1993.
11. Foster, J.V., Ross, H.M., and Ashley, P.A., "Investigation of High-Alpha Lateral-Directional Control Power Requirements for High-Performance Aircraft," AIAA Paper 93-3647, Aug. 1993.

12. Goodrich, K.H., Sliwa, S.M., and Lallman, F.J., "A Closed-form Trim Solution Yielding Minimum Trim Drag for Airplanes with Multiple Longitudinal Control Effectors," NASA TP-2907, May 1989
13. MIL-W-25140 Weight and Balance Control Data for Airplanes and Rotorcraft.
14. Roskam, Jan, *Airplane Design Part V Component Weight Estimation*, Roskam Aviation and Engineering Corporation, Ottawa, Kansas, 1988.
15. MIL 8785C
16. Etkin, B, *Dynamics of Atmospheric Flight*, John Wiley & Sons, Inc., New York, 1972.
17. Holloway, Richard B., and Burris, Paul M., "Aircraft Performance Benefits from Modern Control Systems Technology," *Journal of Aircraft*, Vol. 7, No. 6, Nov.-Dec. 1970, pp. 550-553.
18. Kroo, I., "Tail Sizing for Fuel-Efficient Transports," AIAA Paper 83-2476, 1983.
19. Swanson, S.M., "A Computer Module Used to Calculate the Horizontal Control Surface Size of a Conceptual Aircraft Design," MS Thesis, Cal Poly, San Luis Obispo, Jan. 1990.
20. Lamar, J.E., "A Vortex Lattice Method for the Mean Camber Shapes of Trimmed Non-Coplanar Planforms with Minimum Vortex Drag," NASA TN D-8090, June 1976.
21. Mason, W.H., Wing-Canard Aerodynamics at Transonic Speeds—Fundamental Considerations on Minimum Drag Spanloads," AIAA 82-0097, Jan. 1982.
22. Durham, W.C., "Constrained Control Allocation," *Journal of Guidance and Control and Dynamics*, Vol. 16, No. 4, July-August 1993, pp.717-725

23. Durham, W.C., "Constrained Control Allocation: The Three-Moment Problem," *Journal of Guidance and Control and Dynamics* , Vol. 17, No. 2, March-April 1994, pp. 330-336
24. Lallman, F.J., "Relative Control Effectiveness Technique With Application to Airplane Control Coordination," NASA TP 2416, April 1986.
25. Chody, J. R., Hodgkinson, J. and Skow, A. M., "Combat Aircraft Control Requirements for Agility," AGARD CP-465, Oct. 1989.
26. Nguyen, L. T., Ogburn, M. E., Gilbert, W. P., Kibler, K. S., Brown, P. W., and Deal, P. L., "Simulator Study of Stall/Post-Stall Characteristics of a Fighter Airplane with Relaxed Longitudinal Static Stability," NASA TP-1538, NASA-Langley, Dec. 1979.
27. Durham, W., Lutze, F., and Mason, W.H., "Kinematics and Aerodynamics of the Velocity Vector Roll," AIAA Paper 93-3625, Aug. 1993.
28. Mercadante, R., "Basic Agility/Control Power Requirements for Advanced Supersonic Fighter Configurations," Grumman Memorandum, EG-ARDYN-83-82. Oct. 1983.
29. Nelson, R. C., *Flight Stability and Automatic Control*, McGraw-Hill Co, New York, 1989.
30. Lutze, F. H., Durham, W. C., and Mason, W. H., "Lateral-Directional Departure Criteria," AIAA Paper 93-3650, Aug. 1993.
31. Johnston, D.E., and Heffley, R. K., "Investigation of High AOA Flying Quality Criteria & Design Guides," AFWAL-TR-81-3108, December 1981.
32. Bihrlé, W., Jr. and Barnhart, B., "Departure Susceptibility and Uncoordinated Roll-Reversal Boundaries for Fighter Configurations," *Journal of Aircraft*, Vol. 19, No. 11, Nov. 1982, P. 897.
33. Roskam, J., and Dusto, A., "A Method for Predicting Longitudinal Stability Derivatives of Rigid and Elastic Airplanes," *Journal of Aircraft*, Vol. 6, No.

6, Nov.-Dec. 1969, pp. 525-531.

34. Citurs, K.D., Buckley, J.E., and Doll, K.A., "Investigation of Roll Requirements for Carrier Approach," AIAA Paper 93-3649, Aug. 1993.
35. Bertin, J. and Smith, M., *Aerodynamics for Engineers*, 2nd ed., Prentice Hall, New Jersey, 1989.
36. Katz, J. and Plotkin, A., *Low-Speed Aerodynamics: From Wing Theory to Panel Methods*, McGraw-Hill, Inc. New York, 1991.
37. Roskam, J., *Methods for Estimating Stability and Control Derivatives of Conventional Subsonic Airplanes*, Roskam Aviation and Engineering Corporation, Kansas, 1971.
38. Lamar, J. E. and Gloss, B. B., "Subsonic Aerodynamics Characteristics of Interacting Lifting Surface with Separate Flow Around Sharp Edges Predicted by a Vortex-Lattice Method," NASA TN D-7921, Sept., 1975

Appendix A. Program and Spreadsheet Documentation

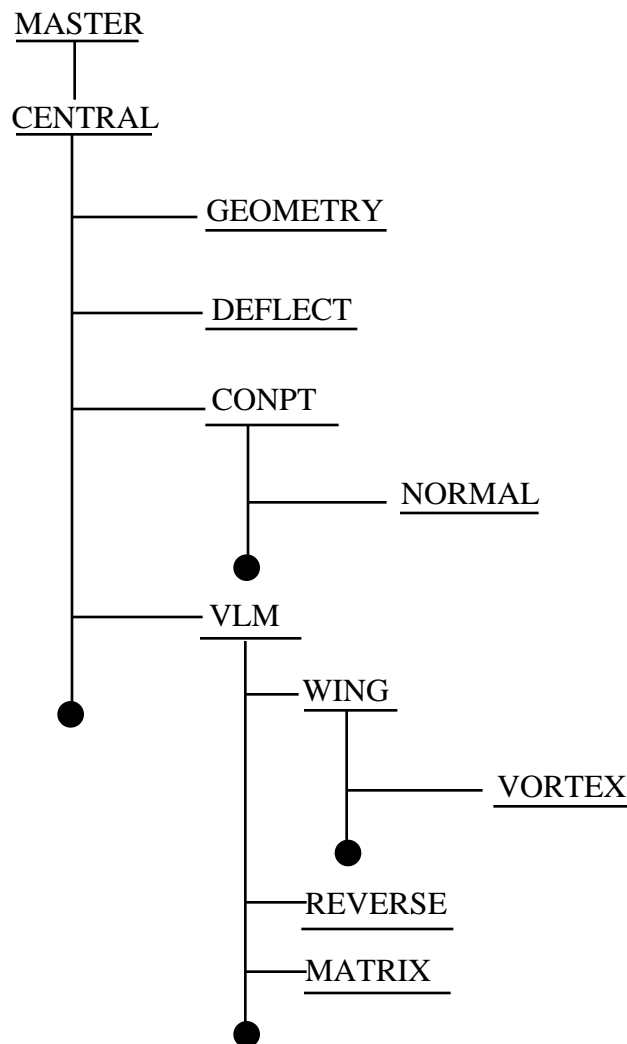
A1. JKayVLM Program

The vortex lattice method (JKayVLM) program developed in this study was written in Microsoft FORTRAN to be used on IBM compatible PCs. It also runs on a Mac using Language Systems FORTRAN and the SGI Workstations. The program's major subroutines and their functions are:

Prgm/Subrtn	Functions
MASTER	User interface. Controls variation in flow. (control deflection, AOA, etc.) Calls CENTRAL. Performs finite difference on forces & moments. Stab. & control derivatives output.
CENTRAL	Reads GEOMETRY & LATGEOM for corner points. Calls GEOMETRY; DEFLECT; CONPT; VLM.
GEOMETRY	Determines corner pts of vortex rings.
DEFLECT	Rotates corner points about the hinge line in 3-D.
CONPT	Determines control point locations. Calls NORMAL.
NORMAL	Determines panels' normal vectors & areas.
VLM	Calls WING to calc. Influence Coefficient. Calls REVERSE to reverse surface deflection for asymmetric deflection. Calls MATRIX to solve for vortex strengths. Calculates Forces and Moments.
WING	Determines the induced velocity at control points by a vortex ring. Calls VORTEX.
VORTEX	Uses Biot-Savart Law to find induced velocity at a point by a vortex segment.
MATRIX	Solves a system of linear equations.
REVERSE	Reverses control surface's deflection for antisymmetric deflection cases.

The connection between JKayVLM's subroutines is illustrated in the diagram below. Note in the output, positive control deflection is TE down and LE up for longitudinal controls and TE right for directional controls. In addition, the lift-curve slope of the horizontal tail due to the downwash of the wing is also available to be used to determine C-m-alpha-dot of the horizontal tail.

JKayVLM Program Subroutine Tree



A2. Spreadsheet to Check Control Authority Requirements

A Lotus-1-2-3 worksheet (now also available in EXCEL) was created to check if the design configuration is able to meet the control authority requirements. It contains items discussed in section 2.1 through 2.2.6. The following is the sample worksheet. The spreadsheet has eleven sections,

1. Nose-wheel Lift-off
2. Nose-down Rotation During Landing Rollout
3. Trimmed 1-G Flight
4. Maneuvering Flight (Pull-up)
5. Short Period & Control Anticipation Parameter (CAP)
6. Pitch Due to Roll Inertial Coupling
7. Time-to-Bank Performance
8. Steady Sideslip Flights (Aileron & Rudder Deflections)
9. Engine-out Trim (Aileron & Rudder Deflections)
10. Roll Pullout
11. Initiate & Maintain Coordinated Velocity Axis Roll

Each one is printed out on the following pages.

1. Nose-wheel Lift-off

 Nose-wheel Lift-off

Input:	Max Takeoff Gross Weight (lbs)	51900
	Max Takeoff Thrust (lbs)	33700
	Thrust Incident Angle (rad)	0
	Reference Area (ft^2)	400
	Reference Chord (ft)	11.52
	Horiz. Dist. CG to main gear axle (ft)	4.2
	Vert. Dist. CG to main gear axle (ft)	5.4
	Horiz. Dist. CG to engine nozzle (ft)	20
	Vert. Dist. CG to engine nozzle (ft)	-0.55
	Rolling Coefficient: tire & runway surface	0.025
	Total C-m with deflected flaps & pitch controllers	0.585
	Total C-L with deflected flaps & pitch controllers	-0.222
	Air Density (slug/ft^3)	0.002376
	Zero-lift Drag Coef, CD0	0.02
	CDi/CL^2	0.055
Calc.	Dynamic Pressure to Start Rotation, (lbs/ft^2)	89.344
	Moment Arm (ft)	6.8410
	Tip-Back Angle (rad)	0.6610
Output:	Speed for Rotation (ft/sec)	274.236
	Speed for Rotation (knots)	162.485

 Integration to check pitch attitude at .9 V-min

Time Increment (s)	0.1
I-y about CG (slug ft^2)	140000

V (ft/s)	AOA(rad)	C-L	C-D	C-m	Dyn Press	AOA"	AOA-dot
274.23	0	-0.222	0.0227	0.585	89.344	0.0000	0
276.4	0	-0.222	0.0227	0.585	90.8061	0.0241	0.0012
278.70	0.00012	-0.2213	0.0226	0.584	92.2803	0.0491	0.0048
280.94	0.00060	-0.2187	0.0226	0.584	93.7669	0.0766	0.0111
283.1	0.00172	-0.2128	0.0224	0.583	95.2658	0.1083	0.0204
285.41	0.00376	-0.2020	0.0222	0.580	96.7769	0.1459	0.0331
287.65	0.00707	-0.1844	0.0218	0.577	98.2996	0.1916	0.0500
289.88	0.01207	-0.1578	0.0213	0.571	99.8335	0.2479	0.0719
292.12	0.01927	-0.1196	0.0207	0.563	101.377	0.3178	0.1002
294.350	0.02930	-0.0663	0.0202	0.552	102.931	0.4043	0.1363
.							
.							
.							
314.51	0.43805	2.10407	0.26349	0.1040	117.515	1.2701	1.0525
317.07	0.54331	2.66300	0.41003	-0.0115	119.441	0.7318	1.1526
319.94	0.65858	3.27508	0.60993	-0.1381	121.606	-0.2486	1.1768

2. Nose-down Rotation During Landing Rollout

 Nose-down Rotation During Landing Rollout

Input:	Max Landing Weight (lbs)	51900	
	Landing Thrust (lbs)	12000	
	Thrust Incident Angle (rad)	0	
	Reference Area (ft ²)	400	
	Reference Chord (ft)	11.52	
	Horiz. Dist. CG to main gear axle (ft)		4.2
	Vert. Dist. CG to main gear axle (ft)	5.4	
	Horiz. Dist. CG to engine nozzle (ft)	20	
	Vert. Dist. CG to engine nozzle (ft)	-0.55	
	Rolling Coefficient: tire & runway surface	0.025	
	Air Density (slug/ft ³)	0.002376	
	I-y about CG (slug ft ²)	140000	
	Zero-lift Drag Coef, CD0	0.02	
	CDi/CL ²	0.055	
	Tip-Back Angle (rad)	0.661043	
	Moment Arm (ft)	6.841052	

Check for Nose-up Moment from T.D. to 0.9 V-min

V (ft/s)	Dyn Press	AOA (rad)	C-L	C-D	C-m	Pitch M	q-dot
305	110.5137	0.262	1.42262	0.1313121	0.29102	194491.0	1.389221
305	110.5137	0.1	0.5624	0.0373961	0.4689	147585.5	1.054182
305	110.5137	0	0.0314	0.0200542	0.5787	82332.01	0.588085
277	91.154052	0.262	1.42262	0.1313116	0.29102	137510.8	0.982220
277	91.154052	0.1	0.5624	0.0373961	0.4689	89272.26	0.637659
277	91.154052	0	0.0314	0.0200542	0.5787	29652.53	0.211803

3. Trimmed 1-G Flight

 Trimmed 1-G Flight

Input:	Weight (lbs)	
	51900	
	Reference Area (ft ²)	400
	Speed (ft/s)	400
	Air Density (slug/ft ³)	0.002376
	C-m-0	0.0181
	C-m-delta E (/rad)	-1.117
	C-L-0	-0.0685
	C-L-delta E (/rad)	0.8688
	C-m / C-L (-Static Margin)	-0.13
	C-L-alpha (/rad)	4

Output:	C-L Required for 1-g trim	0.6826073
	Elevator Deflection for Trim (deg)	-4.53912205
	AOA Required for 1-g Trim (deg)	11.744717

4. Maneuvering Flight (Pull-up)

 Maneuvering Flight (Pull-up)

Input:	Weight (lbs)	51900
	Reference Area (ft ²)	400
	Reference Chord (ft)	11.52
	Speed (ft/s)	1695
	Air Density (slug/ft ³)	0.002376
	Dynamic Pressure (lbf/ft ²)	3413.1537

	C-m-0	0
	C-m-delta E (/rad)	-1.06
	C-L-0	0
	C-L-delta E (/rad)	0.65
	C-m / C-L (-Static Margin)	-0.35
	C-L-alpha (/rad)	5.57
	C-m-q (rad)	-6.22
	C-L-q (rad)	5.51
	Load Factor, (g)	5

Calc.	C-L Required for 1-g trim	0.0380147
	Elevator Deflection for 1-g Trim (rad)	-0.015982
	AOA for 1-g Trim (rad)	0.00868

	RHS1:	0.1463674
	RHS2:	0.0016061

[A]:	5.57	0.65
	-1.9495	-1.06

[A]^1:	0.2285948	0.1401761
	-0.42042	-1.201201

Macro: /dmig160.h161~g163.h164~/dmmg163.h164~h157.h158~h168.h169~

Output:	Delta-alpha (rad)	0.033684
	Delta-delta E (rad)	-0.063465

	Total AOA required (deg)	2.4278492
	Total Elevator Deflection (deg)	-4.551998

NOTE: Press <ALT-M> to recalculate (on a Mac use the menu bar)

5. Short Period & Control Anticipation Parameter (CAP)

 Short Period & Control Anticipation Parameter (CAP)

Input:	Weight (lbs)	34297
	I-y (slug ft ²)	123936
	Reference Area (ft ²)	400
	Reference Chord (ft)	11.52
	Speed (ft/s)	1291
	Density (slug/ft ³)	0.001755
	Dynamic Pressure, q (lbf/ft ²)	1462.5125
	C-L-alpha (/rad)	5.6
	C-m-alpha (/rad)	-1.79
	C-m-q (/rad)	-6.86
	C-m-alpha-dot (/rad)	-1.5
Output:	Natural Frequency (/s)	10.06478
	Damping Ratio	0.2191138
	N-alpha (G/rad)	95.51937
	Control Anticipation Parameter, CAP (rad/sec ² /g)	1.0605157
	Control Anticipation Parameter, CAP (deg/sec ² /g)	60.763075
::		

6. Pitch Due to Roll Inertial Coupling

 Pitch Due to Roll Inertial Coupling

Input:	Weight (lbs)	500
	I-x (slug ft ²)	23168
	I-y (slug ft ²)	123936
	I-z (slug ft ²)	143239
	Reference Area (ft ²)	400
	Reference Chord (ft)	11.52
	Density (slug/ft ³)	0.002376
	Speed (ft/s)	670
	Velocity Axis Roll Rate (deg/sec)	147
	Angle of Attack (deg)	60
	C-m-delta-E (/rad)	-1.23
Output:	Dynamic Pressure, q (lbf/ft ²)	533.2932
	Pitch Moment Coeff. due to Roll Coupling(+ or -)	0.2785349
	Additional Elev. Deflection to Counter Coupling (rad)	0.2264511
	Additional Elev. Deflection to Counter Coupling (deg)	12.974695

7. Time-to-Bank Performance

Time-to-Bank Performance

Input:	I-x (slug ft ²)	26000
	Reference Area (ft ²)	400
	Reference Span (ft ²)	34.72
	Air Density (slug/ft ³)	0.002376
	Speed (ft/sec)	334
	Max Aileron Deflection Rate (rad/sec)	3.1
	Max Aileron Deflection Angle (rad)	0.436
	C-l-delta-Aileron (/rad)	0.17
	C-l-p, roll rate damping (/rad)	-0.4239
	Integration Time Step (sec)	0.05
Output:	Dynamic Pressure (lbf/ft ²)	132.528
	L-delta-Aileron (lbf-ft/rad)	312894.553
	L-p (lbf-ft/rad)	-40552.324
	Time to Max Aileron Deflection (sec)	0.14064

Integration to Check Roll Performance:

Time (sec)	Delta-A (rad)	Delta-A (deg)	L-total (lbf-ft)	p-dot (rad/s ²)	p (rad/sec)	Bank Angle (rad)	Bank Angle (deg)
0	0	0	0	0	0	0	0
0.05	0.155	8.8808	48498.65	1.86533	0.0466	0.001	0.066
0.1	0.31	17.761	95106.22	3.65793	0.1847	0.006	0.398
0.15	0.436	24.980	128931.4	4.95890	0.4001	0.021	1.235
0.2	0.436	24.980	120195.5	4.62290	0.6396	0.047	2.725
0.25	0.436	24.980	110481.4	4.24928	0.8614	0.085	4.875
0.3	0.436	24.980	101486.7	3.90333	1.0653	0.133	7.635
0.35	0.436	24.980	93221.57	3.58544	1.2525	0.191	10.95
0.4	0.436	24.980	85629.38	3.29343	1.4244	0.258	14.79
.							
.							
.							
1	0.436	24.9809	30895.78	1.188299	2.66427	1.546	88.60
1.05	0.436	24.9809	28379.55	1.091521	2.72126	1.681	96.31
1.1	0.436	24.9809	26068.25	1.002625	2.77362	1.818	104.1
1.15	0.436	24.9809	23945.19	0.920968	2.82171	1.958	112.2
.							
.							
.							

8. Steady Sideslip Flights (Aileron & Rudder Deflections)

Steady Sideslip Flights (Aileron & Rudder Deflections)

Input:	Sideslip Angle, beta, (deg)	18.5
	Sideslip Angle, beta, (rad)	0.3228859
	C-l-beta (/rad)	-0.05025
	C-n-beta (/rad)	0.09169
	C-l-delta-Aileron (/rad)	0.171
	C-n-delta-Aileron (/rad)	-0.0045
	C-l-delta-rudder (/rad)	0.0337
	C-n-delta-rudder (/rad)	-0.08988
Output:	Aileron Deflection (rad)	0.0302672
	Aileron Deflection (deg)	1.7341871
	Rudder Deflection (rad)	0.3278727
	Rudder Deflection (deg)	18.785727

9. Engine-out Trim (Aileron & Rudder Deflections)

Engine-out Trim (Aileron & Rudder Deflections)

Input:	C-l-beta (/rad)	-0.0803
	C-n-beta (/rad)	0.0868
	C-Y-beta (/rad)	-0.532
	C-l-delta-Aileron (/rad)	0.171
	C-n-delta-Aileron (/rad)	-0.0046
	C-Y-delta-Aileron (/rad)	0
	C-l-delta-rudder (/rad)	0.033
	C-n-delta-rudder (/rad)	-0.09
	C-Y-delta-rudder (/rad)	0.22
	Thrust Difference (lbf)	15000
	Engine Nozzle's X-dist. from CG (ft)	21
	Engine Nozzle's Y-dist. from CG (ft)	1.5
	Vertical Nozzle Deflection (deg)	0
	Horizontal Nozzle Deflection (deg)	2
	Speed (ft/sec)	250
	Air Density (slug/ft^3)	0.002376
	Weight (lbs)	40000
	Reference Area (ft^2)	400
	Reference Span (ft)	34.72
	Dynamic Pressure (lbf/ft^2)	74.25
	Bank Angle (deg)	3
Calc:	C-Y-delta-Thrust	-0.017626

C-n-delta-Thrust			-0.011145
C-l-delta-Thrust			0
RHS1			-0.052860
RHS2			0
RHS3			0.011145
Matrix A:	-0.532	0.22	0
	-0.0803	0.033	0.171
	0.0868	-0.09	-0.0046
Inverse A:	-3.095578	-0.205583	-7.642349
	-2.940216	-0.497138	-18.480590
	-0.886244	5.847352	-0.0223460
Macros:	/dmid355.f357~d359~/dmmd359.f361~h351.h353~h366~		
Note:	Hit <ALT-I> to Recalculate		
Output:	Sideslip Angle (rad)		0.078455
	Rudder Deflection (rad)		-0.050553
	Aileron Deflection (rad)		0.046597
	Sideslip Angle (deg)		4.495178
	Rudder Deflection (deg)		-2.896488
	Aileron Deflection (deg)		2.669865

10. Roll Pullout

```

*****
Roll Pullout
*****

```

Input:	I-x (slug ft^2)	23168
	I-y (slug ft^2)	123936
	I-z (slug ft^2)	143239
	Reference Area (ft^2)	400
	Reference Span (ft)	34.72
	Density (slug/ft^3)	0.002376
	Speed (ft/s)	400
	Velocity Axis Roll Rate (deg/sec)	180
	Normal Load Factor (g's)	2
	Angle of Attack (deg)	45
	C-n-delta-R (/rad)	-0.08
Output:	Dynamic Pressure (lbf/ft^2)	190.08
	Max. Yaw Coefficient due to Roll Pullout	-0.020478
	Rudder Deflection to Counter (deg)	-14.6666

11. Initiate & Maintain Coordinated Velocity Axis Roll

Initiate & Maintain Coordinated Velocity Axis Roll

Input:	Weight(lbs)			25000
	I-x (slug ft^2)			23168
	I-y (slug ft^2)			123936
	I-z (slug ft^2)			143239
	Reference Area (ft^2)			400
	Reference Span (ft)			34.72
	Density (slug/ft^3)			0.002376
	Speed (ft/s)			670
	C-l-p (/rad)			-0.432
	C-n-p (/rad)			-0.0696
	C-l-r (/rad)			0.03223
	C-n-r (/rad)			-0.183
	C-l-delta-Aileron (/rad)			0.175
	C-n-delta-Aileron (/rad)			-0.00045
	C-l-delta-Rudder (/rad)			0.034
	C-n-delta-Rudder (/rad)			-0.091
	Velocity Axis Roll Rate (deg/s)			180
	Velocity Axis Roll Accel (deg/s^2)			90
	Angle of Attack (deg)			28
	Normal Load Factor (g)			5
Calc:	AOA (rad)			0.4886921
	Dynamic Pressure * Ref. Area * Ref. Span (lbf-ft)			7406376
	L-p (ft-lbf/(rad/sec))			-82901.88
	L-r (ft-lbf/(rad/sec))			6185.0181
	N-p (ft-lbf/(rad/sec))			-13356.41
	N-r (ft-lbf/(rad/sec))			-35118.16
	RHS1 (ft-lbf)			261178.06
	RHS2 (ft-lbf)			275075.86
	Matrix A:	L-del-R	L-del-A	251816.78
		N-del-R	N-del-A	-673980.2
	A^-1:			-3.8E-09
				7.7E-07
				-1.5E-06
				2.9E-07
Macro:	/DMIG439.H440~G442~/DMMG442.H443~H436.H437~H447~			
	Rudder Deflection (rad)			-0.409526
	Aileron Deflection (rad)			0.2810733
	Rudder Deflection (deg)			-23.46413
	Aileron Deflection (deg)			16.104319
NOTE:	Hit <ALT-C> to Recalculate			

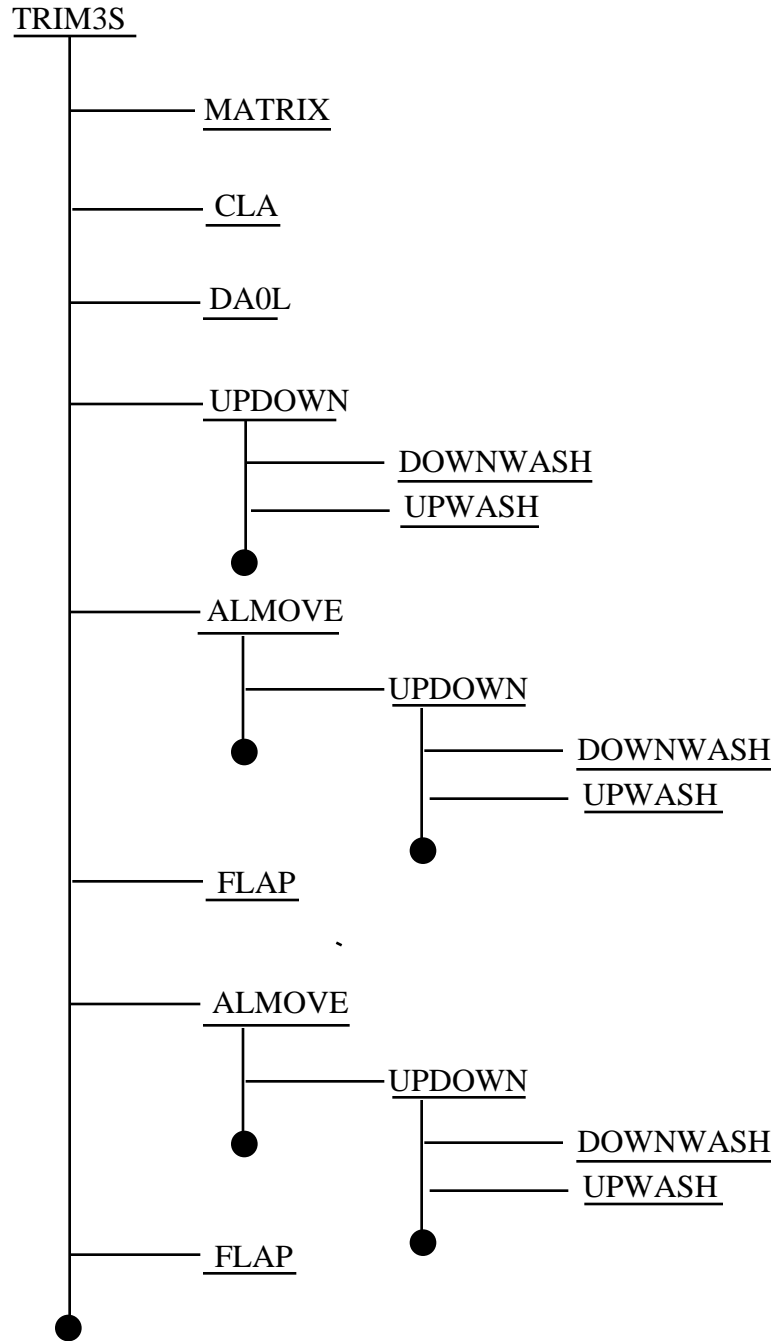
A3. Program FLTCOND

Program FLTCOND was written in Microsoft FORTRAN for IBM compatible PCs. Sample input (with Lotus-123 spreadsheet) and output is shown in Figures 3 & 4 respectively. Note the value column in the input worksheet is to be written to a file FCINPUT.PRN to be read by FLTCOND. In the output of FLTCOND, variables with values of '.900E+16' signifies that the variable need not be specified in the control power requirement check worksheet discussed in A2.

A4. Programs TRIM3S & TRIMTV

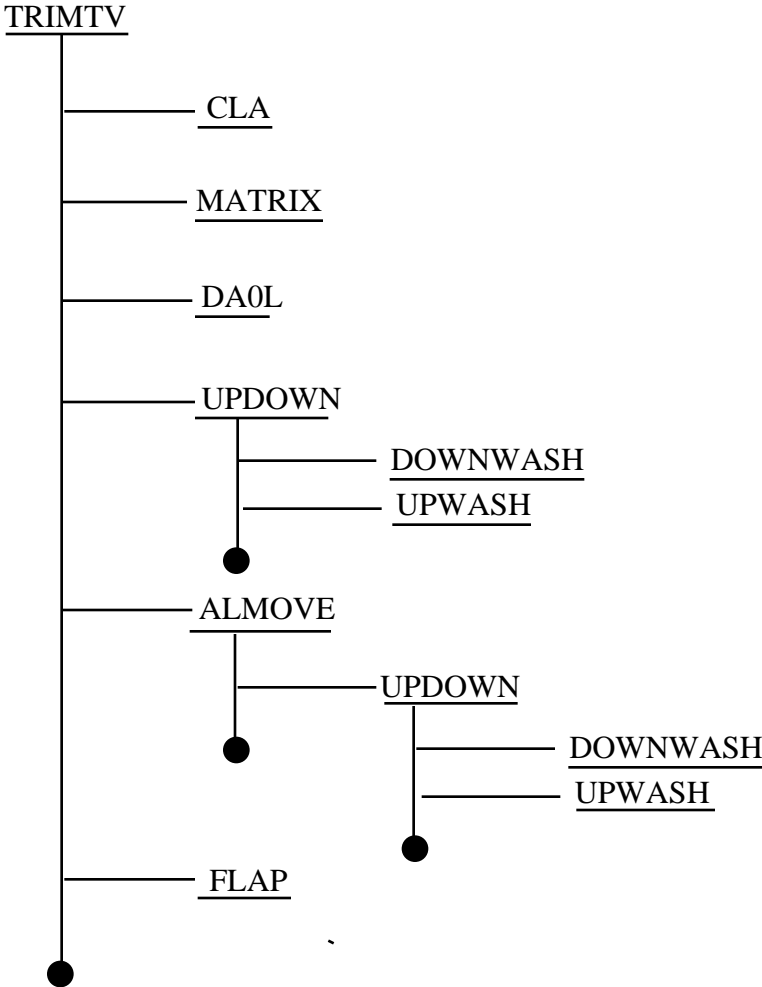
The subroutine tree for TRIM3S is:

TRIM3S Program Subroutine Tree



The subroutine tree for TRIMTV is:

TRIMTV Program Subroutine Tree



Appendix B

Annotated Bibliography and Extended Reference List: Control Power Requirements

Developed partially under NASA/US Navy support
October 15, 1991, rev. May 14, 1992, August 6, 1993

Defining control power requirements for advanced aircraft has become a difficult job. Recently, control power requirements have emerged to produce a first order effect on the aircraft concept. Previously, stability was a key requirement. However, flight control systems can now augment inherent stability, relaxing previous requirements. Instead, the defining issue for concept viability is the capability of the vehicle control effectors to provide the forces and moments required by the control system. Modern concepts employ multiple means of producing these forces and moments. The subject has attracted considerable attention, and this appendix provides a summary of related papers and reports. It follows a tradition, apparently started by Seckel in the aerospace vehicle control world, of providing bibliography lists and sample aircraft characteristics.

Classification of Reports:

The following classification has been used to try to separate papers according to specialized topics. The list is tutorial in that classical textbooks have been included to introduce the aircraft design engineer to the area.

- AGARD Reports
- Textbooks
- A. Traditional (Classical)
 - A-1. Criteria and Methods
- B. Relaxed Static Stability
- C. Lateral/Directional and Roll Performance Issues
- D. High Angle of Attack
 - D-1. Longitudinal
 - D-2. Lateral/Directional, including departure
- E. Agility
- F. Post-Stall Maneuvering
- G. Design Issues Related to Vehicle Control
 - G-1. Canard-Tail Comparisons
- H. Aerodynamic Characteristics
 - H-1. Propulsion related controls
- I. Specific Aircraft
 - I-1. Representative "Math Model" Data
 - I-1. Detailed "Math Models"

AGARD

AGARD reports provide a valuable, focused, source of information, nicely collected by topic. The following list provides an entry into the report series volumes related to control power.

- CP-17 Stability and Control, September 1966
- CP-106 Handling Qualities Criteria, October 1971
- CP-119 Stability and Control, 1972
- CP-147 Aircraft Design Integration and Optimization, 1973
(early impact of CCV on design)
- CP-157 Impact of Active Control Technology on Airplane Design, October 1974
- CP-199 Stall/Spin Problems of Military Aircraft, 1976
- CP-235 Dynamic Stability Parameters
- CP-260 Stability and Control, 1978
- CP-262 Aerodynamic Characteristics of Controls, Sept. 1979
- CP-333 Criteria for Handling Qualities of Military Aircraft, April 1982
- CP-465 Aerodynamics of Combat Aircraft Controls and of Ground Effects,
October 1989
- CP-497 Manoeuvring Aerodynamics, Nov. 1991
(section on stability and control)
- CP-508 Flying Qualities, October 1990

- AR-155A Manoeuvre Limitations of Combat Aircraft, August 1979
- AR-279 Handling Qualities of Unstable Highly Augmented Aircraft, May 1991

- LS-114 Dynamic Stability Parameters, May 1981
- LS-153 Integrated Design of Advanced Fighters, 1987

TextBooks

Ashley, H., *Engineering Analysis of Flight Vehicles*, Addison-Wesley, Reading, 1974. This book has a simple, effective overview presentation of flight mechanics.

Etkin, B., *Dynamics of Atmospheric Flight*, John Wiley & Sons, Inc., New York, 1972.

McRuer, D., Ashkenas, I., and Graham, D., *Aircraft Dynamics and Automatic Control*, Princeton University Press, Princeton, 1973.

Nelson, R. C., *Flight Stability and Automatic Control*, McGraw-Hill Co, New York, 1989.

Roskam, J., *Airplane Flight Dynamics and Automatic Flight Controls*, Parts I and II, Roskam Aviation and Engineering, Ottawa, KS, 1979.

Seckel, E., *Stability and Control of Airplanes and Helicopters*, Academic Press, New York, 1964. He started the practice of including bibliographies in control text books. His book contains an extraordinary bibliography list.

A. Traditional (Classical)

Military Standard, “Flying Qualities of Piloted Vehicles,” MIL-STD 1797A.

Military Specification, MIL-SPEC 8785C.

Buchacker, E., Galleithner, H, Koehler, R., and Marchand, M., “Development of MIL-8785C into a Handling Qualities Specification for a New European Fighter Aircraft,” Flying Qualities, AGARD-508, Oct. 1990.

This paper focused on the introduction of additional criteria (such as higher order system criteria, carefree handling) and the amendments of application of pertinent criteria of MIL-8785C to the development of Handling Qualities Definition Documents (HQDD) for the EFA.

Saunders, T., and Tucker, J., “Combat Aircraft Control Requirements,” Aerodynamics of Combat Aircraft Controls and of Ground Effects, AGARD CP-465, Oct. 1989.

A very good qualitative discussion of functions and requirements of controls with examples from existing British fighter/attack aircraft.

Advisory Group for Aerospace Research & Development, “Manoeuvre Limitations of Combat Aircraft,” AGARD-AR- 155A.

The descriptions of various phenomena limiting aircraft maneuverability, and the approaches to determine the maneuver limits are presented.

Thomas, D., “The Art of Flying Qualities Testing,” Flying Qualities, AGARD CP-508, Oct. 1990.

From a test pilot’s point of view, the author argues for less of the unnecessary numbers and regulations in MIL-specs & FAR. He uses examples to illustrate that an airplane with good flying qualities is one that performs well in actual flight, not just on paper.

Leggett, D., and Black, G., “MIL-STD-1797 is not a Cookbook,” Flying Qualities, AGARD CP-508, Oct. 1990.

The authors claim that the subjective, closed-loop requirements of the MIL-STD-1797 come closer to specifying qualities than do the objective, open loop requirements. They further believe that MIL- STD-1797 should be used as a specification (rather than a guideline), but designers should keep in mind that it’s more important to meet the specifications’ intents than just the specifications’ criteria.

Wanner, J., and Carlson, J., "Comparison of French and United States Flying Qualities Requirements," Handling Qualities Criteria, AGARD CP-106, Oct. 1971.

The goals and intent of the two sets of flying qualities requirements are shown to be generally the same.

Roskam, J., *Airplane Design, Part VII: Determination of Stability, Control and Performance Characteristics: FAR and Military Requirements*, Roskam Aviation and Engineering Corporation, Ottawa, KS, 1988.

Andrews, S., "The Nature and Use of the Rules for Judging the Acceptability for the Flying Qualities of Fixed Wing Aircraft," Handling Qualities Criteria, AGARD CP-106, Oct. 1971.

This paper considers the general content of "Design Requirements for Service Airplanes" and "Flying Qualities of Piloted Aeroplanes" in relation to the requirements of the flight test in the assessment of fighter/attack aircraft.

Sliff, R., and LeSuer, R., "FAA Flying Qualities Requirements," Handling Qualities Criteria, AGARD CP-106, Oct. 1971.

Projected difficulties associated with airplane handling qualities indicates a need for flexibility and change of FAR to accommodate new designs and innovations.

Anderson, S., and Schroers, L., "Revisions to V/STOL Handling Qualities Criteria of AGARD Report 408," Handling Qualities Criteria, AGARD CP-106, Oct. 1971.

Several controversial areas associated with V/STOL aircraft are discussed to show that more research is needed to refine their criteria.

Koven, W., and Wasicki, R., "Flying Qualities Requirement for United States Navy and Air Force Aircraft," AGARD-R-336, October 1961.

Hoh, R., "Concepts and Criteria for a Mission Oriented Flying Qualities Specification," AGARD LS-157, May 1988.

-----, "Standard Evaluation Maneuvers Set Contract - Government and Industry Review," McDonnell Douglas, Hamilton Associates, Inc. and Fighter Command International, WPAFB, July, 1991.

A-1. Criteria and Methods

Vincenti, W.G., "Establishment of Design Requirements: Flying-Quality Specifications for American Aircraft, 1918-1943," in Vincenti, W.G., *What Engineers Know and How They Know It*, Johns Hopkins Univ. Press, Baltimore, 1990, pp. 51-111.

Gibson, J., "The Development of Alternate Criteria for FBW Handling Qualities," Flying Qualities, AGARD-508, Oct. 1990.

This paper presents the development of criteria to address problems in flight path, flight attitude, PIO, and lateral-directional handling.

Shirk, F. J., and Moorehouse, D. J., "Alternative Design Guidelines for Pitch Tracking," AIAA 87-2289, Proceedings AIAA Atmospheric Flight Mechanics Conference, Monterey, CA, August, 1987, pp. 40 - 48.

Bland, M., *et al.*, "Alternative Design Guidelines for Pitch Tracking," AIAA 87-2289, August 1987.

McRuer, D., "Progress and Pitfalls in Advanced Flight Control Systems," AGARD CP-321.

Bosworth, J., and Cox, H., "A Design Procedure for the Handling Qualities Optimization of the X-29A Aircraft," AIAA 89-3428, Boston, Mass., August 1989.

Gibson, J., "Piloted Handling Qualities Design Criteria for High Order Flight Control System," AGARD CP-333, April 1982.

Hodgkinson, J., and LaManna, W., "Equivalent System Approaches to Handling Qualities Analysis and Design Problems of Augmented Aircraft," AIAA Atmospheric Flight Conference, Hollywood, FL, August 1977.

B. Relaxed Static Stability

Holloway, Richard B., Burris, Paul M., and Johannes, Robert P., "Aircraft Performance Benefits from Modern Control Systems Technology," *Journal of Aircraft*, Vol. 7, No. 6, Nov.-Dec. 1970, pp. 550-553.

Beaufriere, H.L., Stratton, A., and Damle, R., "Control Power Requirements for Statically Unstable Aircraft," AFWAL-TR-87-3018, June 1987.

Wunnenberg, Horst., "Handling Qualities of Highly Augmented Unstable Aircraft, Summary of an AGARD-FMP Working Group Effort," Flying Qualities, AGARD-508, Oct. 1990.

This is a very brief outline of AGARD AR-279, that presents methods and criteria as design guides and guides for the evaluation of handling qualities of highly augmented aircraft. AGARD AR-279 was published in May 1991.

Innocenti, M., "Metrics for Roll Response Flying Qualities," Flying Qualities, AGARD-CP-508, Oct. 1990.

The primary focus is the analysis using the Gibson's method, and composed of time domain and frequency domain techniques to evaluate the roll performance and handling qualities of a highly augmented aircraft.

Gibson, J., "Handling Qualities for Unstable Combat Aircraft," ICAS-86-5.3.4, September 1986.

-----, "Evaluation of Alternate Handling Qualities Criteria for Highly Augmented Unstable Aircraft," AIAA Paper 90-2844, 1991.

C. Lateral/Directional and Roll Performance Issues

Pinsker, W., "Directional Stability in Flight with Bank Angle Constraint as a Condition Defining a Minimum Acceptable Value for $n-v$," RAE Report TR 67127.

Doetsch, K. Jr., "Parameters Affecting Lateral-Directional Handling Qualities at Low Speed," Handling Qualities Criteria, AGARD CP-106, Oct. 1971.

Monagan, S., *et al.*, "Lateral Flying Qualities of Highly Augmented Fighter Aircraft," AFWAL-TR-81-3171, Vol. I, 1982.

Juri Kalviste, "Spherical Mapping and Analysis of Aircraft Angles for Maneuvering Flight," *Journal of Aircraft*, Vol. 24, No. 8, Aug. 1987, pp.523-530.

This paper examines the definition of a coordinated roll and a velocity vector roll.

Innocenti, M. Thukral, A., "Roll Performance Criteria for Highly Augmented Aircraft," *Journal of Guidance Control and Dynamics*, Vol. 14, No. 6, Nov.-Dec. 1991, pp. 1277-1286.

Some additional parameters of V/STOL aircraft are found to affect the lateral-directional flying qualities at very low speeds.

Gregory Clemens Krekeler, Jr., "Aircraft Lateral-Directional Control Power Prediction for Advanced Fighter Aircraft Design," MS Thesis, University of Missouri—Rolla, 1992.

This thesis is slightly mistitled. It investigates the determination of the control power requirements rather than the prediction of control power from a given design. In fact, it requires a detailed math model of the design. It uses coordinated rolls and level sideslips to find the required control moments. The author works for McDonnell-Douglas, and the work is closely connected to their program VECTOR.

Durham, W., Lutze, F., and Mason, W.H., "Kinematics and Aerodynamics of the Velocity Vector Roll," AIAA Paper 93-3625, Aug. 1993.

In this model problem, the control moments required to obtain a specified fully coordinated roll are found. It is an inverse problem which uses a program running on a PC to provide the time history of the trajectory and the required moments. From this study, maximum moments are determined for a variety of conditions and compared with new and classical analytic estimates.

Kevin D. Citurs, James E. Buckley and Kenneth A. Doll, "Investigation of Roll Requirements for Carrier Approach," AIAA Paper 93-3649, Aug. 1993.

D. High Angle of Attack

Johnston, D. E. and Heffley, R. K., "Investigation of High AOA Flying Qualities Criteria and Design Guidelines," AFWAL-TR-81-3108, December, 1981.

Heffley, R.B. and Johnston, D.E., "High-Angle-of-Attack Flying Qualities—An Overview of Current Design Considerations," SAE Paper 791085, Dec. 1979.

Krekeler, G., Wilson, D., and Riley, D., "High Angle of Attack Flying Criteria," AIAA 90-0219, Jan. 1990.

Beaufriere, H., "Flight Plan Development for a Joint NASA/Navy High Angle of Attack Flight Test Program," Grumman Contract No. NASA 2965, March 1983.

Kalviste, J., "Aircraft Stability Characteristics at High Angle of Attack," Paper 29, Dynamic Stability Parameters, AGARD CP-235, November 1978.

D-1. Longitudinal

Nguyen, L.T., and Foster, J.V., "Development of a Preliminary High-Angle-of-Attack Nose-Down Pitch Control Requirement for High-Performance Aircraft," NASA TM 101684, Feb. 1990.

Ogburn, M.E., Foster, J.V., Nguyen, L.T., Breneman, K.P., McNamara, W.G., Clark, C.M., Rude, D.D., Draper, M.G., Wood, C.A., and Hynes, M.S., "High-Angle-of-Attack Nose-Down Pitch Control Requirements for Relaxed Static Stability Combat Aircraft," NASA High-Angle-of-Attack Technology Conference, Oct. 30-Nov. 1, 1990.

Ogburn, Marilyn E., John Foster, J. Pahle, J. Wilson, and James Lackey, "Status of the Validation of High-Angle-of-Attack Nose-Down Pitch Control Margin Design Guidelines," AIAA Paper 93-3623, Aug. 1993.

D-2. Lateral/Directional, including departure

Weissman, R. "Criteria for Predicting Spin Susceptibility of Fighter Type Aircraft," AST TR 72-48.

Bihrlle, W., Jr., and Barnhart, B., "Departure Susceptibility and Uncoordinated Roll-Reversal Boundaries for Fighter Aircraft," *Journal of Aircraft*, Nov. 1982, pp. 897-903.

J. Kalviste, "Coupled Static Stability Analysis for Nonlinear Aerodynamics," AIAA Paper 83-2069, Aug. 1983.

Pelikan, R. J., "F/A-18 High Angle of Attack Departure Resistant Criteria for Control Law Development," AIAA-83-2126, Atmospheric Flight Mechanics Conference, Gatlinburg, TN, August, 1983.

Anderson, S.B., "Handling Qualities Related to Stall/Spin Accidents of Supersonic Fighter Aircraft," AIAA 84-2093, 1984.

Juri Kalviste and Bob Eller, "Coupled Static and Dynamic Stability Parameters," AIAA Paper 89-3362, Aug. 1989.

Lutze, F., Durham, W., and Mason, W.H., "Lateral-Directional Departure Criteria," AIAA Paper 93-3650, Aug. 1993.

John V. Foster, Holly M. Ross and Patrick A. Ashley, "Investigation of High-Alpha Lateral-Directional Control Requirements for High-Performance Aircraft," AIAA Paper 93-3647, Aug. 1993.

E. Agility

Bitten, R., "Qualitative and Quantitative Comparison of Government and Industry Agility Metrics," *Journal of Aircraft*, Vol. 27, No. 3 March, 1990, pp. 276-282.

Drajeske, M.H., and Riley, D.R., "Relationships Between Agility Metrics and Flying Qualities," SAE Paper 901003, April 1990.

Tamrat, B., "Fighter Aircraft Agility Assessment Concepts and Their Implications on Future Agile Fighter Design," AIAA 88-4400, Sept. 1988.

Hodgkinson, J., Skow, A., Ettinger, R., Lynch, U., Laboy, O., Chody, J., and Cord, T.J., "Relationship Between Flying Qualities, Transient Agility, and Operational Effectiveness of Fighter Aircraft," AIAA 88-4329, 1988.

Eggold, D., Valasek, J., and Downing, D., "The Measurement of the Lateral Agility of the F-18," AIAA 91-2880, Proceedings Atmospheric Flight Mechanics Conference, New Orleans, LA, August, 1991, pp. 315-322.

Chody, J., Hodgkinson, J. and Skow, A., "Combat Aircraft Control Requirements for Agility," Aerodynamics of Combat Aircraft Control and of Ground Effects, AGARD CP- 465, Oct. 1989, Section 2.0 - 3.3.

Additional lateral-directional stability criteria are introduced to augment the traditional criteria in the preliminary design process.

Mazza, C. "Agility: A Rational Development of Fundamental Metrics and Their Relationship to Flying Qualities," Flying Qualities, AGARD CP-508, Oct. 1990.

The Frenet approach and the Newtonian approach for the assessment of aircraft agility are discussed.

Murphy, P. C., and Davidson, J. B., "Control Design for Future Agile Fighters," AIAA-91-2882-CP, Proceedings Atmospheric Flight Mechanics Conference, New Orleans, LA, August, 1991, pp. 331 - 241.

Skow, Andrew M., "Agility as a Contributor to Design Balance," *Journal of Aircraft*, Vol. 29, No. 1, Jan.-Feb. 1992, pp. 34-46.

Kalviste, J., "Measures of Merit for Aircraft Dynamic Maneuvering," SAE Technical Paper 901005, April 1990.

F. Post-Stall Maneuvering

I have not seen papers specifically considering control power design for post-stall maneuvering. They are probably classified.

G. Design Issues Related to Vehicle Control

Kehrer, W.T., "Flight Control and Configuration Design Considerations for Highly Maneuverable Aircraft," AGARD CP-262, May 1979.

Mangold, P., "Integration of Handling Quality Aspects into the Aerodynamic Design of Modern Unstable Fighters," Flying Qualities, AGARD-CP-508, Oct. 1990.

Issues relating instabilities in longitudinal and lateral-directional controls and flying qualities are discussed.

Mangold, P. and Wedekind, G., "Integration of Aerodynamic, Performance, Stability and Control Requirements into the Design Process of Modern Fighter Aircraft Configurations," AGARD LS 153.

Stephen Mark Swanson, "A Computer MOdule to Calculate the Horizontal Control Surface Size of a Conceptual Aircraft Design," MS Thesis, Cal Poly, San Luis Obispo, January 1990.

This thesis describes a module for ACSYNT. It includes a discussion of the determination of the center of gravity position and the considerations required to determine a size of an aft tail or canard. Thrust vectoring considerations for landing are also included.

McKay, K. and Walker, M. "A Review of High Angle of Attack Requirements for Combat Aircraft," Flying Qualities, AGARD CP-508, Oct. 1990.

The paper examines qualitatively the implications of designing for high angle of attack on aircraft design configuration.

Mangold, Peter, "Transformation of Flightmechanical Design Reguirements for Modern Fighters into Aerodynamic Characterestics," AGARD CP-147, Nov. 1991.

Joseph R. Boland, David R. Riley and Kevin D. Citurs, "Aircraft Control Requirements and Achievable Dynamics Prediction," AIAA Paper 93-3648, Aug. 1993.

This paper is very close to Wayne Durham's control allocation work.

James M. Simon, William B. Blake and Dieter Multhopp, "Control Concepts for a Vertical Tailless Fighter," AIAA Paper 93-4000, Aug. 1993.

This paper includes a lot of aerodynamic data on control effectiveness, and a discussion of the control requirements associated with the typical requirement for a vertical tail.

G-1. Canard-Tail Comparisons

Fellers, W., Bowman, W., and Wooler, P., "Tail Configuration for Highly Maneuverable Combat Aircraft," AGARD CP-319, Combat Aircraft Maneuverability, Oct. 1981.

A comparison in maneuverability for three tail configurations, aft tail, tailless (with and without thrust vectoring) and canard configuration is presented. This is one of the first papers to discuss nose down pitching moment requirements at high angle-of-attack as a primary design criterion.

Wedekind, G., "Tail Versus Canard Configuration: An Aerodynamic Comparison with Regard to the Suitability for Future Tactical Combat Aircraft," ICAS-82-1.2.2, 1982.

Nicholas, W.U., Naville, G.L., Hoffschwelle, Huffman, J.K., and Covell, P.F., "An Evaluation of the Relative Merits of Wing-Canard, Wing-Tail, and Tailless Arrangements for Advanced Fighter Applications," ICAS-84-2.7.3, 1984.

Landfield, J.P., and Rajkovic, D., "Canard/Tail Comparison for an Advanced Variable-Sweep-Wing Fighter," *Journal of Aircraft*, Vol. 23, No. 6, June 1986, pp. 449-454 (also AIAA Paper 84-2401).

This paper provides an excellent survey of the control power issues arising in the design process, and the interplay between relaxed static stability and various control effector possibilities. It also references most of the other design studies comparing aft tail and canard design.

H. Aerodynamic Characteristics

Greer, H., "Summary of Directional Divergence Characteristics of Several High Performance Aircraft Configurations," NASA-TN D-6993, Nov. 1972.

Nominal characteristics of the following: XP-92, YF-102, XF4D-1, F-8, F-86D, Mig 15, Bell D-188A, X-15, A-7, F-4E, F-111, F-5, XB-58, Winged missile, Lockheed SST, Initial Boeing SST B2707, NASA Generic SST.

Brandon, J. and Nguyen, L., "Experimental Study of Effects of Forebody Geometry on High Angle of Attack Static and Dynamic Stability," AIAA 86-0311, 1986.

Chambers, J. and Anglin E., "Analysis of Lateral- directional Stability Characteristics of a Twin Jet Fighter Airplane at High Angles of Attack," NASA TN-D- 5361.

Carr, P.C., and Gilbert, W.P., "Effects of Fuselage Forebody Geometry on Low Speed Lateral Directional Characteristics of a Twin-Tail Fighter Model at High Angles of Attack," NASA TP-1592, Dec. 1979.

Maul, M. and Paulson, J., "Dynamic Lateral Behavior of High Performance Aircraft," NASA RML58E16, March 1958.

Skow, A., and Titiriga, A. Jr., "A Survey of Analytical and Experimental Techniques to Predict Aircraft Dynamic Characteristics at High Angle of Attack," AGARD-CP-235, Dynamic Stability Parameters, November 1978, pp. 19.1 - 19.37.

Ross, A.J., and Thomas, H.H.B.M., "A Survey of Experimental Data on the Aerodynamics of Controls, in the Light of Future Needs," AGARD CP-262, May 1979.

Includes a massive bibliography on control surface effects. The bibliography was obtained from the ESA Information Retrieval System, and covered 1961-1978. The classification is by Control Surface: Pitch, Roll, Yaw and Lift and Side Force "Motivators", Jet controls and Hinge Moments.

Agnew, J.W., and Mello, "Correlation of F-15 Flight and Wind Tunnel Test Control Effectiveness," AGARD CP-262, May 1976.

Orlik-Rückemann, K.J., "Aerodynamic Aspects of Aircraft Dynamics at High Angles of Attack," *Journal of Aircraft*, Vol. 20, No. 9, September 1983, pp. 737-752.

H-1 Propulsion related controls

Skow, A., "Forebody Vortex Blowing - A Novel Control Concept to Enhance Departure/ Spin Recovery Characteristics of Fighter & Trainer Aircraft," AGARD CP-262, Paper 24.

Mangold, P. and Wedekind G., "Inflight Thrust Vectoring: A Further Degree of Freedom in the Aerodynamic/Flight Mechanical Design of Modern Fighter Aircraft," AGARD CP-465, Madrid 1989.

Moorhouse, D. Laughrey, J. and Thomas, R., "Aerodynamic Propulsive Control Development of the STOL and Maneuver Technology Demonstrator," AGARD CP-465, October 1989.

Hahne, D.E., Luckring, J.M., Covell, P.F., Phillips, W.P., Gatlin, G.M., Shaughnessy, J.D., and Nguyen, L.T., "Stability Characteristics of a Conical Aerospace Plane Concept," SAE Paper 892313, Sept. 1989.

I. Specific Aircraft

Moorhouse, D.J., Citurs, K., Thomas, R., and Crawford, M., "The Handling Qualities of the STOL & Maneuver Technology Demonstrator from Specification to Flight Test," Flying Qualities, AGARD-508, Oct. 1990.

This paper presents the analytical development of the handling qualities specifications of the S/MTD aircraft. Simulator verification and flight test results are also included.

Renzo, B., "Flying Qualities Experience on the AMX Aircraft," Flying Qualities, AGARD-CP-508, Oct. 1990.

The application of modern handling qualities criteria to the AMX lead to alleviation of PIO tendencies and accomplish lateral-directional precision tracking tasks.

Sobata, M., "B-1B High AOA Testing in the Evaluation of a Stall Inhibitor System," Flying Qualities, AGARD CP- 508, Oct. 1990.

This paper summarizes the application of Stall Inhibitor System/Stability Enhancement Function (SIS/SEF) to address the longitudinal instability problem of the B-1B.

Walchli, L., and Smith, Rogers, "Flying Qualities of the X-29 Forward Swept Wing Aircraft," Flying Qualities, AGARD CP-508, Oct. 1990.

A brief description of the flight control system and a summary of the subsequent high and low AOA flight test results of the flying qualities is the focus of the paper.

Gallagher, J., and Nelson, W., Jr., "Flying Qualities of the Northrop YF-17 Fighter Prototypes," Business Aircraft Meeting, Wichita, March 1977.

Clark, C., and Bernens, M., "High Angle-of-Attack Flight Characteristics of the YF-22," AIAA Paper 91-3194, Sept. 1991.

Includes nose down capability as a function of angle of attack including thrust vectoring (no scales) and max roll rate as a function of α (with scales) with and w/o thrust vectoring.

Klein, V., and Noderer, K.D., "Aerodynamic Parameters of the X-31 Drop Model Estimated from Flight Data at High Angles of Attack," AIAA Paper 92-43??, 1992.

Includes extensive C_n and C_l derivatives ($\beta, p, r, \delta r$) as a function of angle of attack.

Taylor, J. H., and Skow, A. M., "F-5E Departure Warning System Algorithm Development and Validation," *Journal of Aircraft*, Vol. 25, No. 9, September 1988.

Herbst, W., "X-31 at First Flight," Flying Qualities, AGARD CP-508, Oct. 1990.

The motivation and design goals are discussed along with the expected performance in terms of "supermaneuverability", pp. 783 - 789.

Behel, I.M., and McNamara, W.G., "F/A-18A High Angle of Attack/Spin Testing," Society of Experimental Test Pilots Silver Anniversary 1981 Report to the Aerospace Profession, Sept. 1981, *Technical Review*, Vol. 15, No. 2, 1981.

I-1. Representative "Math Model" Data

<u>Model</u>	<u>Source</u>
Cessna 172	Roskam
North American Navion	Nelson
Beech Model 99	Roskam
Grumman OV-1 "Mohawk"	Seckel
Douglas A-4D "Skyhawk"	Nelson; McRuer, Ashkenas, and Graham
SIAI-Marchetti S211	Roskam
Northrop F-89 "Scorpion"	McRuer, Ashkenas, and Graham
North American F-100 "Super Saber"	Seckel
Lockheed F-104A "Starfighter"	Nelson
Convair F-106B "Delta Dart"	McRuer, Ashkenas, and Graham
McDonnell F-4E "Phantom II"	Roskam
Convair B-58 "Hustler"	Seckel
North American XB-70 "Valkyrie"	Ashley
Douglas C-47 "Skytrain"	McRuer, Ashkenas, and Graham
Boeing 707	Seckel
Douglas DC-8	McRuer, Ashkenas, and Graham
Convair 880	Nelson
Boeing 747	Nelson; Roskam
Lockheed Jetstar	Nelson
Gates Learjet M24	Roskam
Bell X-1	Seckel
North American X-15	Seckel
LTV-Hiller XC-142	McRuer, Ashkenas, and Graham
Douglas-Doak VZ-4	McRuer, Ashkenas, and Graham
Sikorsky S-58 (H-35 Choctaw)	Seckel
Sikorsky S-55 (H-19 Chickasaw)	McRuer, Ashkenas, and Graham
Bristol F.2B "Brisfit"	McRuer, Ashkenas, and Graham

I-2. Detailed Math Models

F-16

Nguyen, L.T., Ogburn, M.E., Gilbert, W.P., Kibler, K.S., Brown, P.W., and Deal, P.L., "Simulator Study of Stall/Post-Stall Characteristics of a Fighter Airplane With Relaxed Static Stability," NASA TP-1538, Dec. 1979.

Stevens, B.L., and Lewis, F.L., *Aircraft Control and Simulation*, John Wiley & Sons, New York, 1992.

Boeing 747

Hanke, C.R., "The Simulation of a Large Jet Transport Aircraft, Vol. I: Mathematical Model, NASA CR-1756, March 1971, Vol. II: Modeling Data, Sept. 1970, N73-10027 Boeing Doc. D6-30643, with D.R. Nordwall as an additional author.

XB-70

"Wind-Tunnel/Flight Correlation Study of a Large Flexible Supersonic Cruise Aircraft (XB-70-1)", Part I, NASA TP 1514, by James C. Daugherty, Nov. 1979. Part II, NASA TP 1515, by John B. Peterson, Jr., Mike Mann, Russell Sorrells, Wally Sawyer and Dennis Fuller, Feb. 1980, and Part III, NASA TP 1516, by Henry Arnaiz, John B. Peterson, Jr. and James C. Daugherty, Mar. 1980

Chester H. Wolowicz and Roxanah B. Yancy, "Summary of Stability and Control Characteristics of the XB-70 Airplane," NASA TM X-2933,, October 1973.

Arnaiz, H.H., "Flight Measured Lift and Drag Characteristics of a Large, Flexible, High Supersonic Cruise Airplane," NASA TM X-3532, May 1977.

Powers, B.G., "A Review of Transport Handling Qualities in Terms of Preliminary XB-70 Flight Experience," NASA TMX-1584, May 1968.

Wolowicz, C.H., Strutz, L.W., Gilyard, G.B., and Matheny, N.W., "Preliminary Flight Evaluation of the Stability and Control Derivatives and Dynamic Characteristics of the Unaugmented XB-70-1 Airplane including Comparisons with Predictions," NASA TND-4578, May, 1968.

Wykes, J.H. and Lawrence, R.E., "Estimated Performance and Stability and Control Data for Correlation with XB-70-1 Test Data," NASA CR-114335, July 1971.

Martin, A.W. and Beaulieu, W.D., "XB-70 Flight Test Data Comparisons with Simulation Predictions of Inlet Unstart and Buzz," NASA CR-1631, June 1970.